OFFICE OF CIVILIAN RADIOACTIVE WASTE MANAGEMENT
ANALYSIS/MODEL COVER SHEET
Complete Only Applicable Items

1. QA: QA
Page: 1 of: 102

2. ☐ Analysis ☐ Engineering
☐ Performance Assessment
☐ Scientific

3. ☒ Model ☒ Conceptual Model Documentation
☒ Model Documentation
☒ Model Validation Documentation

4. Title:
Geologic Framework Model (GFM3.1)

5. Document Identifier (including Rev. No. and Change No., if applicable):
MDL-NBS-GS-000002 REV 00 ICN 01

6. Total Attachments:
5

7. Attachment Numbers - No. of Pages in Each:
I - 0 pp.; II - 8 pp.; III - 2 pp., IV - 4 pp.; V - 6 pp.

	Printed Name	Signature	Date
8. Originator	Robert Clayton	[signature]	01/27/00
9. Checker	Gerald Nieder-Westermann	[signature]	01/27/00
10. Lead/Supervisor	Clinton Lumm	[signature]	1/27/00
11. Responsible Manager	Dwight Hoxie	[signature]	1/27/00

12. Remarks:

NM3507
WM-11

OFFICE OF CIVILIAN RADIOACTIVE WASTE MANAGEMENT
ANALYSIS/MODEL COVER SHEET
Complete Only Applicable Items

1. QA: QA
Page: 1 of: 102

2. ☐ Analysis ☐ Engineering
☐ Performance Assessment
☐ Scientific

3. ☒ Model ☒ Conceptual Model Documentation
☒ Model Documentation
☒ Model Validation Documentation

4. Title:
Geologic Framework Model (GFM3.1)

5. Document Identifier (including Rev. No. and Change No., if applicable):
MDL-NBS-GS-000002 REV 00 ICN 01

6. Total Attachments:
5

7. Attachment Numbers - No. of Pages in Each:
I - 0 pp.; II - 8 pp.; III - 2 pp., IV - 4 pp.; V - 6 pp.

	Printed Name	Signature	Date
8. Originator	Robert Clayton		01/27/00
9. Checker	Gerald Nieder-Westermann		01/27/00
10. Lead/Supervisor	Clinton Lumm		1/27/00
11. Responsible Manager	Dwight Hoxie		1/27/00

12. Remarks:

INFORMATION COPY
LAS VEGAS DOCUMENT CONTROL

OFFICE OF CIVILIAN RADIOACTIVE WASTE MANAGEMENT
ANALYSIS/MODEL REVISION RECORD

Complete Only Applicable Items

2. Analysis or Model Title:

Geologic Framework Model (GFM3.1)

3. Document Identifier (including Rev. No. and Change No., if applicable):

MDL-NBS-GS-000002 REV 00 ICN 01

4. Revision/Change No.	5. Description of Revision/Change
00	Initial issue.
00/01	ICN 01 incorporates DOE comments and editorial changes. Changes are designated by a change bar in the right margin.

CONTENTS

Page

ACRONYMS 9

1. PURPOSE 11

2. QUALITY ASSURANCE 15

3. COMPUTER SOFTWARE AND MODEL USAGE 17

4. INPUTS 19
   4.1 DATA AND PARAMETERS 19
   4.2 CRITERIA 21
   4.3 CODES AND STANDARDS 21

5 ASSUMPTIONS 23

6. GEOLOGIC FRAMEWORK MODEL 25
   6.1 DATA REDUCTION 25
      6.1.1 Selection of Boreholes 25
      6.1.2 Selection of Faults 31
   6.2 MODEL DEVELOPMENT (GFM1.0 TO GFM3.1) 33
      6.2.1 Changes From GFM1.0 to GFM2.0 35
      6.2.2 Changes From GFM2.0 to GFM3.0 35
   6.3 METHODOLOGY 38
      6.3.1 GFM Conceptual Models 45
      6.3.2 Overview of GFM3.1 Methodology 45
      6.3.3 Construction of Faults 48
      6.3.4 Construction of Reference Horizons and Model-Isochores 49
      6.3.5 Assembly of Faults and Rock Layers 50
   6.4 RESULTS AND DISCUSSION 50
      6.4.1 Interpretation Of Rock Units 52
      6.4.2 Interpretation of Faults 78
   6.5 UNCERTAINTIES AND LIMITATIONS 80
      6.5.1 Uncertainty Estimates for Constrained Areas 81
      6.5.2 Uncertainty Estimates for Less Constrained Areas 86
      6.5.3 Limitations and Alternative Interpretations 86
      6.5.4 Effect of To Be Verified (TBV) Input on the GFM 88
   6.6 GFM VALIDATION 88
      6.6.1 Validation Criteria 88
      6.6.2 Predictions for Boreholes SD-6 and WT-24 and the ECRB Cross-Block Drift 89
      6.6.3 Validation Results 93

CONTENTS (CONTINUED)

Page

7. CONCLUSIONS 96

8. INPUTS AND REFERENCES 98
   8.1 DOCUMENTS CITED 98
   8.2 CODES, STANDARDS, REGULATIONS, AND PROCEDURES 100
   8.3 SOURCE DATA, LISTED BY DATA TRACKING NUMBER 101
   8.4 SOFTWARE 102

ATTACHMENTS

I DOCUMENT INPUT REFERENCE SYSTEM (DIRS) REMOVED

II EXCLUDED BOREHOLE DATA

III PREDICTED AND ACTUAL UNIT THICKNESSES FOR THE UZN BOREHOLES

IV PREDICTED AND ACTUAL UNIT THICKNESSES FOR BOREHOLES a#1, a#7, c#1, AND c#3

V METHODOLOGY FOR UNCERTAINTY ANALYSES

FIGURES

Page

1. Area of Integrated Site Model, Showing Model Boundaries 12
2. Relationships of Component Models, Integrated Site Model, and Downstream Uses 13
3. Locations of Boreholes, ESF, and Cross-Block Drift 26
4. Surface Traces of Faults Modeled in GFM 27
5. Locations of Measured Sections, Gravity Profiles, and Seismic Profiles 28
6. Locations of Boreholes Not Used in the GFM 29
7. Map Showing the C-Hole Complex, Mapped Faults, and Grid Nodes 32
8. Changes Between GFM Versions 34
9. Interpretive Constraints 36
10. Isochore Method 43
11. Schematic Cross Section Showing The Relation of Partial Thickness to Model Units 46
12. Elevation Map of Basal Tiva Reference Horizon 51
13. Model Surficial Geology (Vertical View of GFM; Same Area as Figure 1) 53
14. Wedge of Post-Tiva Rocks in Solitario Canyon (View to North of Slice Through GFM) 54
15. Model-Isochore Map of Alluvium 56
16. Model-Isochore Map of Tiva Canyon Tuff Crystal-Poor Member Vitric Zone Densely Welded Subzone (Tpcpv3) 57
17. Model-Isochore Map of Yucca Mountain Tuff (Tpy) 59
18. Model-Isochore Map of Pah Canyon Tuff (Tpp) 60
19. Model-Isochore Map of Paintbrush Tuff Nonwelded Unit (Ptn) 61
20. Model-Isochore Map of Topopah Spring Tuff (Tpt) 62
21. Model-Isochore Map of Topopah Spring Tuff Crystal-Poor Member Vitric Zone Densely Welded Subzone (Tptpv3) 64
22. Model-Isochore Map of Topopah Spring Tuff Crystal-Poor Member Lithic-Rich Zone (Tptf) 65
23. Model-Isochore Map of Repository Host Horizon (RHH) 66
24. Model-Isochore Map of Calico Hills Formation (Ta) 68
25. Model-Isochore Map of Prow Pass Tuff (Tcp) 69
26. Model-Isochore Map of Bullfrog Tuff (Tcb) 71

FIGURES (Continued)

Page

27. Model-Isochore Map of Tram Tuff (Tct) 72
28. Elevation Map of Top of Older Tertiary Units (Tund) 74
29. Elevation Map of Tertiary-Paleozoic Unconformity 76
30. Comparison of Geophysical and GFM Interpretations of Tertiary-Paleozoic Unconformity 77
31. Map of Constrained and Less Constrained Areas 82
32. Model-Isochore Map of Topopah Spring Tuff Crystal-Rich Member Vitric Zone Densely Welded Subzone (Tptrv1) 84
33. Model-Isochore Map of Repository Host Horizon Showing Less Constrained Areas 85
34. SD-6 Comparison of Predicted Versus Actual Contact Depths 90
35. WT-24 Comparison of Predicted Versus Actual Contact Depths 94
V-1. Predicted Errors From the Piecewise Reconstruction Uncertainty Assessment for Tptpv3 (Lower Vitrophyre) V-3
V-2. Method for Evaluating Contouring Uncertainty V-5

TABLES

Page

1. Model-Development Documentation for GFM 15
2. Information for Model Software 17
3. Data Input 19
4. Boreholes Excluded From GFM 25
5. Correlation Chart for Model Stratigraphy 39
6. Predicted Versus Actual Contacts in Borehole SD-6 92
7. Predicted Versus Actual Contacts in Borehole WT-24 95
8. Locations of Predicted and Actual Stratigraphic Contacts for the ECRB Cross-Block Drift 96

INTENTIONALLY LEFT BLANK

ACRONYMS

AMR	Analysis/Model Report
CFR	Code of Federal Regulations
CRWMS	Civilian Radioactive Waste Management System
DI	document identifier
DIRS	Document Input Reference System
DOE	United States Department of Energy
DTN	data tracking number
ECRB	Enhanced Characterization of the Repository Block
ESF	Exploratory Studies Facility
FR	Federal Register
GFM	Geologic Framework Model
GFM3.1	Geologic Framework Model, Version 3.1
ISM	Integrated Site Model
MI	media identifier
MM	Mineralogic Model
M&O	Management and Operating Contractor
NRC	Nuclear Regulatory Commission
Q	qualified
QA	quality assurance
QARD	Quality Assurance Requirements and Description
RHH	Repository Host Horizon
RIB	Reference Information Base
RPM	Rock Properties Model
STN	Software Tracking Number
SZ	saturated zone
TBV	to be verified
TDMS	Technical Data Management System
TSPA	Total System Performance Assessment
USGS	United States Geological Survey
UZ	unsaturated zone
YMP	Yucca Mountain Site Characterization Project

INTENTIONALLY LEFT BLANK

1. PURPOSE

The purpose of this report is to document the Geologic Framework Model (GFM), Version 3.1 (GFM3.1) with regard to data input, modeling methods, assumptions, uncertainties, limitations, and validation of the model results, qualification status of the model, and the differences between Version 3.1 and previous versions.

The GFM represents a three-dimensional interpretation of the stratigraphy and structural features of the location of the potential Yucca Mountain radioactive waste repository. The GFM encompasses an area of 65 square miles (170 square kilometers) and a volume of 185 cubic miles (771 cubic kilometers). The boundaries of the GFM (shown in Figure 1) were chosen to encompass the most widely distributed set of exploratory boreholes (the Water Table or WT series) and to provide a geologic framework over the area of interest for hydrologic flow and radionuclide transport modeling through the unsaturated zone (UZ). The depth of the model is constrained by the inferred depth of the Tertiary-Paleozoic unconformity. The GFM was constructed from geologic map and borehole data. Additional information from measured stratigraphy sections, gravity profiles, and seismic profiles was also considered.

This work was conducted in accordance with the *Work Plan for Integrated Site Model* (CRWMS M&O 1998a). The constraints, caveats, and limitations associated with this model are discussed in the appropriate text sections that follow.

The GFM is one component of the Integrated Site Model (ISM) (Figure 1), which has been developed to provide a consistent volumetric portrayal of the rock layers, rock properties, and mineralogy of the Yucca Mountain site. The ISM consists of three components:

- Geologic Framework Model (GFM)
- Rock Properties Model (RPM)
- Mineralogic Model (MM).

The ISM merges the detailed project stratigraphy into model stratigraphic units that are most useful for the primary downstream models and the repository design. These downstream models include the hydrologic flow models and the radionuclide transport models. All the models and the repository design, in turn, will be incorporated into the Total System Performance Assessment (TSPA) of the potential radioactive waste repository block and vicinity to determine the suitability of Yucca Mountain as a host for the repository. The interrelationship of the three components of the ISM and their interface with downstream uses are illustrated in Figure 2.

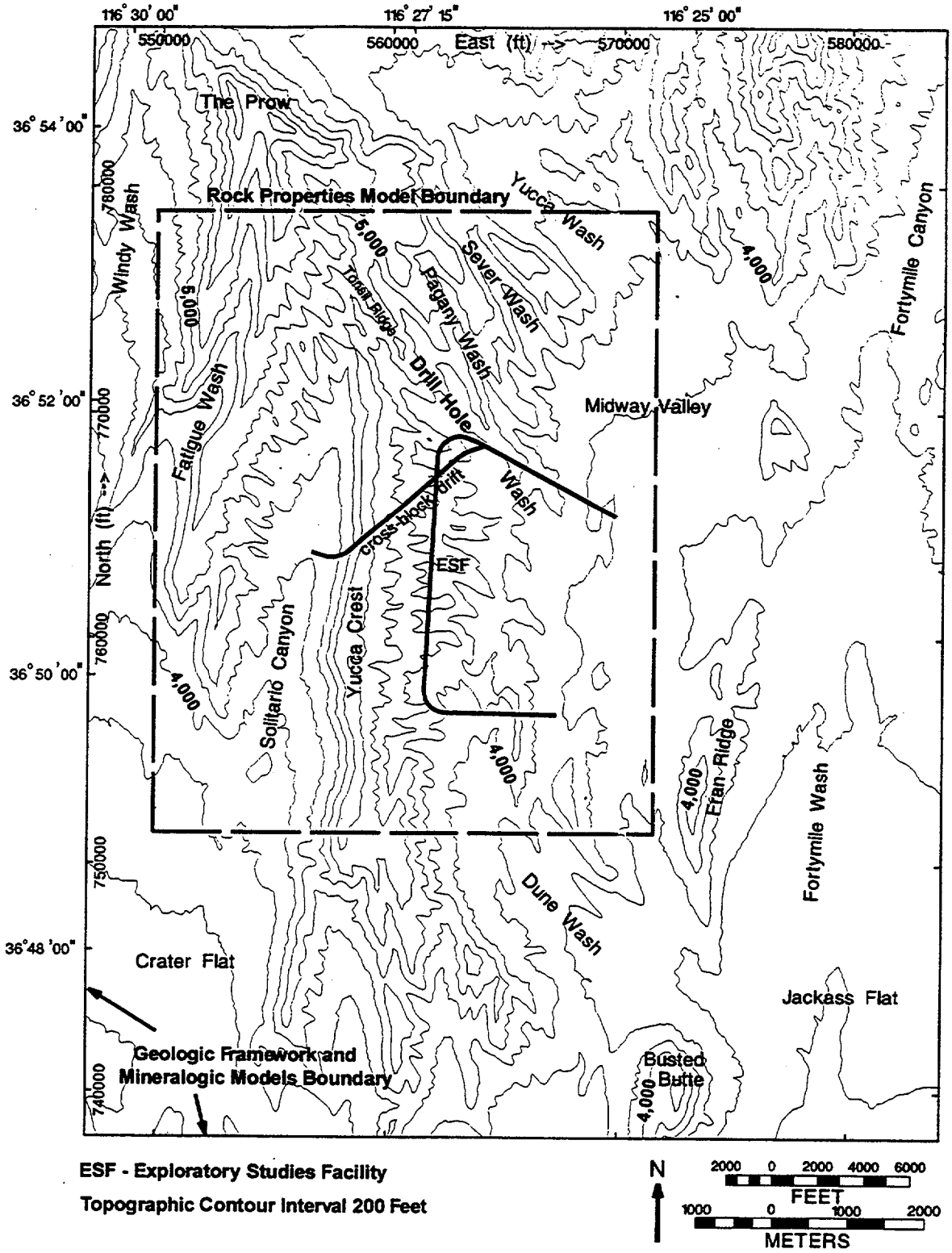

Figure 1. Area of Integrated Site Model, Showing Model Boundaries

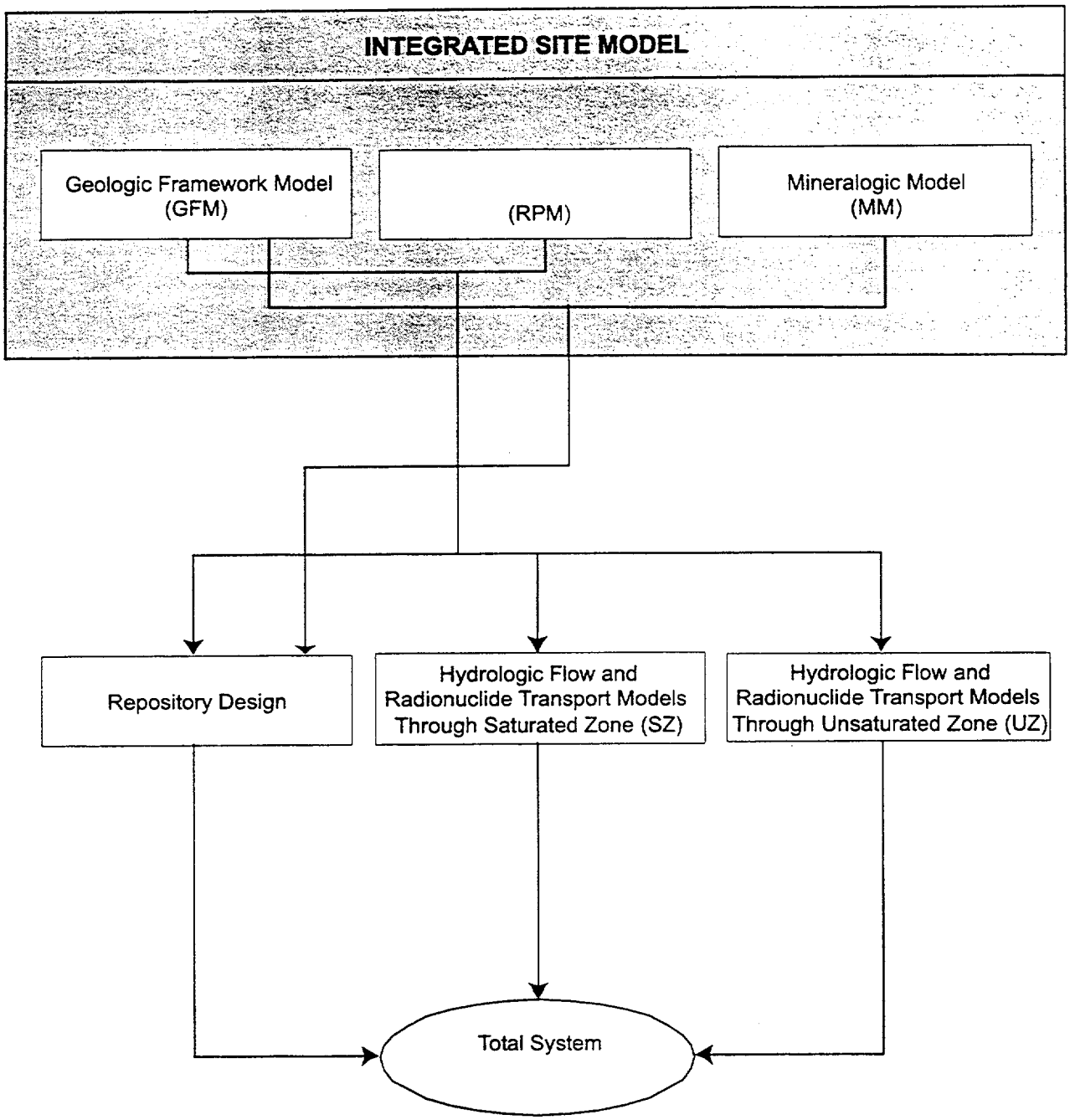

Figure 2. Relationships of Component Models, Integrated Site Model, and Downstream Uses

INTENTIONALLY LEFT BLANK

2. QUALITY ASSURANCE

Pursuant to evaluations (CRWMS M&O 1999a, 1999b) performed in accordance with QAP-2-0, *Conduct of Activities*, it was determined that activities supporting the development of the GFM are quality affecting and subject to the requirements of the *Quality Assurance Requirements and Description* (QARD) (DOE 1998a). Accordingly, efforts to conduct the analysis have been performed in accordance with approved quality assurance (QA) procedures under the auspices of the Yucca Mountain Site Characterization Project (YMP) Management and Operating Contractor (M&O) Quality Assurance program, using procedures identified in the work direction and planning document for preparation of this Analysis/Model Report (AMR) (CRWMS M&O 1999c). This AMR has been planned and prepared in accordance with procedure AP-3.10Q, *Analyses and Models*.

Modeling work was performed and documented in accordance with QA procedures QAP-SIII-3 (*Scientific Notebooks*) and AP-SIII.1Q (*Scientific Notebooks*). The work plan for the modeling activity was developed in accordance with QAP-SIII-1, *Scientific Investigation Control*. The model was technically reviewed in accordance with QAP-SIII-2, *Review of Scientific Documents and Data*. Documentation is listed in Table 1.

Table 1. Model-Development Documentation for GFM

Planning Document	Procedures	Scientific Notebook
CRWMS M&O 1998a CRWMS M&O 1999c	QAP-SIII-1 (*Scientific Investigation Control*) QAP-SIII-2 (*Review of Scientific Documents and Data*) QAP-SIII-3 (*Scientific Notebooks*) AP-SIII.1Q (*Scientific Notebooks*) AP-3.10Q (Analysis and Models)	SN-M&O-SCI-008-V1 (Clayton 1999)

INTENTIONALLY LEFT BLANK

3. COMPUTER SOFTWARE AND MODEL USAGE

The GFM was constructed with EARTHVISION Version 4.0 (EARTHVISION) software, which is designed for three-dimensional geologic modeling. EARTHVISION was qualified under QAP-SI-0, *Computer Software Qualification*, and managed under QAP-SI-3Q, *Software Configuration Management*. The software was obtained from Configuration Management, is appropriate for this application, and was used within the range of validation in accordance with AP-SI.1Q, *Software Management*. The Software Tracking Number (STN) is 30035 V4.0. The media identifier (MI) number is 30035-M09-001. The document identifier (DI) number is 30035-2003 Rev 0. Software information is listed in Table 2 and its qualification status is indicated in the Document Input Reference System (DIRS). EARTHVISION version 4.0 was used to construct GFM model versions 2.1, 3.0, and 3.1.

Table 2. Information for Model Software

Computer Type	Software Name	Version	Qualification Procedure	STN
Silicon Graphics Octane	EARTHVISION	4.0	QAP-SI-0	30035 V4.0

During construction and use of the GFM, the model is stored on internal computer disks, backup tapes, and compact discs. The electronic files for GFM3.1 were submitted to the Technical Data Management System (TDMS) in EARTHVISION binary format or ASCII format, depending on the file type. Data files and instructions necessary to reconstruct the GFM are available in the TDMS, (DTN: MO9901MWDGFM31.000). Reconstruction of GFM3.1 or use of the EARTHVISION binary format files requires EARTHVISION software Version 4.0 or higher. ASCII format files containing all modeled horizons and faults are also provided in the TDMS under the same data tracking number (DTN) for input to other software used in downstream modeling. The total size of the GFM3.1 binary and ASCII files is approximately 1,200 megabytes.

INTENTIONALLY LEFT BLANK

4. INPUTS

4.1 DATA AND PARAMETERS

Input data for the GFM include borehole lithostratigraphic contacts, tunnel contacts, maps of geology and topography, and measured stratigraphic sections (transects of stratigraphy measured at the surface). In addition, interpretations from geophysical data were used to interpret structures beneath alluvium in Midway Valley. The sources of input data are listed in Table 3. The qualification status (Q or non-Q) of data used in the construction of the GFM is indicated on the Document Input Reference System (DIRS).

Table 3. Data Input

Data Description	Data Tracking Number
Geologic Map	GS970808314221.002
Borehole Lithostratigraphic contacts	MO9811MWDGFM03.000
SD-6 contacts	SNF40060298001.001
WT-24 contacts	SNF40060198001.001
Borehole locations	MO9807COV98003.000
ESF North Ramp geology	GS960908314224.020
ESF South Ramp geology	GS970808314224.016
Tertiary/Paleozoic unconformity	LB980130123112.003

Data Description	Data Tracking Number
Measured section SC#1	GS940708314211.035
Measured section PTn#1	GS950108314211.001
Measured section PTn#2	GS950108314211.002
Measured section PTn#3	GS950108314211.003
Measured section PTn#4	GS950108314211.004
Measured section PTn#5	GS950108314211.005
44 measured sections	GS950608314211.025
ECRB cross-drift contacts	GS981108314224.005

With the exception of a fault modeled under Fortymile Wash (see Section 6.1.2), the fault traces modeled in the GFM are based on the bedrock geologic map of the Yucca Mountain area (DTN: GS970808314221.002). This map was superseded in the TDMS after its incorporation into the GFM. The newer version (DTN: GS980608314221.002) includes minor typographic changes, including omitted labels and line segments that have no technical impact on the GFM.

Fault offsets, where modeled, were also derived from the bedrock geologic map of the Yucca Mountain area (DTN: GS970808314221.002). An exception to this was a feature interpreted from gravity and magnetic profiles beneath Midway Valley as a horst, with vertical displacements of 246 feet (75 meters) on the faults bounding the structure. (Ponce and Langenheim 1994, p.6). The location of this feature was integrated with geologic map information during the creation of the bedrock geologic map of the Yucca Mountain area (DTN: GS970808314221.002), and is included in the GFM.

Data from the Exploratory Studies Facility (ESF) (DTN: GS960908314224.020; GS970808314224.016) and Cross-Block Drift (DTN: GS981108314224.005) were used to constrain the elevation of the reference horizon at the base of the Tiva Canyon Tuff. Only data for the elevation of this horizon were used as input to the GFM because the ESF data do not provide thickness information for the modeled rock layers. For the non-reference horizon units,

model unit thicknesses were adjusted to honor the lithostratigraphic contact elevations as mapped in the ESF and ECRB cross-block drift.

The data tracking number for borehole collar location data (DTN: MO9807COV98003.000) was changed (for administrative reasons) in the TDMS to DTN: MO9906GPS98410.000 after construction of the GFM. Because only the DTN was changed and no data were affected, there is no impact on the GFM.

The group of 44 measured sections listed in Table 3 (DTN: GS950608314211.025) are located primarily in and north of Yucca Wash and provide qualitative data on stratigraphic thicknesses of the shallow units in the northern part of the model. They provide support to the conceptual model (discussed in Section 6.3.1), but were not used as direct input to the model for the following reasons:

- They are non-Q and there are no current plans for these data to be qualified
- They are located in an area of rapid lithologic change and most cannot be confidently correlated to the borehole data
- The United States Geological Survey (USGS) Bedrock Geologic Map (DTN: GS970808314221.002) provides a more appropriate and qualified source of input.

In contrast, the Q measured sections listed in Table 3 are located near the potential repository area where lithologic changes are less rapid and the data can be correlated to nearby boreholes.

Including the 44 measured sections would add an unacceptable level of uncertainty to the model when compared to the value added The specific qualitative information from the non-Q measured sections in support of the conceptual model are the thicknesses of three units of the Topopah Spring Tuff (Tptrv1, Tptf, and Tptpv3), but these data were not input to the model. The sections containing relevant information are as follows: Tptrv1 (sections Tpt-2, -3, -4a, -4b, -5, -6, -8, -9a, -14, -16, -20a, -20b, -23, -30), Tptf (sections Tpt-2, -3, -5, -8, -11, -20a, -21, -22, -23, -32), and Tptpv3 (sections Tpt-1, -3, -4a, -5, -8, 9b, -11, -20c, -22, -31, -33, -35). Because the 44 measured sections are located away from the potential repository area and are in part redundant with the geologic map (DTN: GS970808314221.002), they do not affect the critical characteristics or results of the GFM, nor are the data directly relied upon to address safety and waste isolation issues. Therefore, the 44 measured sections do not require qualification.

Interpretations of seismic reflection profiles (Brocher et al. 1998, pp. 947–971) were used qualitatively to formulate three-dimensional fault geometries and interpret tilted strata. The seismic profiles are not sufficient to provide quantitative model input data because of noise and uncertainties regarding rock velocity. The depth to the top of Paleozoic strata in the GFM was adapted from a gravity inversion study (DTN: LB980130123112.003). This surface was modified to show vertical displacement along the faults modeled in the GFM.

In general, although gravity, aeromagnetic, and seismic reflection and refraction data are available they do not provide sufficient spatial resolution to be used as direct model input. A summary of these data is presented in Oliver et al. (1995). For input, a model requires spatial

location (x-y coordinates and elevation) and specific geometry and identity of faults and stratigraphic units, which is not generally provided by the data obtainable from these geophysical methods.

The surface topography used in the GFM (DTN: MO9901MWDGFM31.000, file name "topography.2grd") was obtained from an undocumented source. For this reason the topographic grid was compared with a digital terrain model (DTN: MO9811COV98591.000) and surveyed borehole collar elevations (DTN: MO9807COV98003.000). The elevation of each grid was calculated at the surveyed locations and these results were compared. Because the vertical error of the GFM grid at the survey locations was consistently less than that of the digital terrain model, it was assumed that the GFM grid provided a more accurate depiction of topography throughout the model area. This assumption is documented in Section 5.

4.2 CRITERIA

This AMR complies with the DOE interim guidance (Dyer 1999). Subparts of the interim guidance that apply to this analysis or modeling activity are those pertaining to the characterization of the Yucca Mountain site (Subpart B, Section 15), the compilation of information regarding geology of the site in support of the License Application (Subpart B, Section 21(c)(1)(ii)), and the definition of geologic parameters and conceptual models used in performance assessment (Subpart E, Section 114(a)).

4.3 CODES AND STANDARDS

No codes and standards are applicable to the GFM.

INTENTIONALLY LEFT BLANK

5 ASSUMPTIONS

The assumptions underlying the construction of the GFM are methodological in nature and entail the use of standard geologic techniques for the analysis, interpretation, and representation of stratigraphic and structural features and relationships at Yucca Mountain. Specific techniques that are assumed to be applicable include the correlation of stratigraphy through the analysis of geophysical borehole logs; the isochore method, as adapted for use in constructing the GFM (and referred to as model-isochore as discussed in Section 6.3 Methodology); and the minimum tension algorithm for constructing model grids. The use of these techniques is described in detail in Section 6. The applicability of these techniques to the Yucca Mountain site is supported by the information currently available pertaining to the geologic setting of the site as described in CRWMS M&O 1998b, page 3.6-6, and requires no further confirmation.

Additionally, it is assumed that the topography used in constructing the GFM was adequate for the intended purposes of the GFM, based on comparisons to surveyed points in DTN: MO9811COV98591.000 as discussed in Section 4.1, and requires no further confirmation.

INTENTIONALLY LEFT BLANK

6. GEOLOGIC FRAMEWORK MODEL

Yucca Mountain is located in the southwestern Nevada volcanic field and consists of tilted fault blocks composed of layered sequences of ash-flow, ash-fall, and bedded tuffs of Miocene age (Sawyer et al. 1994, pp. 1304-1318). Additional information regarding the geologic setting of the Yucca Mountain site and model area is provided in CRWMS M&O 1998b, Chapter 3.2. The stratigraphic nomenclature used in this report is adapted from DTN: MO9510RIB00002.004.

This section describes the GFM in terms of data reduction, development of the model, the modeling methodology, the model results, and the uncertainties and limitations of the model. Model validation is discussed in Section 6.6. The Nevada State Plane coordinates of the GFM boundaries shown in Figure 2 are N738,000 to N787,000 feet (N224,943 to N239,878 meters) and E547,000 to E584,000 feet (E166,726 to E178,004 meters).

As described in Section 4.1, the GFM is based primarily on the geologic map of the Yucca Mountain area (DTN: GS970808314221.002) and data from boreholes (DTN: MO9811MWDGFM03.000), shown in Figure 3. (For brevity, the location identifiers (e.g., USW and UE-25) of boreholes are not used in this report.) The faults included in the GFM, shown in Figure 4, were input from the geologic map (DTN: GS970808314221.002). Locations of geophysical data, and measured sections, described in Section 4, are shown in Figure 5.

6.1 DATA REDUCTION

6.1.1 Selection of Boreholes

The primary input data for the geologic framework are stratigraphic contacts from boreholes and the geologic map of the Yucca Mountain area (Table 3). Of the 82 boreholes listed in the input data (DTN: MO9811MWDGFM03.000), 33 were excluded, for the reasons presented in Table 4 and discussed below. The locations of the excluded boreholes are shown on Figure 6. The specific contacts excluded from the GFM input data, and the reasons for exclusion, are listed in Attachment II. Additionally, data from sources outside the model boundaries cannot be directly input to the model; however, model units were developed to allow reasonable extrapolation to these data sources. The off-site data include boreholes VH-1, VH-2, JF#3, and J#12. Distances from the model boundaries to these boreholes ranges from 0.9 to 3.9 miles (1.4 to 6.3 kilometers).

Table 4. Boreholes Excluded From GFM

Borehole ID	Reason for Exclusion
WT#5	Not included in borehole data correlation exercise; not included in DTN: MO9811MWDGFM03.000
UZN holes	Not included in borehole data correlation exercise
c#1, 3	Used c#2 to represent the three-borehole complex
a#1	Used nearby b#1 instead
a#7, NRG #2b	Data upload error
NRG #2a, c, d, NRG #3	Insufficient depth of penetration

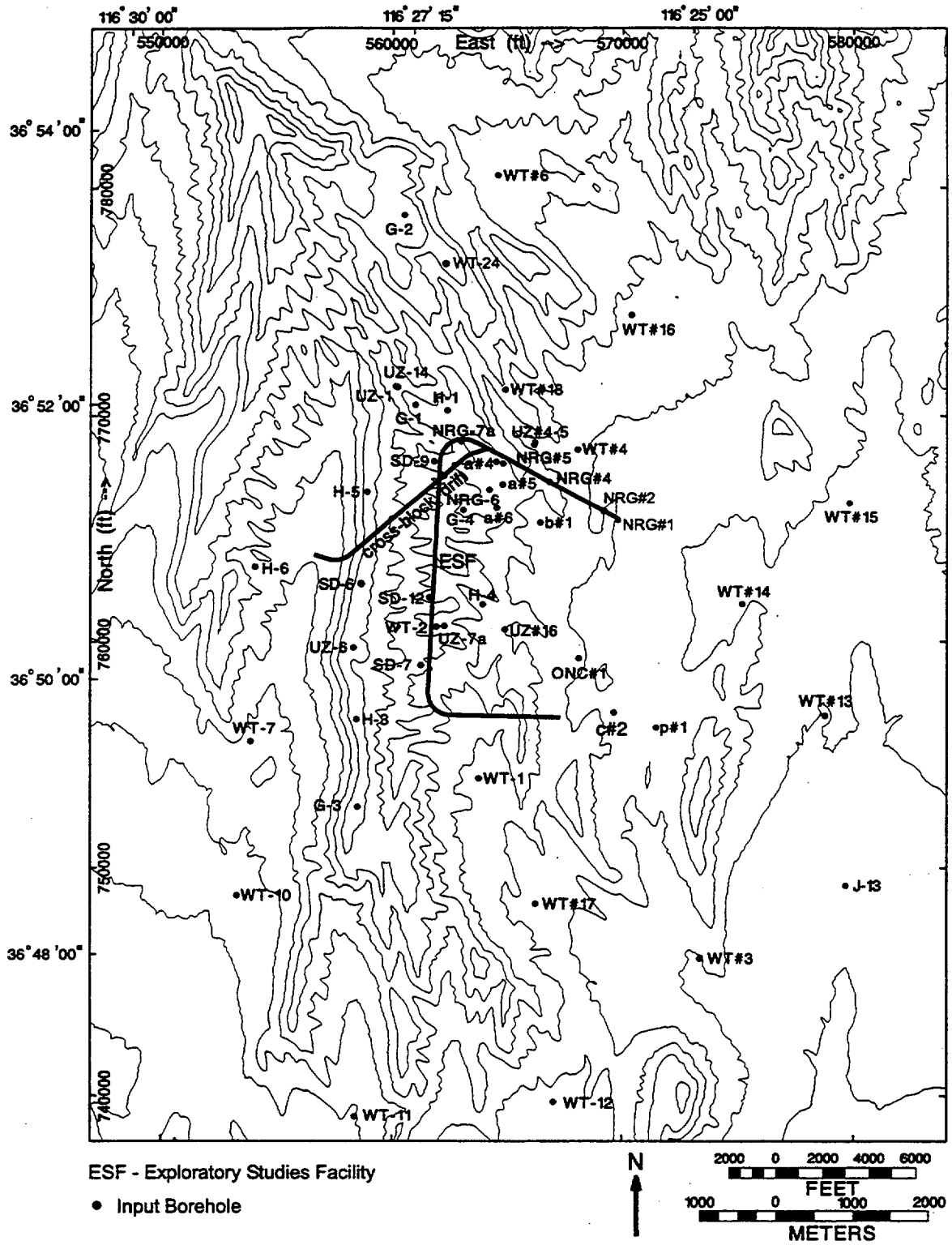

Figure 3. Locations of Boreholes, ESF, and Cross-Block Drift

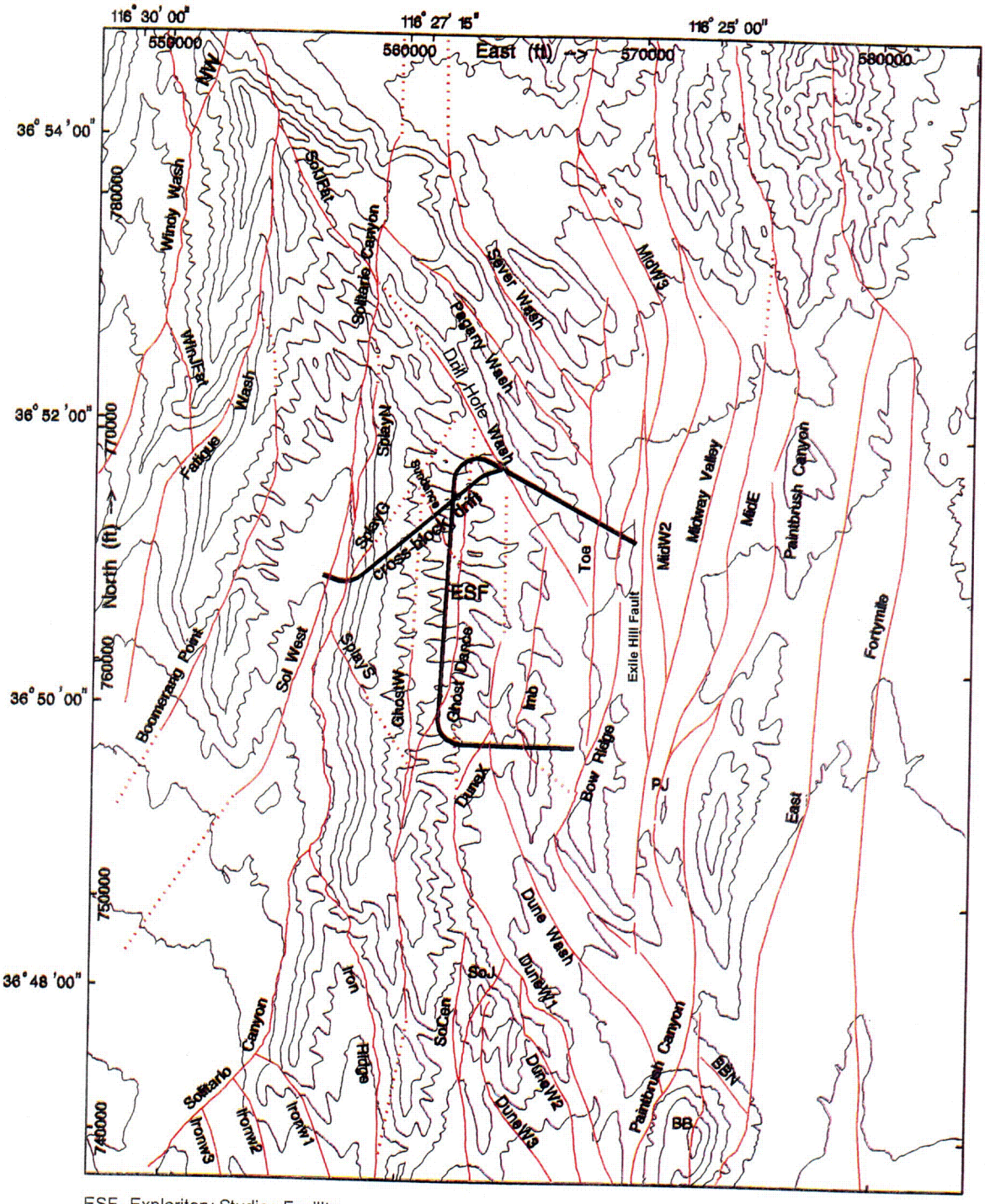

ESF- Exploritory Studies Facility

Fault Trace Inputs Dotted Where Fault is Buried Or Extended

Note: Fault names shown here are for GFM modeling purposes only.

N

2000 0 2000 4000 6000
FEET

1000 0 1000 2000
METERS

Figure 4. Surface Traces of Faults Modeled in GFM

C 001

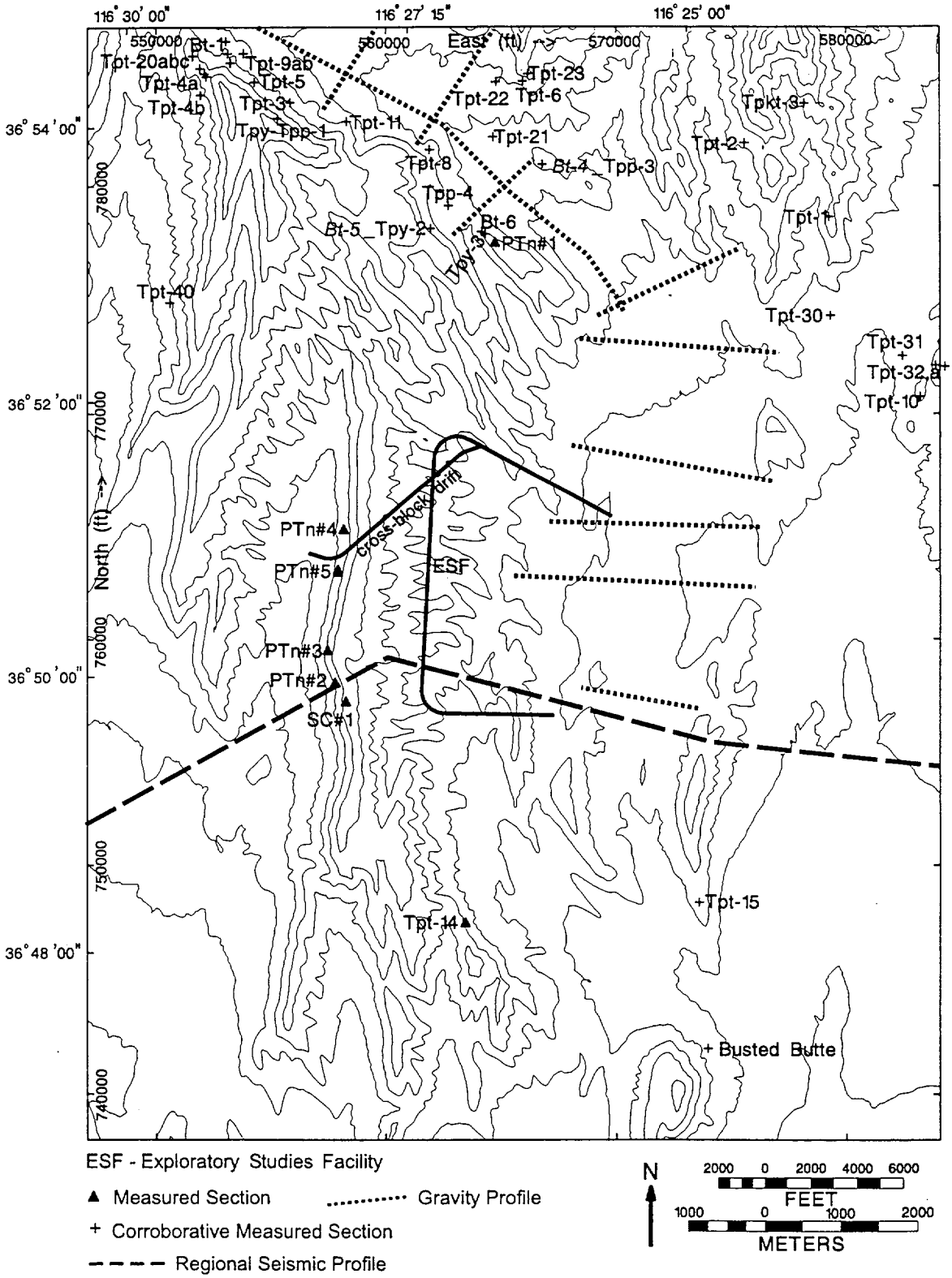

Figure 5. Locations of Measured Sections, Gravity Profiles, and Seismic Profiles

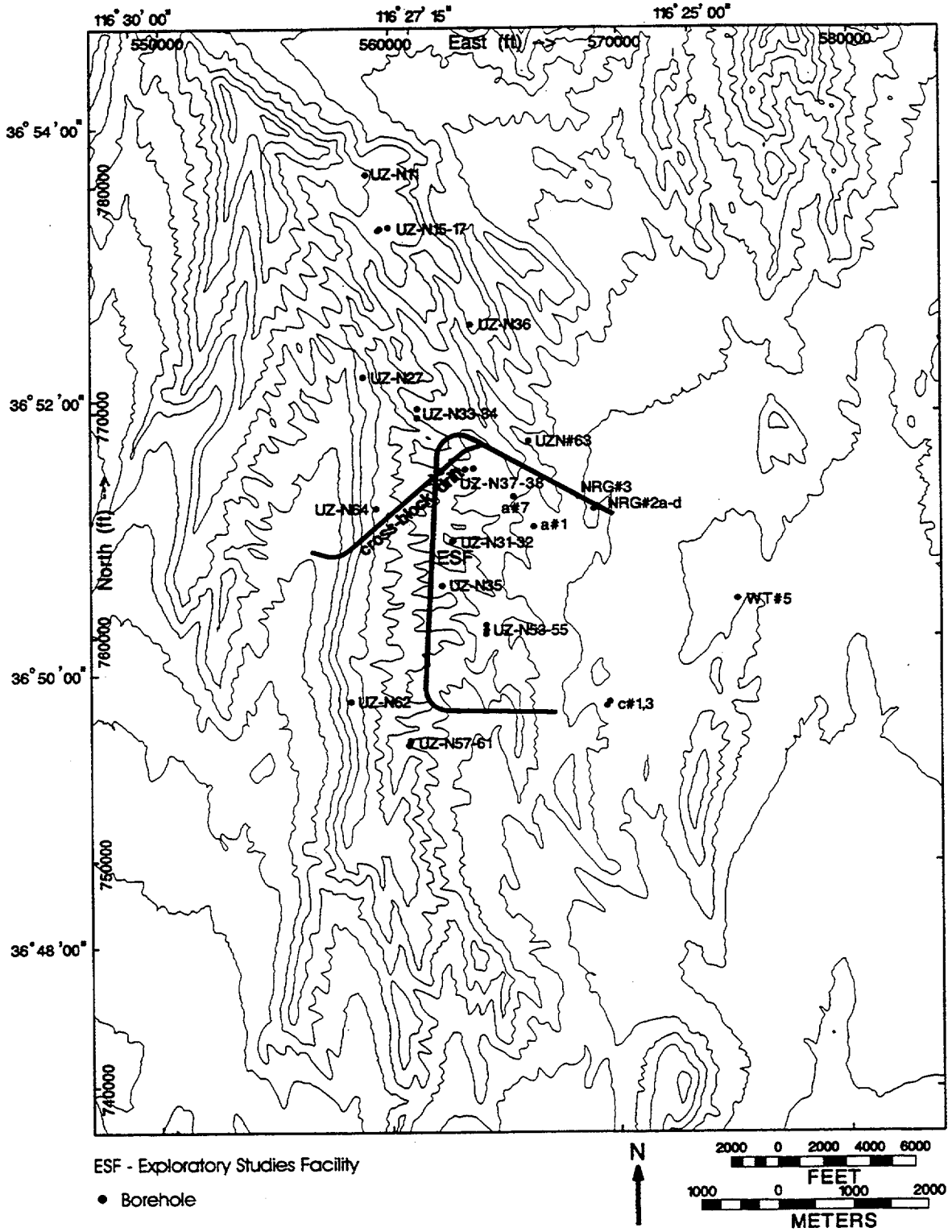

Figure 6. Locations of Boreholes Not Used in the GFM

The basic inclusion criterion for borehole data was correlation. Data correlation is a comparison and adjustment of all data to a common standard. In this case, the common standard was the geophysical logs because they are the most widely available data among the boreholes. All available borehole data were considered in determining the stratigraphic contacts, but the geophysical logs were used as the primary data set.

The data correlation task performed by the GFM modeling group was deemed essential to the technical quality of a geologic model because it establishes consistency throughout the input data set and reduces uncertainty in the model. When input data are correlated, the results of the model can be confidently interpreted in terms of geologic factors. When input data are not correlated, the results of the model are more difficult to interpret because the source of variability is unknown. Uncorrelated data add an unacceptable amount of uncertainty to the model when compared to the value added.

A data correlation activity was the basis for most of the input borehole data (DTN: MO9811MWDGFM03.000), but all data were not included in the correlation activity. The 23 UZN boreholes were excluded from the GFM because they were not included in the data correlation activity. Only 10 of the UZN boreholes provide information on the modeled stratigraphic units, and only 6 of those boreholes penetrate below the pre-Tiva Canyon Tuff bedded tuff. The deepest unit penetrated by the UZN boreholes is in the upper Topopah Spring Tuff, unit Tptrn. The UZN boreholes were used, however, to infer the thickness of alluvium, which is not sensitive to correlation by geophysical logs. Comparison of Figure 6 and Figure 3 shows that the UZN boreholes are all located near deeper boreholes, so that the impact of excluding them is minimized.

The difference between rock layer thicknesses in the GFM and the thicknesses in the UZN data are shown in Attachment III. The table was calculated by subtracting the thicknesses in the GFM from the recorded data (DTN: MO9811MWDGFM03.000). The table shows two important conclusions. First, most of the differences are small. Second, closely spaced UZN boreholes sometimes have differences in thickness that would be difficult to capture in a model of the size and scale of the GFM. The differences between the closely spaced boreholes are difficult to verify without data to correlate to other boreholes (geophysical logs), and so the origins of the differences are uncertain. For these reasons, exclusion of the UZN boreholes is anticipated to have little to no impact on downstream users of the GFM.

In addition to correlation, the geophysical logs are valuable for verifying input data when questions arise during modeling. Using the geophysical logs, anomalous data were re-examined and verified during construction of the GFM to provide confidence in the model. Where geophysical logs are not available for correlation and contact verification, as is the case for the UZN holes, the data were not input to the model. Additional contacts excluded from the model because geophysical logs are not available are listed in Attachment II.

In certain instances where the uncorrelated data were determined to be critical to constraining the subsurface over a large area of the model, an exception was made. Specifically, data from borehole H-6 were needed to constrain units Tpcpv3 and Tpbt4, even though the data are not based on geophysical logs, because these data are the only constraints for these units over a large area.

Faulting and small-scale stratigraphic variations can cause abrupt elevation or thickness variations of units between closely spaced boreholes. Three groups of closely spaced boreholes are within the model boundaries; these are boreholes a#1 and b#1; c#1, c#2, and c#3; and UZ-1 and UZ-14. Because small-scale features are not intended to be represented in a model of the size and scale of the GFM, one borehole was selected from each of the closely-spaced groups. Borehole b#1 was chosen instead of a#1 because it has a more complete geophysical log suite than borehole a#1. Borehole c#2 was chosen because of its higher quality geophysical log signatures, although any of the c-holes could have been used. The geophysically logged intervals of UZ-1 and UZ-14 were used as input, even though they are very close together, because they do not overlap stratigraphically. The unit thicknesses for the unused boreholes (a#1, a#7, c#1, and c#3) (DTN: MO9811MWDGFMN03.000) compared with GFM predictions are presented in Attachment IV.

In gridding, closely spaced borehole data that have disparate elevations can cause unintended flexure of the grid and incorrect model output. The flexure is caused by abruptly different elevations calculated for the grid nodes nearest each borehole, and can affect the grid for hundreds of feet around the boreholes. Figure 7 shows the c-holes, faults, and the actual grid nodes used in the GFM for all surfaces. The three boreholes are separated by faults which are too small to meet the model inclusion criteria. Because the calculated value of unit thicknesses at each grid node is influenced most strongly by the nearest borehole, adjacent grid nodes at the c-hole complex can have abruptly different values and produce unintended model results.

Additionally, boreholes a#7 and NRG #2b were not properly uploaded into EARTHVISION and were thus inadvertently omitted. The impact of omitting borehole a#7 is illustrated in Attachment V, which shows that all model unit thicknesses were closely predicted by the GFM. The impact of omitting borehole NRG#2b is minimal because the borehole only penetrates as deep as model unit Tpbt2 and is near several other boreholes (see Figures 3 and 6).

During the modeling process, the borehole input data (DTN: MO9811MWDGFM03.000) were reexamined and 14 values were corrected. The affected data are in the PTn stratigraphic interval in boreholes H-4, H-5, and H-6. Additionally two data entry errors were also corrected—Tptrl in SD-7 and Tptf in WT#4. The corrected data are in the GFM3.1 model files (DTN: MO9901MWDGFM31.000 in the file named "pix99el.dat").

6.1.2 Selection of Faults

Criteria were developed to determine which mapped faults would be included in the GFM. Due to the large number of faults in the modeled area and limitations in modeling technology, guidelines are needed to select the faults that can realistically be modeled. The fault selection guidelines presented herein were determined by a group of subject matter experts from the USGS, M&O, Sandia National Laboratories, and Lawrence Berkeley National Laboratory in an informal 1995 workshop. These experts determined the fault selection criteria needed to meet both the requirements of model users and provide a level of detail that was technically feasible to model while providing an adequate representation of the structure of Yucca Mountain. This workshop was informal, and as such was not documented. In general if no downstream users needed a fault and omitting the fault did not adversely affect the GFM, the fault was not modeled. In consideration of the impact that faults may have on repository design, more stringent criteria were developed for the potential repository area in the vicinity of the ESF. Inclusion criteria for faults in the GFM are provided in the following lists.

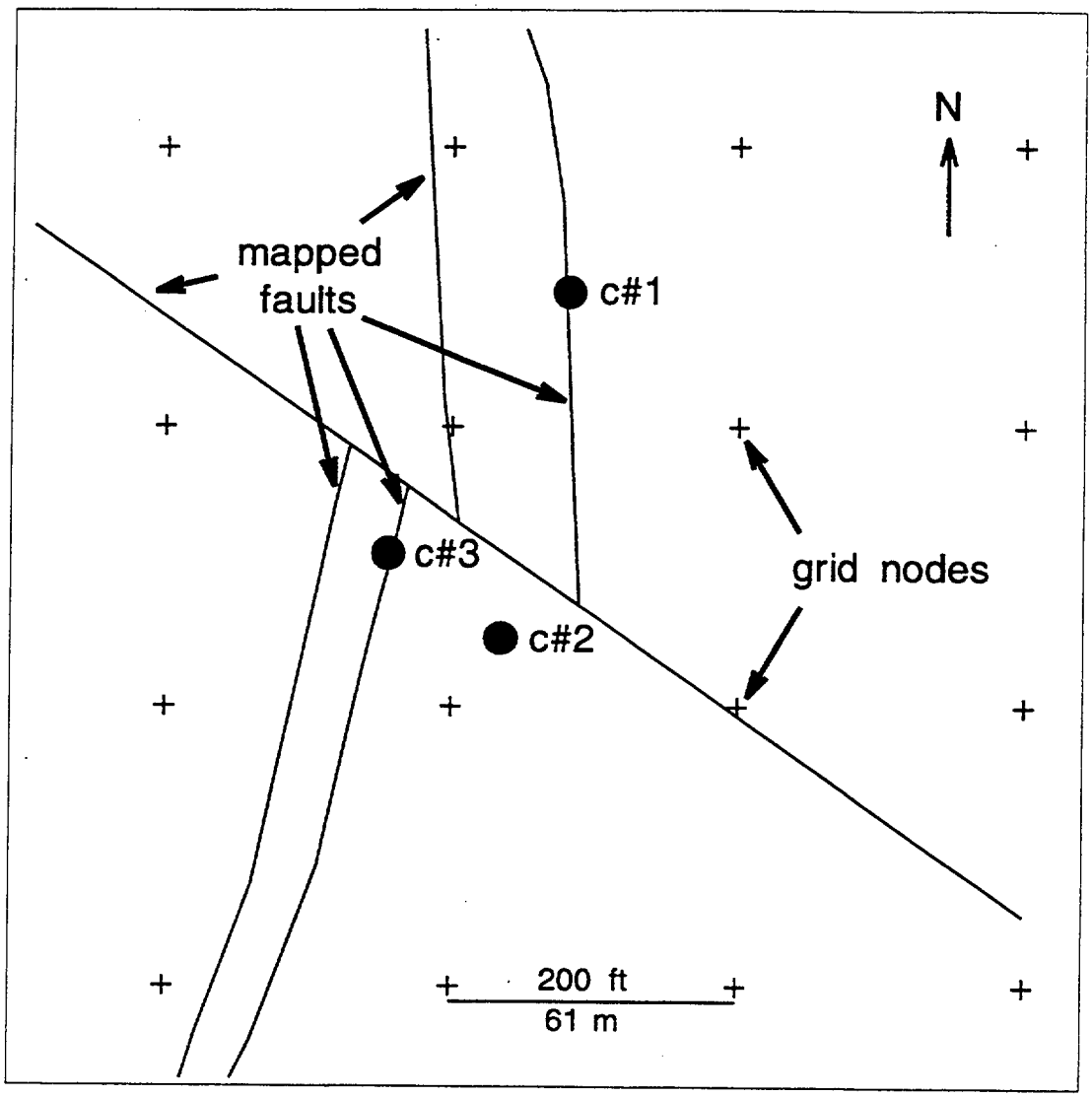

Locations of c-holes

Figure 7. Map Showing the C-Hole Complex, Mapped Faults, and Grid Nodes

In the vicinity of the ESF, the potential repository area (the area bounded by the Solitario Canyon fault, the northward projection of the Dune Wash fault, and the westward projections of the ESF north and south ramps):

- The mapped trace length is 1 mile (1.6 kilometer) or greater.

and

- The maximum vertical displacement is at least 100 feet (30 meters).

or

- The mapped fault intersects with the ESF or cross-block drift.

Outside the vicinity of the ESF:

- The mapped trace length is 2 miles (3.2 kilometers) or greater.

and

- The maximum vertical displacement is at least 100 feet (30 meters).

or

- Omitting the fault would produce an unacceptable mismatch between the model and the geologic map.

The locations of fault traces (Figure 4) were established by the geologic map of the site area (DTN: GS970808314221.002). Fault displacements were estimated from borehole data (DTN: MO9811MWDGFM03.000) and the geologic map. Fault displacements and geometries were iterated during technical reviews of each model iteration to incorporate feedback from YMP scientists.

An additional fault was added beneath Fortymile Wash, as shown on Figure 4, to account for geometric relations between outcrop data and boreholes WT#13, WT#15, and J-13. Location and extent of this fault have a high degree of uncertainty which increases towards the south. Interpretation of gravity and magnetic data in Fortymile Wash indicates that faults beneath the wash, if present, have vertical displacements that are small compared to the Paintbrush Canyon fault (Ponce et al. 1992, pp 6-7). The fault modeled in the GFM has a displacement of about 100 feet (30 meters), which although not directly supported by these interpretations is not in conflict with them.

6.2 MODEL DEVELOPMENT (GFM1.0 TO GFM3.1)

As of the preparation of this report, GFM3.1 was the most current version of the GFM. Each revision improved on the previous version and incorporated new data. Figure 8 summarizes the changes between model versions. The following subsections describe the changes from version to version.

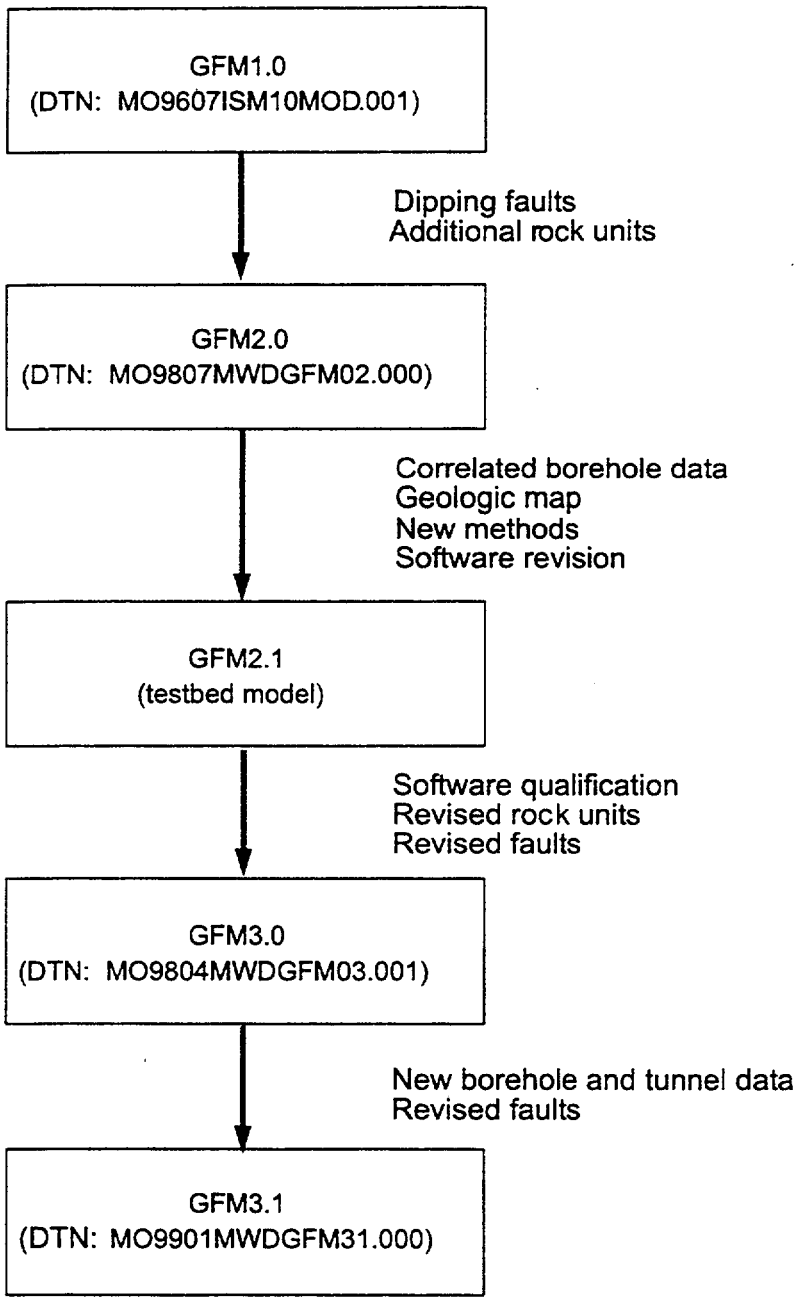

Figure 8. Changes Between GFM Versions

6.2.1 Changes From GFM1.0 to GFM2.0

GFM1.0 (DTN: MO96071SM10MOD.001) provided an initial portrayal of the geoloic framework, with simplified fault geometry. GFM2.0 (DTN: MO9807MWDGFM02.000) improved on GFM1.0 by the inclusion of dipping faults and additional rock units.

6.2.2 Changes From GFM2.0 to GFM3.0

The primary difference between GFM3.0 (DTN: MO9804MWDGFM03.001) and its predecessor (GFM2.0) was use of the bedrock geologic map of the Yucca Mountain area (DTN: GS970808314221.002) and a set of correlated and standardized borehole lithostratigraphic data (DTN: MO9811MWDGFM03.000). The geologic map provided wider, more accurate data coverage than was previously available for the construction of faults, reference horizons, and model-isochores. The GFM adapts the isochore method described in Section 6.3, Methodology, for use in model construction units which are constructed using this methodology are referred to as model-isochores in this report. The number of rock layers modeled also increased to meet the needs of model users.

All model-isochores and reference horizons were reconstructed on the basis of the new borehole and map data so that each rock layer in GFM3.0 was changed from that in GFM2.0. The Tertiary-Paleozoic unconformity (top of Paleozoic) was also recalculated using the new gravity-based Paleozoic surface in DTN: LB980130123112.003.

In the transition from GFM2.0 to GFM3.0, an interim GFM was constructed. This version (GFM2.1) was used as a test bed for modeling parameters and methods. Because GFM2.1 used preliminary input data and the software (EARTHVISION, Version 4.0) had not yet been qualified, GFM2.1 was neither qualified nor circulated to other modelers for use. Details of modeling are discussed in the scientific notebooks for GFM2.1 (Clayton 1998a) and GFM3.0 (Clayton 1998b).

GFM2.1 was used to derive many of the methods described in this text and used to develop GFM3.0 and GFM3.1. The major improvements in GFM2.1 that were incorporated in all later model versions are described in the following subsections.

6.2.2.1 Gridding

Gridding (the process of calculating a surface to pass through input data) was improved by iterative experiment. Grids were constructed first with the use of field data (as listed in Section 4.1) and then with the addition of interpretive constraints, based on the conceptual model described in Section 6.3.1, to produce the final grids and prevent unreasonable extrapolations. Interpretive constraints are illustrated in Figure 9 (see Section 6.3.2.2), which shows the input data and interpretive constraints for the thickness of the Pah Canyon Tuff (Tpp). Interpretive constraints were placed only where needed to prevent unreasonable extrapolations. In GFM2.1, it was found that distributing interpretive constraints evenly across the model area and locating them at least five grid nodes (1,000 feet (300 meters)) away from field data produce grids that both honor the field data more closely and yield internally consistent results. This method eliminated grid anomalies that were present in previous model versions.

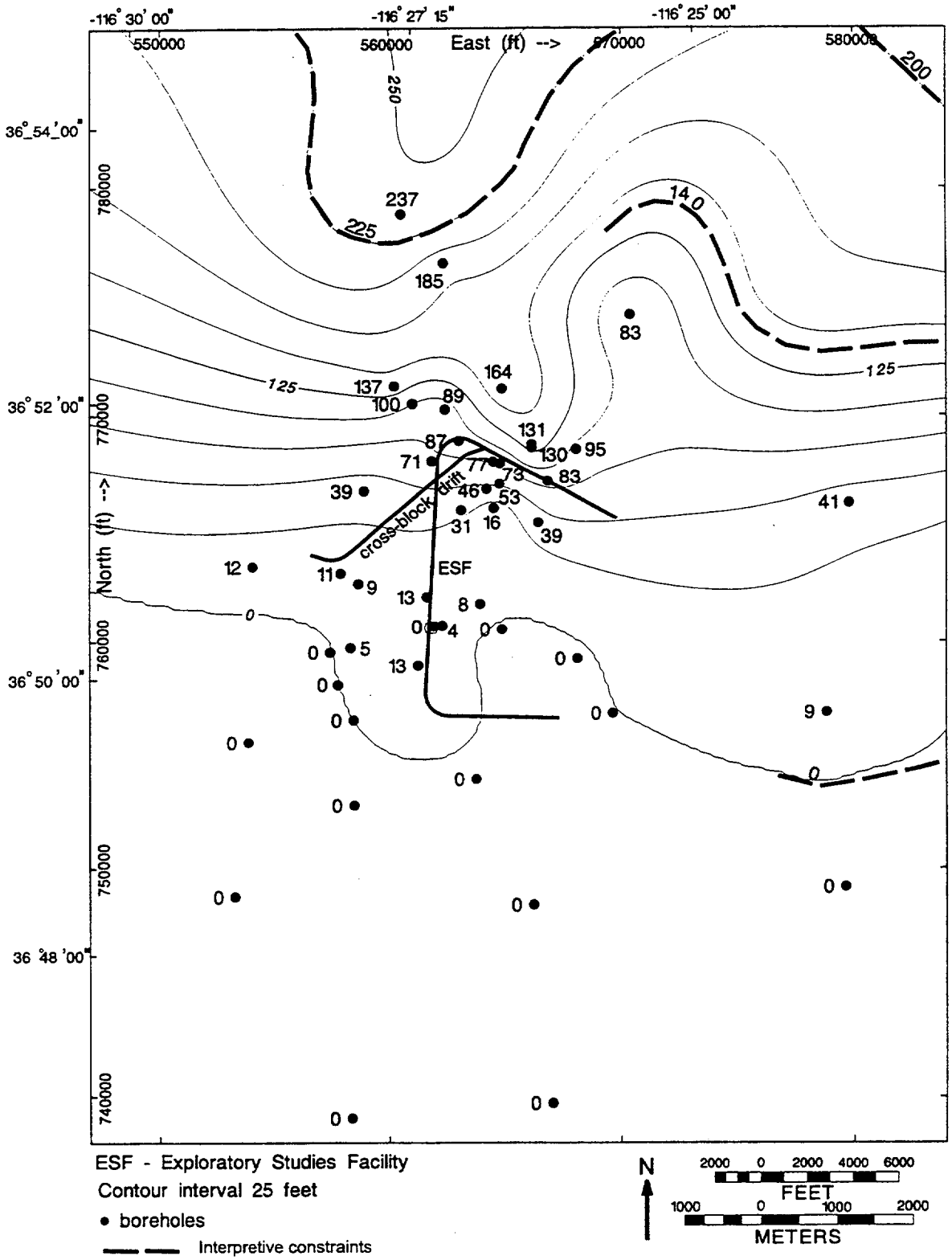

Figure 9. Interpretive Constraints

6.2.2.2 Grid Node Spacing

Iterative testing of possible grid node spacings conducted during the normal course of modeling indicated that a grid node spacing of 200 feet was sufficient to accurately represent the input data and provide output comparable to the 100-foot (30-meter) spacing of earlier model versions. At greater intervals, closely spaced borehole or map data are not honored sufficiently well to preserve the detail of thin rock units, which are in some cases 2 to 5 feet (1 to 2 meters) thick and therefore sensitive to the averaging of data during gridding. The 200-foot (61-meter) grid spacing allowed faster computation times and more iterations, which resulted in higher quality model results.

6.2.2.3 Reference Horizon

A reference horizon establishes the elevation, shape, and fault displacement of all horizons that are added to or subtracted from it. In GFM2.1, iterative experiment showed that reference horizons can be placed at the top, middle, and bottom of the stratigraphic sequence to adequately control fault displacements so that the displacements remain relatively constant with depth. This method improved the consistency of fault displacements over previous model versions, which used only one reference horizon at the top of the stratigraphic section.

6.2.2.4 Geologic Map

The bedrock geologic map of the Yucca Mountain area (DTN: GS970808314221.002) was first used as input data in GFM2.1. It was demonstrated in this interim model version that the map in digital format could be used directly in the modeling process. The geologic map was shown to be consistent with borehole, tunnel, and other data used in the GFM.

6.2.2.5 Data File Isolation

To prevent inadvertent changes, field data were kept physically isolated from interpretive constraints by the maintenance of separate electronic files. Such a data separation also allows field data to be given priority over interpretive constraints during the gridding process by means of tools within the modeling software. This is done by first gridding the field data plus interpretive constraints and then shifting the grid to explicitly match the field data (without the interpretive constraints). Grids constructed by this method more closely honor field data, while implementing the appropriate geologic concepts.

6.2.2.6 Solitario Canyon Fault

In GFM2.0, the Solitario Canyon fault was constructed as two separate fault plane surfaces (grids) joined at Tonsil Ridge, one surface dipping east and the other dipping west. In GFM3.0, however, the Solitario Canyon fault was constructed as a single surface. From Tonsil Ridge north, the fault plane has a nearly vertical westward dip, although the map indicates a steep eastward dip. This simplification was made because a fault plane that dips in two directions cannot be constructed using a rectilinear grid, which must cover the entire model area and contain no gaps or nulls. It was concluded that the two-surface approach used in GFM2.0

created geometries, at the depth where the surfaces intersected, that were more problematic technically and geologically than those created by the single-surface approach used in GFM3.0.

Changes From GFM3.0 to GFM3.1

GFM3.1 was constructed to incorporate new data from boreholes SD-6 (DTN: SNF40060298001.001) and WT-24 (DTN: SNF40060198001.001) and the cross-block drift excavated during the Enhanced Characterization of the Repository Block (ECRB) (DTN: GS981108314224.005). Figure 3 shows the locations of boreholes SD-6 and WT-24 and the ECRB cross-block drift. In addition, GFM3.1 includes an additional fault (from DTN: GS970808314221.002), which is located at the Prow (Figure 1) and is designated *NW* on Figure 4. The new fault was included to properly model the Calico Hills Formation and Prow Pass Tuff outcrops.

GFM3.1 was constructed with more curvature on the dominant faults to be consistent with cross sections published with the bedrock geologic map of the Yucca Mountain area (DTN: GS970808314221.002) and to account for field relations showing rotated hanging wall strata (CRWMS M&O 1998b, p. 3.6-6). The revised geometries include a slight decrease in fault dip with depth, resulting in fault planes that are slightly concave-upward to account for field relations. Planes of minor faults are depicted as planar.

6.3 METHODOLOGY

The GFM was constructed in the following general steps, which are discussed in Scientific Notebook SN-M&O-SCI-008-V1 (Clayton 1999, pp 7-23):

1. Development of grid construction and contouring methodology
2. Construction of faults
3. Construction of reference horizons
4. Construction of model-isochores
5. Assembly of faults and rock layers
6. Assessment and iteration.

Table 5 presents the correlation between the stratigraphic units modeled in the GFM and the YMP stratigraphy (DTN: MO9510RIB00002.004). Most of the GFM units correlate with the YMP stratigraphy; however, two nonstratigraphic units were included in the model because of their significance for users of the model—a *low-density zone* (TpcLD) and the *Repository Host Horizon* (RHH). The TpcLD occurs above the Tiva Canyon Tuff lower vitric units (Tpcpv3 and Tpcpv2). The RHH is the body of rock in which the potential repository is proposed to be excavated (CRWMS M&O 1997, pp. 43–50). It spans four lithostratigraphic zones (the lower part of the Tptpul, Tptpmn, Tptpll, and Tptpln). The model unit designated as RHHtop is within the lower part of the Topopah Spring Tuff upper lithophysal zone (Tptpul). This RHHtop unit is defined by a density log signature intermediate between the remainder of the upper lithophysal zone above and the middle nonlithophysal zone below. The RHH includes model units RHHtop, Tptpmn, Tptpll, and Tptpln.

Table 5. Correlation Chart for Model Stratigraphy

Stratigraphic Unit (Group / Formation / Member / Zone / Subzone)	Abbreviation[a]	RHH[b]	Geologic Framework Model Unit
Alluvium and Colluvium	Qal, Qc		Alluvium
Timber Mountain Group	Tm		
Rainier Mesa Tuff	Tmr		
Paintbrush Group	Tp		
Post-tuff unit "x" bedded tuff	Tpbt6		
Tuff unit "x"[c]	Tpki (informal)		
Pre-tuff unit "x" bedded tuff	Tpbt5		
Tiva Canyon Tuff	Tpc		
Crystal-Rich Member	Tpcr		
Vitric zone	Tpcrv		
Nonwelded subzone	Tpcrv3		
Moderately welded subzone	Tpcrv2		
Densely welded subzone	Tpcrv1		
Nonlithophysal subzone	Tpcrn		
Subvitrophyre transition subzone	Tpcrn4		
Pumice-poor subzone	Tpcrn3		
Mixed pumice subzone	Tpcrn2		
Crystal transition subzone	Tpcrn1		
Lithophysal zone	Tpcrl		Tiva and
Crystal transition subzone	Tpcrl1		Post-Tiva
Crystal-Poor Member	Tpcp		
Upper lithophysal zone	Tpcpul		
Spherulite-rich subzone	Tpcpul1		
Middle nonlithophysal zone	Tpcpmn		
Upper subzone	Tpcpmn3		
Lithophysal subzone	Tpcpmn2		
Lower subzone	Tpcpmn1		
Lower lithophysal zone	Tpcpll		
Hackly-fractured subzone	Tpcpllh		
Lower nonlithophysal zone	Tpcpln		
Hackly subzone	Tpcplnh		
			Tpcp
Columnar subzone	Tpcplnc		TpcLD
Vitric zone	Tpcpv		
Densely welded subzone	Tpcpv3		Tpcpv3

Table 5. Correlation Chart for Model Stratigraphy (Continued)

Stratigraphic Unit					Abbreviation[a]	RHH[b]	Geologic Framework Model Unit
Group	Formation	Member	Zone	Subzone			
				Moderately welded subzone	Tpcpv2		Tpcpv2
				Nonwelded subzone	Tpcpv1		Tpcpv1
		Pre-Tiva Canyon bedded tuff			Tpbt4		Tpbt4
	Yucca Mountain Tuff				Tpy		Yucca
		Pre-Yucca Mountain bedded tuff			Tpbt3		Tpbt3_dc[d]
	Pah Canyon Tuff				Tpp		Pah
		Pre-Pah Canyon bedded tuff			Tpbt2		Tpbt2
	Topopah Spring Tuff				Tpt		
		Crystal-Rich Member			Tptr		
			Vitric zone		Tptrv		
				Nonwelded subzone	Tptrv3		Tptrv3
				Moderately welded subzone	Tptrv2		Tptrv2
				Densely welded subzone	Tptrv1		Tptrv1
			Nonlithophysal zone		Tptrn		
				Dense subzone	Tptrn3		
				Vapor-phase corroded subzone	Tptrn2		
				Crystal transition subzone	Tptrn1		Tptrn
			Lithophysal zone		Tptrl		
				Crystal transition subzone	Tptrl1		Tptrl
		Crystal-Poor Member			Tptp		
			Lithic-rich zone		Tptpf or Tptrf		Tptf
							Tptpul
			Upper lithophysal zone		Tptpul	RHH	RHHtop
			Middle nonlithophysal zone		Tptpmn		
				Nonlithophysal subzone	Tptpmn3		
				Lithophysal bearing subzone	Tptpmn2		
				Nonlithophysal subzone	Tptpmn1		Tptpmn
			Lower lithophysal zone		Tptpll		Tptpll
			Lower nonlithophysal zone		Tptpln		Tptpln
			Vitric zone		Tptpv		
				Densely welded subzone	Tptpv3		Tptpv3
				Moderately welded subzone	Tptpv2		Tptpv2
				Nonwelded subzone	Tptpv1		Tptpv1
		Pre-Topopah Spring bedded tuff			Tpbt1		Tpbt1
	Calico Hills Formation				Ta		Calico
		Bedded tuff			Tacbt		Calicobt

Table 5. Correlation Chart for Model Stratigraphy (Continued)

Stratigraphic Unit					Abbreviation[a]	RHH[b]	Geologic Framework Model Unit
Group	Formation	Member	Zone	Subzone			
Crater Flat Group					Tc		
	Prow Pass Tuff				Tcp		
			Prow Pass Tuff upper vitric nonwelded zone		(Tcpuv)[e]		Prowuv
			Prow Pass Tuff upper crystalline nonwelded zone		(Tcpuc)[e]		Prowuc
			Prow Pass Tuff moderately-densely welded zone		(Tcpmd)[e]		Prowmd
			Prow Pass Tuff lower crystalline nonwelded zone		(Tcplc)[e]		Prowlc
			Prow Pass Tuff lower vitric nonwelded zone		(Tcplv)[e]		Prowlv
		Pre-Prow Pass Tuff bedded tuff			(Tcpbt)[e]		Prowbt
	Bullfrog Tuff				Tcb		
			Bullfrog Tuff upper vitric nonwelded zone		(Tcbuv)[e]		Bullfroguv
			Bullfrog Tuff upper crystalline nonwelded zone		(Tcbuc)[e]		Bullfroguc
			Bullfrog Tuff welded zone		(Tcbmd)[e]		Bullfrogmd
			Bullfrog Tuff lower crystalline nonwelded zone		(Tcblc)[e]		Bullfroglc
			Bullfrog Tuff lower vitric nonwelded zone		(Tcblv)[e]		Bullfroglv
		Pre-Bullfrog Tuff bedded tuff			(Tcbbt)[e]		Bullfrogbt
	Tram Tuff				Tct		
			Tram Tuff upper vitric nonwelded zone		(Tctuv)[e]		Tramuv
			Tram Tuff upper crystalline nonwelded zone		(Tctuc)[e]		Tramuc
			Tram Tuff moderately-densely welded zone		(Tctmd)[e]		Trammd
			Tram Tuff lower crystalline nonwelded zone		(Tctlc)[e]		Tramlc
			Tram Tuff lower vitric nonwelded zone		(Tctlv)[e]		Tramlv
		Pre-Tram Tuff bedded tuff			(Tctbt)[e]		Trambt
		Lava and flow breccia (informal)			Tll		
		Bedded tuff			Tllbt		
	Lithic Ridge Tuff				Tr		
		Bedded tuff			Tlrbt		
		Lava and flow breccia (informal)			Tll2		
		Bedded tuff			Tllbt		

Table 5. Correlation Chart for Model Stratigraphy (Continued)

Stratigraphic Unit						Abbreviation[a]	RHH[b]	Geologic Framework Model Unit
Group	Formation	Member	Zone	Subzone				
		Lava and flow breccia (informal)				Tll3		
		Bedded tuff				Tll3bt		
		Older tuffs (informal)				Tt		
			Unit a (informal)			Tta		
			Unit b (informal)			Ttb		
			Unit c (informal)			Ttc		
		Sedimentary rocks and calcified tuff (informal)				Tca		
		Tuff of Yucca Flat (informal)				Tyf		Tund
Pre-Tertiary sedimentary rock								
	Lone Mountain Dolomite					Slm		
	Roberts Mountain Formation					Srm		Paleozoic

NOTES: Shaded rows indicate header lines for subdivided units.
RHH = Repository Host Horizon
[a] Source: DTN: MO9510RIB00002.004
[b] Source: CRWMS M&O 1997, pp. 43–50.
[c] Correlated with the rhyolite of Comb Peak (Buesch et al. 1996, Table 2).
[d] Includes rhyolite of Delirium Canyon north of Yucca Wash (DTN: GS970808314221.002).
[e] For the purposes of GFM3.1, each formation in the Crater Flat Group was subdivided into six zones based on the requirements of the users of the Geologic Framework Model. The subdivisions are upper vitric (uv), upper crystalline (uc), moderately to densely welded (md), lower crystalline (lc), lower vitric (lv), and bedded tuff (bt) (Buesch and Spengler 1999, pp. 62-64).

The GFM stratigraphy was constructed by the thickness (or isochore) method, which consists of adding or subtracting (as appropriate) thicknesses from one or more reference horizons as illustrated in Figure 10. An *isochore* represents the thickness of a geologic unit in the vertical direction, regardless of dip. This contrasts with an *isopach*, which is thickness of a unit measured perpendicular to bedding. Because the structural dips at Yucca Mountain are low (generally less than 10 degrees), an isochore is nearly identical to an isopach. This method was chosen for several reasons:

- In volcanic units, thickness tends to be systematically distributed over large areas as a function of factors including magma type, eruptive processes, wind speed and direction, pre-existing topography, and erosion. Thicknesses directly reflect these processes and can, therefore, be constructed with the use of those processes as guides.

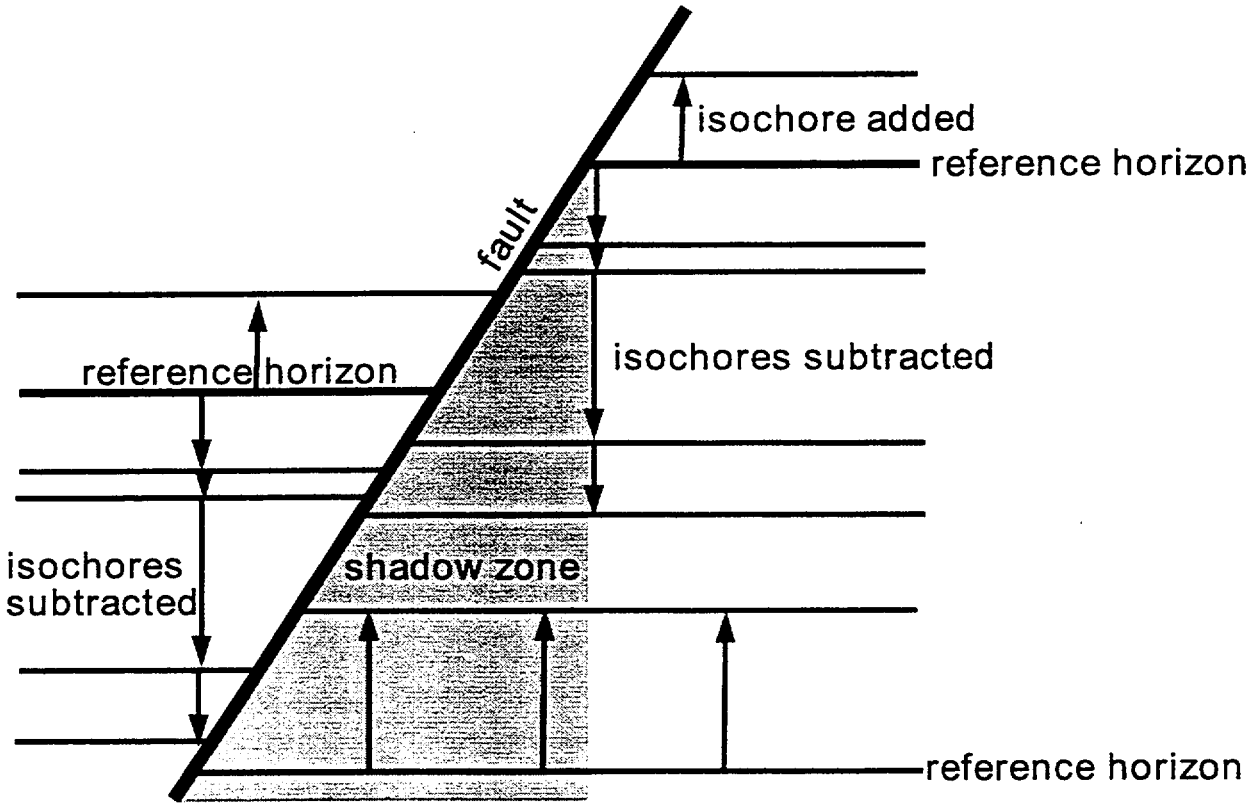

NOTE: Isochores are added or subtracted from reference horizons to assemble the rock units in the model. Because the process does not cross faults, a shadow zone develops beneath dipping faults.

Figure 10. Isochore Method

- Because the volcanic strata at Yucca Mountain consist of many units that pinch out, are very thin, and/or have highly variable thicknesses (creating highly variable differences between the elevations of stratal tops and bottoms), the use of model-isochores prevents the top and bottom grids from intersecting unintentionally.

- Construction of stratigraphy by model-isochores results in fewer thickness anomalies than the construction of each surface as an elevation grid.

Isochores are derived from the borehole contacts data by subtracting the bottom contact elevation of a rock unit from the top elevation. When the model is assembled, the isochores are tied to the elevations of the reference horizons, and all borehole contacts data are honored by the model.

The drawback of the isochore method is the possible generation of unintended surface undulations; however, none of significance has been noted in GFM3.1. Another potential drawback is development of "shadow zones" beneath dipping faults. As illustrated in Figure 11, the shadow zone develops because the addition or subtraction of isochores from a reference horizon is strictly a vertical process. A reference horizon has no influence from above a fault to below, so that surfaces below the fault are unconstrained. Surfaces in the shadow zone were controlled by the use of reference horizons in the deeper units and building the model-isochores upwards into the shadow zone.

The isochore maps in the following sections may differ from true isochores because they may contain artifacts of the modeling process used in construction of the GFM. For this reason, the maps are referred to as "model-isochores." A true isochore map would not include partial thicknesses caused by faulting, but the model-isochores must in cases where the fault is not included in the model. As illustrated in Figure 11, in a computer-based model around an unmodeled fault, a partial thickness is required during model construction to maintain true elevations of the units above and below. In general, a fault that can not be mapped areally can not be modeled in three dimensions. In addition to the inclusion criteria, for a fault to be included in the model it must have a defined extent, strike, and dip. For a fault which intersects a borehole but is not mapped at the surface, extent, strike, and often dip are unknown. Where an unmapped, unmodeled fault displaces a unit in a borehole, resulting in a partial thickness (not a true stratigraphic thickness) in the borehole, the partial thickness must be used to honor the remaining borehole data as the model is assembled.

The model-isochore maps presented in this report are the maps used to construct the model, and therefore may contain artifacts of the modeling process like partial thicknesses. In this regard, the model and its components including isochore maps, structure maps, and cross sections may differ from results of more traditional analysis of geologic maps.

Additionally, most of the model-isochore maps presented in this report are composites of several model units as shown in Table 5. The composite maps are constructed by adding isochore grids together. The resultant maps may contain artifacts of this additive process, including abrupt contour bends and trends, and closed contours away from data.

6.3.1 GFM Conceptual Models

As discussed in the following sections, interpretive constraints were used to guide the shapes of model-isochores (thickness maps), which are the fundamental building blocks of the GFM. The conceptual model described below was used to formulate the interpretive constraints.

The basic conceptual model used to construct the GFM considers that Yucca Mountain is composed of volcanic rocks deposited from variously located calderas or vent sources (DOE 1998b, p. 2-15). The following principles derived from the conceptual model were applied to construct the GFM:

- Volcanogenic rocks generally thin away from their sources.
- The major deposits in the subsurface at Yucca Mountain generally filled in preexisting topography, so that the top of a formation may be more planar than the base.
- The top of a formation may have eroded after deposition.
- The lower vitric zones of the Topopah Spring and Tiva Canyon Tuffs blanketed preexisting topography and began the process of filling in topographic lows.
- Topopah Spring Tuff lithophysal and nonlithophysal zones were produced by multiple processes and, although approximating a planar geometry, these zones may have irregular thickness distributions.

6.3.2 Overview of GFM3.1 Methodology

The conceptual model was applied to shape each model-isochore between and away from the locations of input data. Where suggested by the data, the conceptual model was applied to extrapolate away from unusually thick and thin data values to provide an internally consistent volumetric representation.

The methodology for constructing GFM3.1 included a combination of mathematical grid construction (gridding) and the application of interpretive constraints. In this way, the model honors the measured data while allowing for interpretations in areas where data are sparse or where a grid generated by the model may initially conflict with the accepted conceptual model.

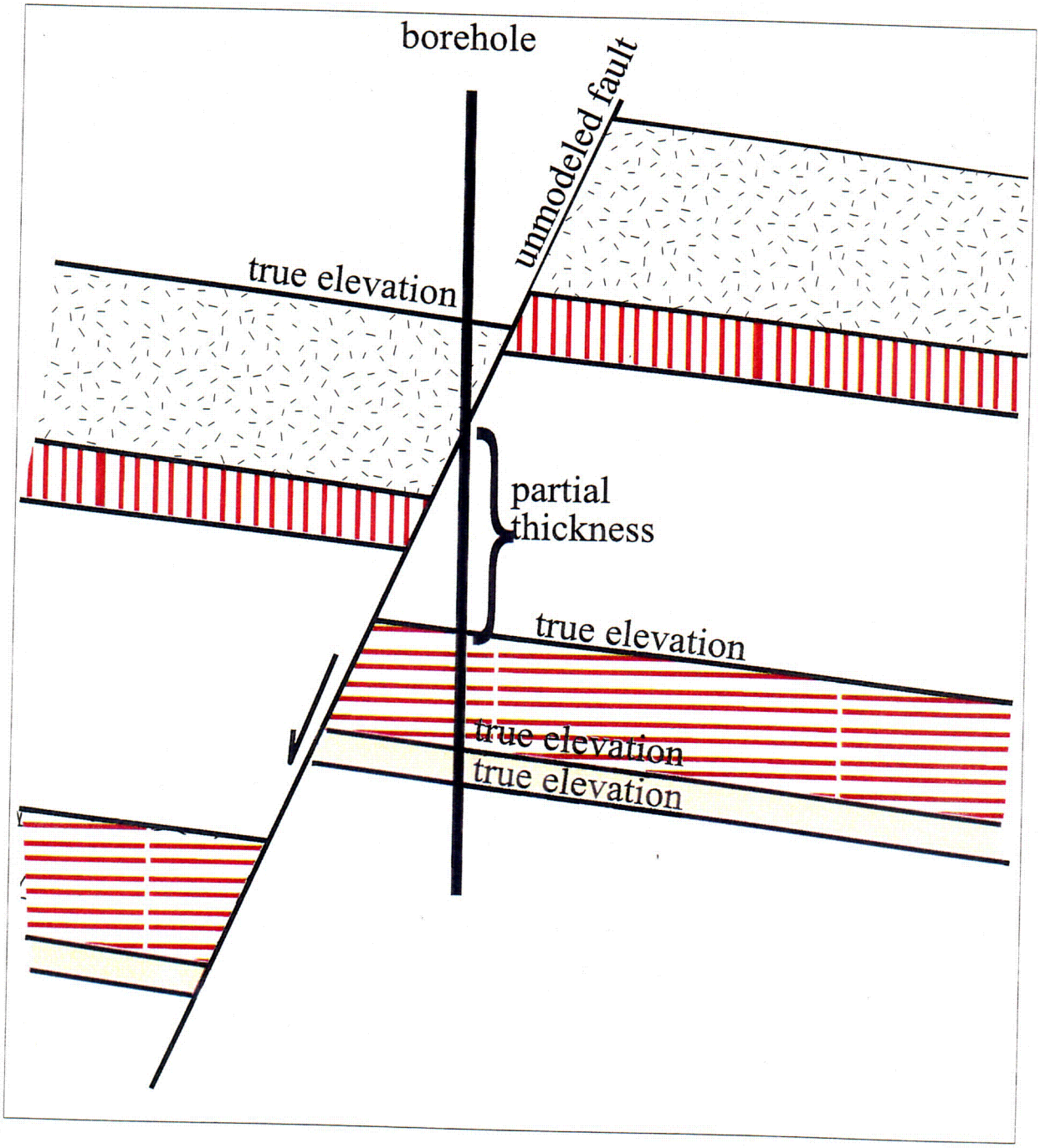

C002

Figure 11. Schematic Cross Section Showing the Relation of Partial Thickness to Model Units

6.3.2.1 Grid Construction

A grid is a systematic array of points, or *nodes*. In three dimensions, a grid forms a surface. Topography is an example of a surface which can be represented by a grid. Gridding is the process of creating a surface (grid) across an area based on widely and variably spaced input data. Many methods (both mathematical and interpretive) are available for use in creating surfaces in a model. Examples include triangulation, hand contouring, linear interpolation, geostatistical methods, and various mathematical algorithms. The gridding method used in the GFM is based on a *minimum tension* mathematical algorithm that calculates a surface passing through the input data and is an option in EARTHVISION. For every grid in the GFM, the minimum tension algorithm is constrained by field data (from boreholes, tunnels, measured sections, or the geologic map) and interpretive constraints in the form of contour segments (discussed in Section 6.3.2.2). Grid node spacing for all grids except topography is 200 by 200 feet (61 by 61 meters). The topographic grid spacing is 100 by 100 feet (30 by 30 meters) to accurately represent details of the ground surface.

In the GFM, the grids represent the geologic surfaces or unit thicknesses (isochores) and are the fundamental building blocks of the model. Grids are created to define fault planes, reference horizons, and model-isochores. For fault planes and reference horizons, each node contains an elevation. For model-isochores, each node contains a thickness value. The advantage of a grid as compared to scattered data is that the grid can be operated on mathematically or can be used to apply mathematical or geologic rules to interpolate a surface between data points.

The minimum tension algorithm produces grids with as few abrupt changes as allowed by the input data, while still honoring all input data. Testing of the minimum tension algorithm during model construction and software qualification (CRWMS M&O 1998f) indicated that it produces internally consistent surfaces which closely honor the input data.

Minimum tension gridding begins with an initial grid estimate in which data around each grid node are sampled to calculate a value for that grid node. In the estimate, only the data nearest to the node are sampled. The data values are averaged using an inverse-distance weighting function, with weighting also dependent on the angular distribution of the data. This weighted average is the initial estimate and includes both interpretive constraints and field data. The initial estimated grid node values are then reevaluated by means of a biharmonic cubic spline function within EARTHVISION. This function serves to distribute curvature across the surface rather than forming sharp flexures at data points. The final step is refitting the grid to the field data (without the interpretive constraints) and one last distribution of curvature by the biharmonic cubic spline function.

6.3.2.2 Interpretive Constraints

As illustrated in Figure 9, interpretive constraints in the form of contour segments inserted into the model were used to control the shapes of grids to insure the appropriate adherence to the conceptual model. The reference horizon, fault, and model-isochore grids in the GFM were calculated with the use of both field data and the interpretive segments. None of the grids represent a purely minimum tension interpretation of field data.

During model development, the following issues associated with the use of interpretive contours in the gridding process were identified, and techniques were developed to correct them:

- Interpretive contours can conflict with gridding mathematics
- Interpretive contours can override input data
- Gridding algorithms can extrapolate unreasonably.

Interpretive constraints can conflict with gridding mathematics when the contours define a shape that does not conform to the underlying equations of the algorithm. If interpretive contours were placed too close together, unintended flexures of the grid resulted when the gridding algorithm was reapplied. Similarly, when interpretive contours were placed too close to input data, the input data were not honored because the grid averaged the interpretive contour values with the input data. A different issue arose when interpretive contours were *not* placed in an area with no data—the algorithm sometimes made unreasonable extrapolations that were inconsistent with geologic interpretations.

A technique was developed to prevent all three problems. It was discovered that the minimum tension algorithm produces the most reasonable, predictable results when the input data and interpretive contours are distributed more or less evenly across the model area. Therefore, interpretive contours were placed only in data gaps and never closer than about five grid nodes (1,000 feet (300 meters)) to input data. The wide distribution of interpretive contours also prevented unreasonable extrapolations. In this way, a balance was struck between the mathematical prediction of the gridding algorithm and the geologic interpretation.

The process for creating grids for faults, reference horizons, and model-isochores consisted of the following steps:

1. The field data were first gridded without any interpretive constraint. These results were analyzed to determine whether interpretive constraints were needed and to choose the most appropriate locations for their use.

2. The grid was then modified by introducing interpretive contours and regridding.

3. The process was iterated until the grid represented the interpretation being applied by the modeler.

6.3.3 Construction of Faults

Grids representing faults were constructed primarily with the use of data from the geologic map, boreholes, and tunnel intercepts. Interpretive contours were calculated to create the proper dip of the fault plane, and the grid was calculated with the use of the field data and interpretive contours. The interpretive contours were then modified as needed to produce the consistent results. Seismic profile data (Brocher et al. 1998, pp. 947-971) were used to confirm the geometries of the Paintbrush Canyon and Solitario Canyon faults and by comparison of the data to a cross section through the model at the same location. High resolution seismic refraction data (Majer et al., 1996) were also used to confirm stratal geometries.

6.3.4 Construction of Reference Horizons and Model-Isochores

In geologic modeling, a reference horizon is an elevation grid that establishes the strike and dip of the rock layers and the displacement of rock layers along faults. Where the grid crosses a fault, the grid is displaced by the appropriate amount. The grid is constructed with the use of data from the geologic map, boreholes, and tunnels. Thicknesses (isochores) of other rock layers are then added to or subtracted from the reference horizon to create the other rock units in the model, as illustrated in Figure 10. The reference horizon and model-isochore grids were constructed by the methods discussed in Section 6.3. In all, three reference horizons were constructed. The reference horizons are:

- Base of Tiva Canyon Tuff
- Top of Calico Hills Formation
- Top of Older Tertiary Unit.

The first reference horizon constructed was at the base of the Tiva Canyon Tuff (top of Tpbt4, the pre-Tiva bedded tuff). This horizon was chosen because it is well constrained by geologic-map and borehole data. It is also a major lithologic break that is readily correlated from one data set to another; thus, the available data are both widespread and consistent. This reference horizon is illustrated in Figure 12, as output from the assembled GFM.

To control the shadow zone effect, illustrated in Figure 10, two more reference horizons were constructed: one at the top of the Calico Hills Formation (Ta) and one at the top of the older Tertiary unit (Tund) (base of the pre-Tram Tuff bedded tuff (Tctbt)). The Calico reference horizon was constructed first by means of the isochore method, building downward from the basal Tiva reference horizon. The Calico reference horizon was then extracted from the resulting model as an elevation grid. This elevation grid was edited to make fault displacements more consistent with the shallower units. The isochore grids for the lower part of the model were then reconstructed, building upward from Calico reference horizon to the Topopah Spring Tuff lower nonlithophysal zone (Tptpln) and downward to the lowest Tertiary unit (defined in the GFM as Tund). Tptpln was chosen as the buffer zone between surfaces built downward and those built upward because of its thickness. Any small elevation changes in the reference horizon would not appreciably affect the thickness of the Tptpll unit.

The deepest reference horizon, the contact between the base of the pre-Tram bedded tuff (Tctbt) and the undifferentiated Tertiary unit (model unit Tund), was constructed in the same way as the Calico reference horizon. Model-isochores were built upward to the Bullfrog Tuff lower crystalline nonwelded zone (Tcblc), again because the unit above was sufficiently thick and would not be appreciably affected by the construction of the reference horizon.

In addition to borehole and geologic map data, the GFM uses tunnel data to establish the elevation of the base-Tiva reference horizon (base of Tpcpv1). To match the elevations of other rock units in the tunnels, the thicknesses of units between Tpcpv1 and the tunnels were adjusted in the GFM. The resulting rock units in the GFM closely match the elevations of rock units in the ESF and ECRB Cross-Block Drift.

The Tertiary-Paleozoic unconformity (Table 3) and the topography (Section 5) were provided as grids and no model-isochore were constructed. The Tpcr/Tpcp boundary was constructed as an elevation grid directly from abundant geologic map data because it is severely eroded in the area and few borehole data are available, making model-isochore mapping impractical.

6.3.5 Assembly of Faults and Rock Layers

The reference horizon grids, model-isochore grids, and fault grids were combined to produce the final model. In the combination, calculations were performed in the EARTHVISION software routines to determine the intersections of faults and rock units, and this information was stored with each grid. The final model consists of a grid for each rock unit in each fault block (the volume of rock between faults) and a grid for each fault. The total number of grids in GFM3.1 is 2,193, as shown in the following equation:

$$50 \text{ units} \times 43 \text{ fault blocks} + 43 \text{ faults} = 2{,}193 \text{ grids} \qquad \text{(Eq. 6-1)}$$

Not included in the total are 46 model-isochore grids used to calculate the geologic surfaces. Information about how all the grids fit together was recorded in a parameter file called a "sequence" file. The sequence file can be used for subsequent analyses or operations on the model; it is included in the GFM3.1 data submittal (DTN: MO9901MWDGFM31.000).

To visually examine the model, a graphical construction called a "faces model" in EARTHVISION was also created. The faces model uses the grids of reference horizons and faults to create a three-dimensional display. In the display, rock layers and faults can be shown individually or in combination. Examples of the faces models are provided in Figures 13 and 14.

6.4 RESULTS AND DISCUSSION

The results of the GFM provide an interpretation of the spatial position and geometry of rock units and faults. To fulfill the needs of users of the GFM without the prohibitive length and repetition of explicitly discussing all 50 modeled units, this section discusses the model results in terms of rock units and faults that are important to other ISM component models (RPM and MM) and downstream users. Some rock units are grouped into thermal-mechanical units (PTn), and others are discussed by depositional formation (Topopah Spring Tuff, Calico Hills Formation, etc.). The maximum and minimum thicknesses of rock units are discussed in terms of input borehole and geologic map data, not in terms of model interpretations. On the thickness maps in this section, only boreholes that completely penetrated a unit and could be used as input are included. The borehole thickness values were rounded to the nearest foot before subtraction to calculate the thickness value. As a result, subtraction using the decimals in the source data may differ from those on the map by 1 foot. This rounding was only performed during figure generation. It was not done in model construction.

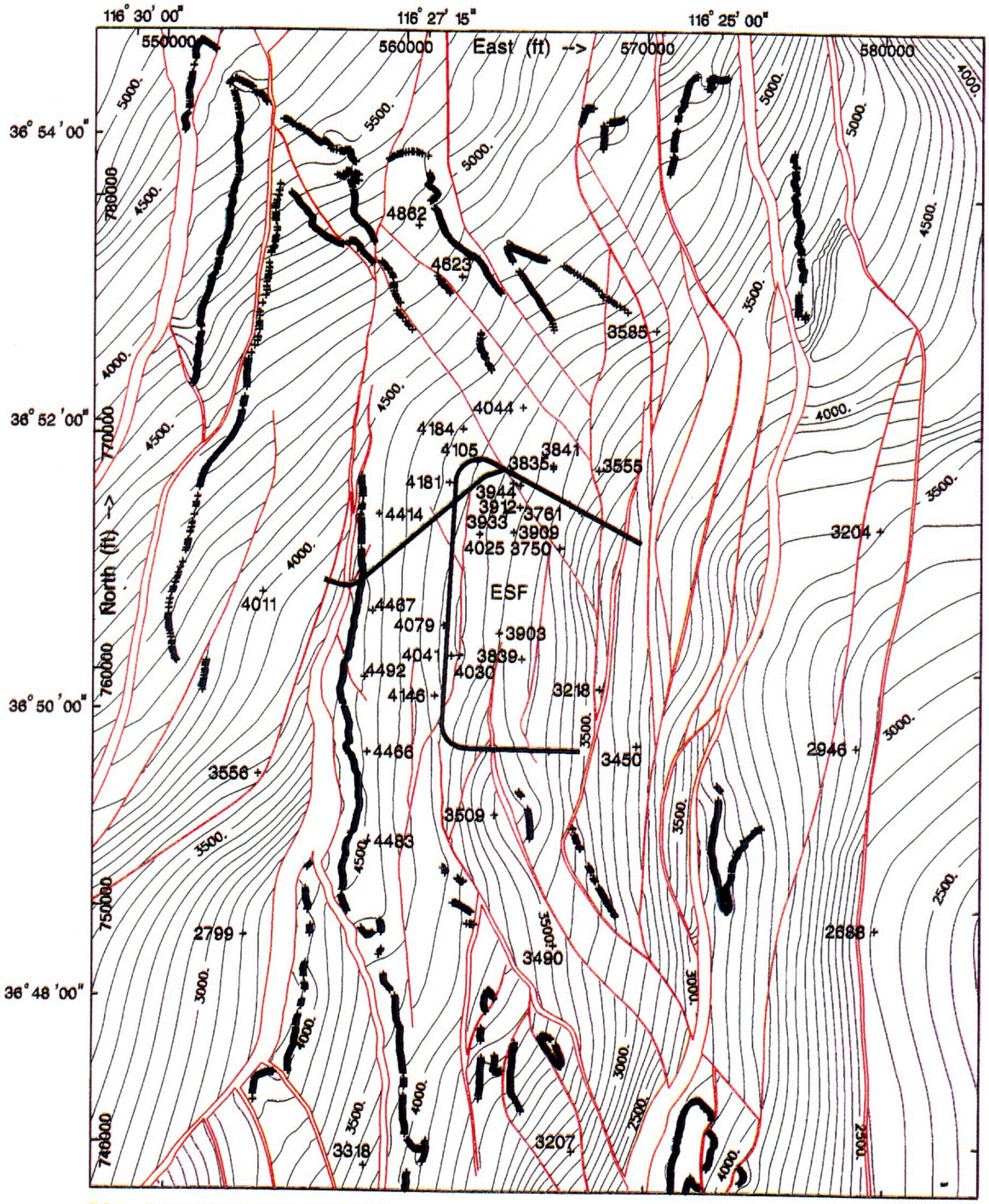

ESF - Exploratory Studies Facility

Fault

Contour Interval 100 Feet

\+ Input Data From Geologic Map and Boreholes

NOTE: Blank areas represent fault displacements.

N

2000 0 2000 4000 6000 FEET

1000 0 1000 2000 METERS

Figure 12. Elevation Map of Basal Tiva Reference Horizon

C 003

6.4.1 Interpretation Of Rock Units

This section describes the geometry and distribution of rock units in the GFM that are important for the ISM, RPM, and MM, as well as the major direct and indirect downstream uses of the ISM (repository design and hydraulic flow modeling through the unsaturated zone (UZ) and the saturated zone (SZ)). Each geologic formation is described, as well as the Paintbrush Tuff nonwelded (PTn) thermal-mechanical unit, the undifferentiated older Tertiary unit (Tund), and the Tertiary-Paleozoic unconformity. Subunits of the formations that are particularly important for GFM uses are also described. Regional stratigraphy and structure, deposition, origin, age, and lithology of the rock layers modeled in the GFM are discussed in the Yucca Mountain Site Description (CRWMS M&O 1998b, chapters 3.2 and 3.5).

6.4.1.1 Alluvium and Post-Tiva Units

Overview–The alluvium (Qal) and post-Tiva rock units (Table 5) in the GFM account for a very small amount of the total model volume (much less than 1 percent), and they occur well above and outside the vicinity of the ESF.

Data Distribution and Unit Geometry–The distribution of modeled alluvium is illustrated in Figure 15. Alluvial thickness was interpreted with the use of the site area geologic map (DTN: GS970808314221.002) and available borehole data (DTN: MO9811MWDGFM03.000), including the UZN boreholes as discussed in Section 6.1.1. Where no thickness data were available, alluvial thickness was estimated by projecting adjacent topographic slopes to depth. The areal extent of alluvium is well constrained by geologic mapping; however, because some boreholes did not penetrate to bedrock, the alluvial thickness is constrained by limited subsurface information. The map, therefore, should be considered more representative of a minimum alluvial thickness or an interpretation based on sparse data rather than of an absolute thickness.

As shown in map view (Figure 13), the post-Tiva rock units are only sparsely encountered in the modeled area. The distribution is based on the geologic map (DTN: GS970808314221.002) and borehole data (DTN: MO9811MWDGFM03.000). South of Yucca Wash, these units are typically preserved in wedges on the downthrown sides of faults. For example, in Figure 14, a wedge of the Tiva Canyon Tuff Crystal-Rich Member and post-Tiva unit is shown on the downthrown side of the Solitario Canyon fault.

6.4.1.2 Tiva Canyon Tuff (Tpc)

Overview–In the GFM, the Tiva Canyon Tuff (Table 5) consists of the Crystal-Rich Member (Tpcr, grouped with post-Tiva rocks) and the Crystal-Poor Member (Tpcp), which is undivided in the GFM except for the three basal vitric subzones (Tpcpv1, Tpcpv2, and Tpcpv3) and a low-density zone (TpcLD). The Tiva Canyon Tuff makes up most of the exposed bedrock in the modeled area (Figure 13).

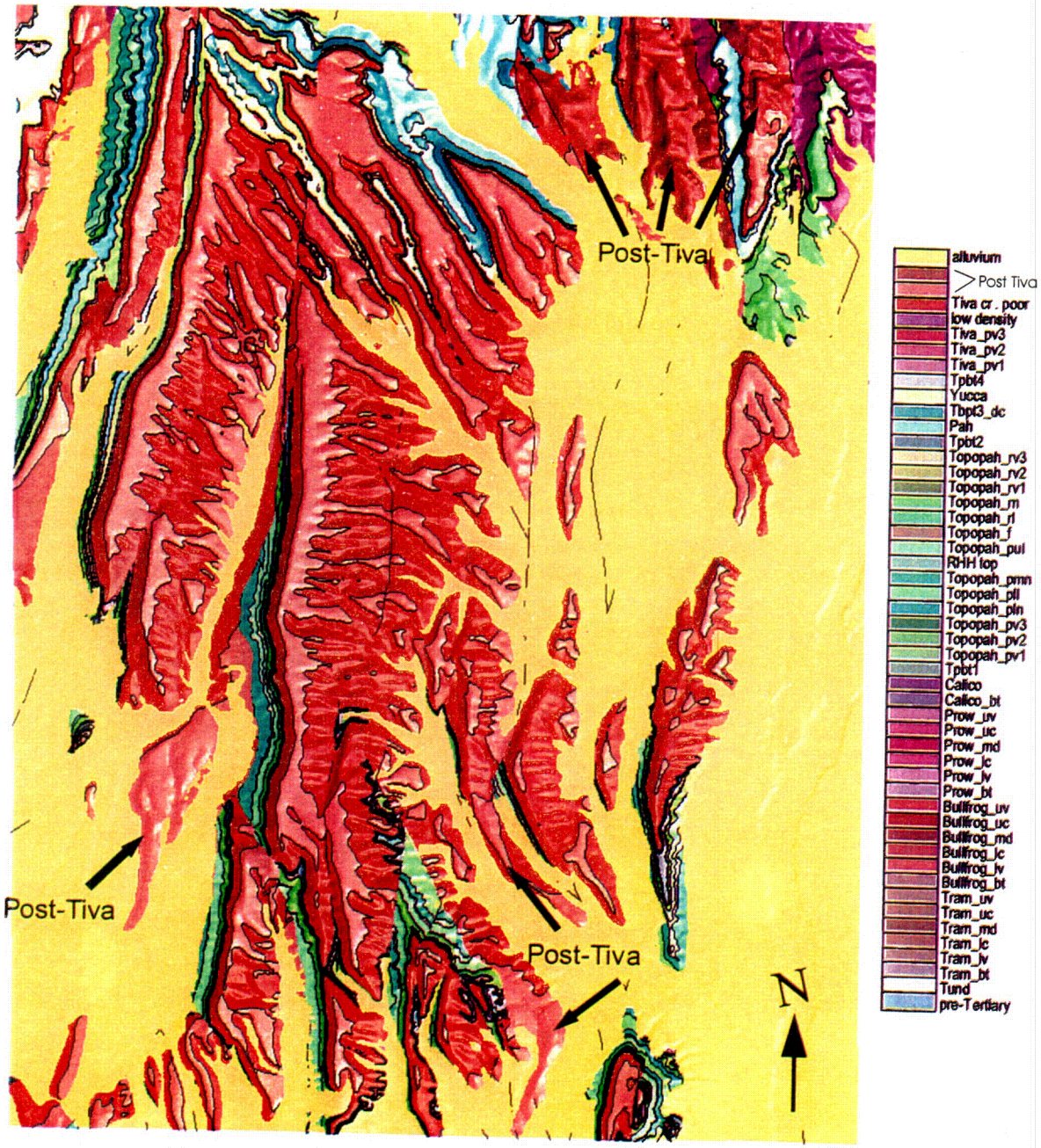

NOTES: Formation names are spelled out in the color key for clarity. Refer to Table 5 for stratigraphic nomenclature.

This figure is a perspective view and not to scale. The area displayed is equivalent to the GFM model boundaries.

Figure 13. Model Surficial Geology (Vertical View of GFM, Same Area as Figure 1)

C004

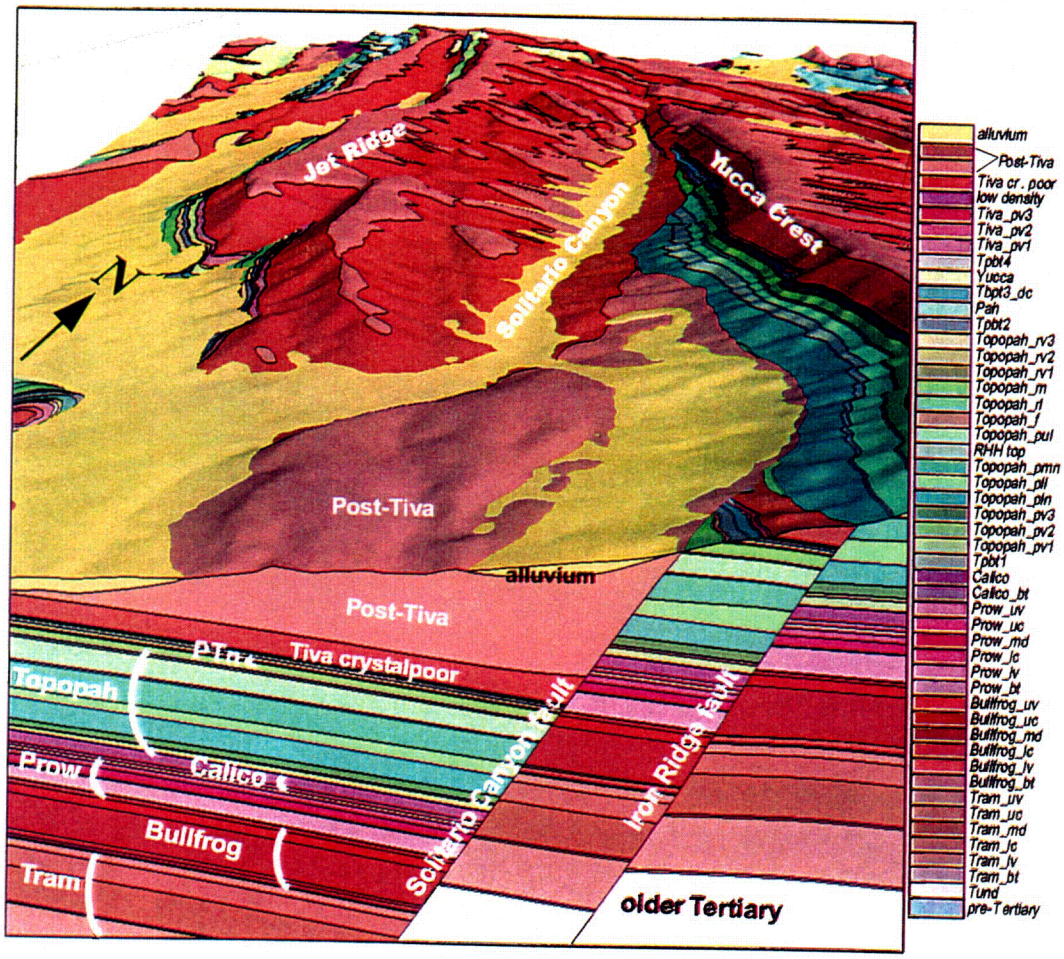

NOTE: Formation names are spelled out in the color key for clarity.
Refer to Table 5 for stratigraphic nomenclature.

Figure 14. Wedge of Post-Tiva Rocks in Solitario Canyon (View to North of Slice Through GFM)

C005

Because the Tiva Canyon Tuff makes up most of the exposed bedrock on Yucca Mountain, it is important in hydrologic infiltration modeling. The distribution of the lower vitrophyre (Tpcpv3) may be important in hydrologic modeling because, like the other vitrophyres, the lower vitrophyre is one of the layers in the mountain having the lowest porosity (Rautman and McKenna 1997, p. 142).

Data Distribution and Unit Geometry–The distribution and thickness of Tpcpv3 are illustrated in Figure 16. The model interpretation for this unit is based on borehole data (DTN: MO9811MWDGFM03.000) and abundant geologic map data (DTN: GS970808314221.002). Because the top of the Tiva Canyon Tuff is extensively eroded in the model area, none of the input boreholes penetrate the entire formation, and a true thickness map cannot be produced. The Tiva Canyon Tuff is thickest in the center of the modeled area and thins to the east, west, and south. The crystal-poor densely welded vitric subzone (Tpcpv3) is present only in the southwestern part of the area and appears to be distributed as pods or in a web-like pattern (Figure 16).

6.4.1.3 Paintbrush Tuff Nonwelded (PTn) Unit

Overview–The PTn unit (defined in Table 5) is a grouping of rock layers used in hydrologic and thermal-mechanical modeling. Stratigraphically, it consists of the rock units Tpcpv2, Tpcpv1, Tpbt4, Tpy, Tpbt3, Tpp, Tpbt2, Tptrv3, and Tptrv2.

Because the mostly nonwelded rocks of the PTn unit are distinct from the welded rocks above and below, the distribution and thickness of the PTn unit are important in hydrologic modeling.

The PTn unit has been hypothesized to attenuate and spatially re-distribute downward flow (DOE 1998b, p. 2-38).

Data Distribution and Unit Geometry–The model interpretation for the PTn unit is based on input data from 41 boreholes that fully penetrated the unit (DTN: MO9811MWDGFM03.000) and abundant geologic map data (DTN: GS970808314221.002). Two additional boreholes partially penetrated the PTn unit but did not provide information on total thickness. The major formations of the PTn unit, the Yucca Mountain Tuff (Tpy) (Figure 17) and Pah Canyon Tuff (Tpp) (Figure 18), both thicken dramatically to the north and northwest but are absent over the southern half of the modeled area. In the southern half of the modeled area, the PTn unit comprises bedded tuffs (Tpbt2, Tpbt3, and Tpbt4) and the vitric units of the lower Tiva Canyon Tuff (Tpcpv1 and Tpcpv2) and the Topopah Spring Tuff (Tptrv2 and Tptrv3). In the vicinity of the ESF, the PTn unit is 75 to 250 feet (23 to 76 meters) thick and thickens rapidly to the north to more than 550 feet (168 meters). An model-isochore map of this unit is shown in Figure 19.

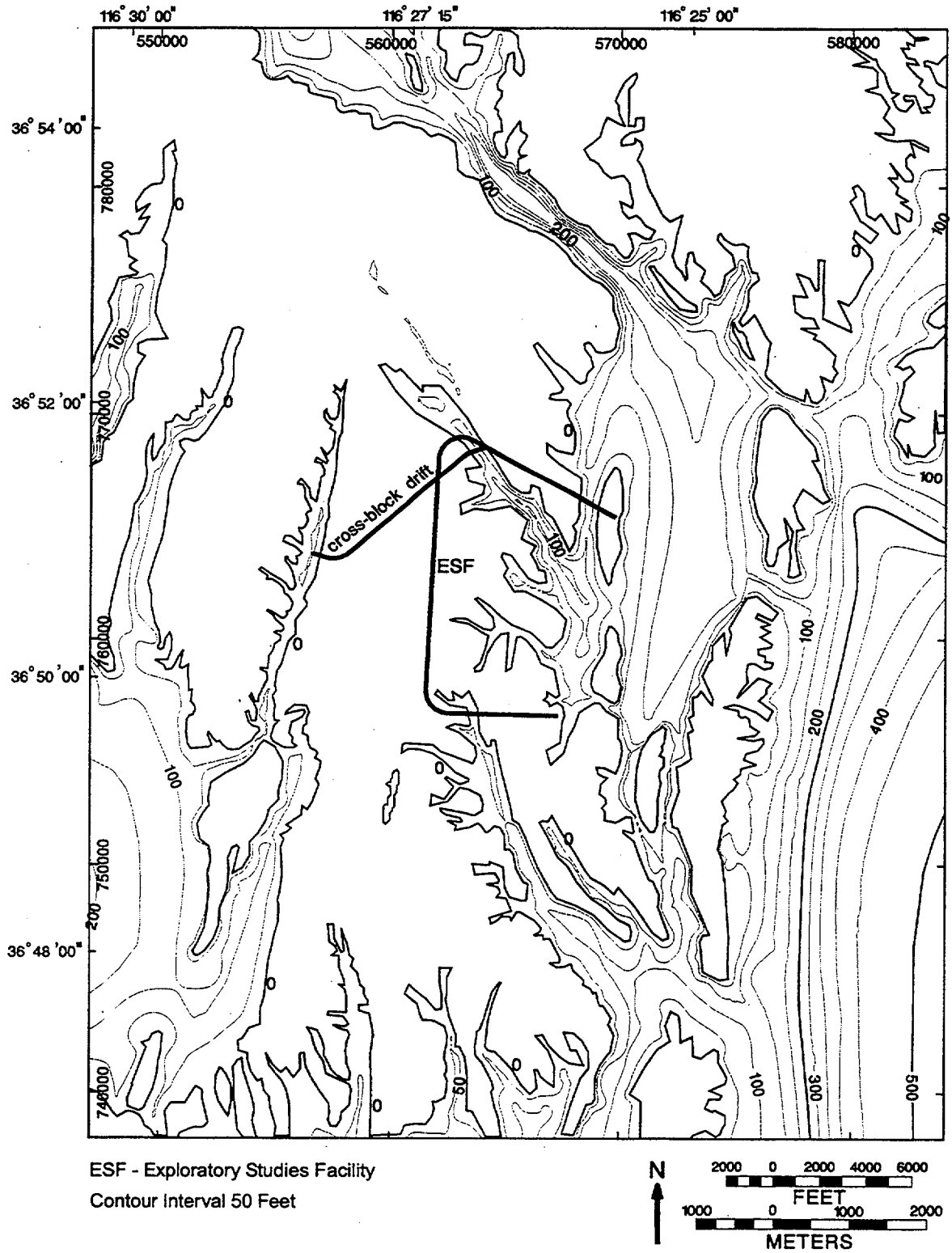

Figure 15. Model-Isochore Map of Alluvium

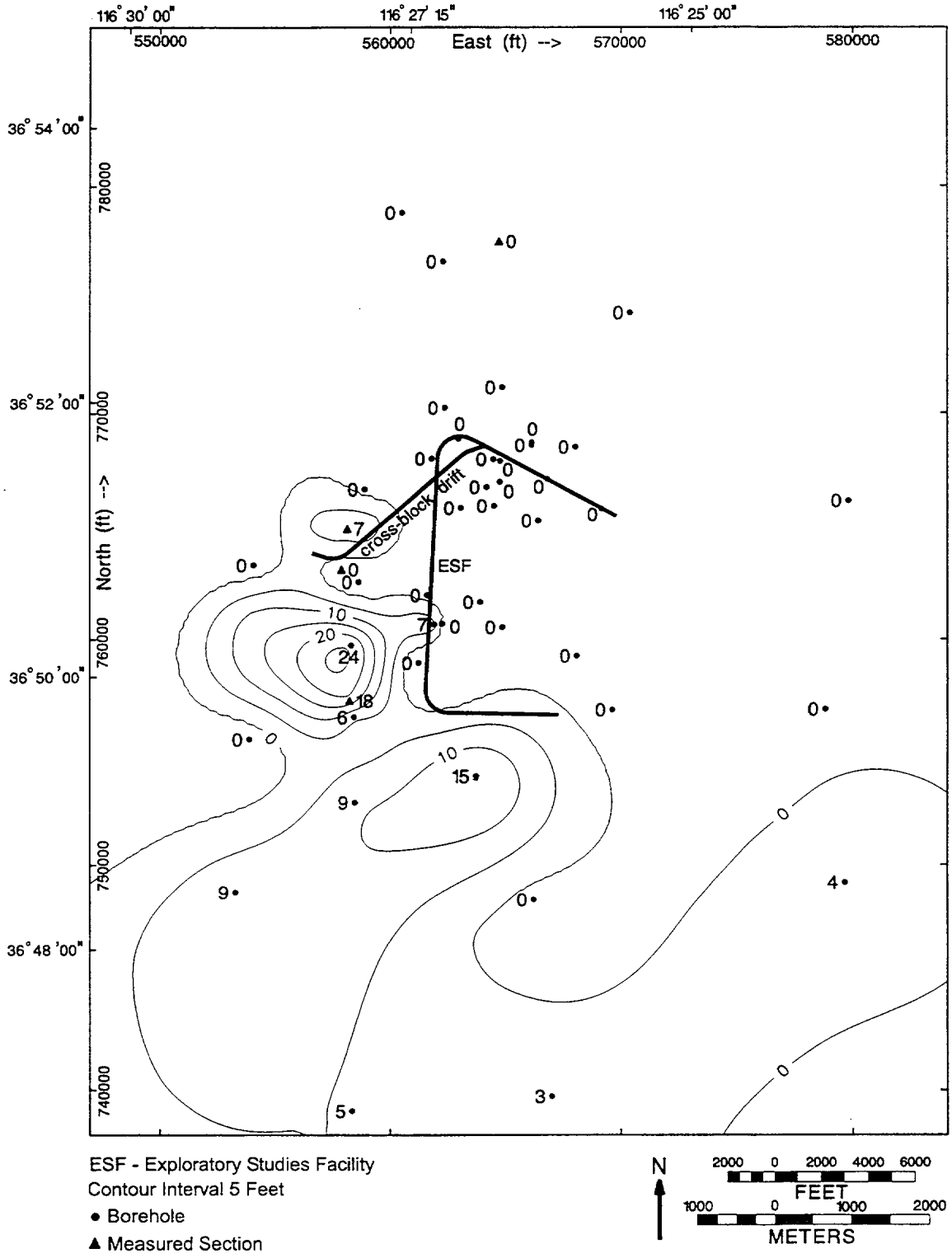

Figure 16. Model-Isochore Map of Tiva Canyon Tuff Crystal-Poor Member Vitric Zone Densely Welded Subzone (Tpcpv3)

6.4.1.4 Topopah Spring Tuff (Tpt)

Overview–The Topopah Spring Tuff encompasses the proposed RHH (identified in Table 5) as well as lithologically distinct units used in modeling rock properties, mineralogy, and hydrologic flow. The Topopah Spring Tuff is exposed locally in the northern, western, and southeastern parts of the modeled area, as can be seen in Figure 13.

The Topopah Spring Tuff is important for the repository design because it encompasses the RHH. The distributions and thicknesses of the densely welded vitric subzones of the Topopah Spring Tuff are important for hydrologic modeling because these subzones have very low porosities and affect hydrologic flow (DOE 1998b, p. 2-38). In addition, the distribution of the Topopah lower densely welded vitric subzone (Tptpv3) is important because it bounds the bottom of the RHH. The lithic rich unit (referred to in the GFM as Tptf) is important for the geologic interpretation of the Topopah Spring Tuff because it provides information on the transition from crystal-poor to crystal-rich units.

Data Distribution and Unit Geometry–The model interpretation for this formation is based on input data from 30 boreholes that fully penetrated the formation (DTN: MO9811MWDGFM03.000), tunnel data (DTN: GS960908314224.020; GS970808314224.016), and abundant geologic map data (DTN: GS970808314221.002). Fifteen additional input boreholes partially penetrated the formation but did not provide information on total thickness. North of Yucca Wash, the model was constructed using the geologic map data (DTN: GS970808314221.002) and the conceptual model discussed in Section 6.3.1. In addition, corroborating data (DTN: GS950608314211.025) were considered to support the conceptual model. Based on the input data, the Topopah Spring Tuff reaches a maximum thickness of more than 1,200 feet (365 meters) along a northwest-southeast axis located across the vicinity of the ESF (Figure 20). The Topopah Spring Tuff thins rapidly toward the northeast and pinches out at the far northeastern corner of the modeled area (DTN: GS970808314221.002). To the southeast, the thickness diminishes to less than 750 feet (210 meters).

The crystal-rich densely welded vitric subzone (Tptrv1) near the top of the Topopah Spring Tuff is less than 10 feet (3 meters) thick over most of the modeled area, but is absent in a few isolated areas. The vitrophyre (densely welded vitric subzone) near the bottom of the formation (Tptpv3) is much thicker, ranging from 46 to 114 feet (14 to 35 meters) over the proposed repository area and from 0 to 115 feet (0 to 35 meters) across the total modeled area (Figure 21). It pinches out only where the formation pinches out, in the northeastern corner of the modeled area. The thicknesses of both vitrophyre units vary by as much as 300 percent over distances as short as 2,000 feet (610 meters). The thickness of Tptpv3 in the southwestern corner of the modeled area is unconstrained, but was extrapolated to allow projection to the 150-foot (46-meter) thickness observed in borehole VH-2 in Crater Flat (DTN: MO9811MWDGFM03.000), approximately 4 miles (6 kilometers) west-southwest of the boundary of the modeled area.

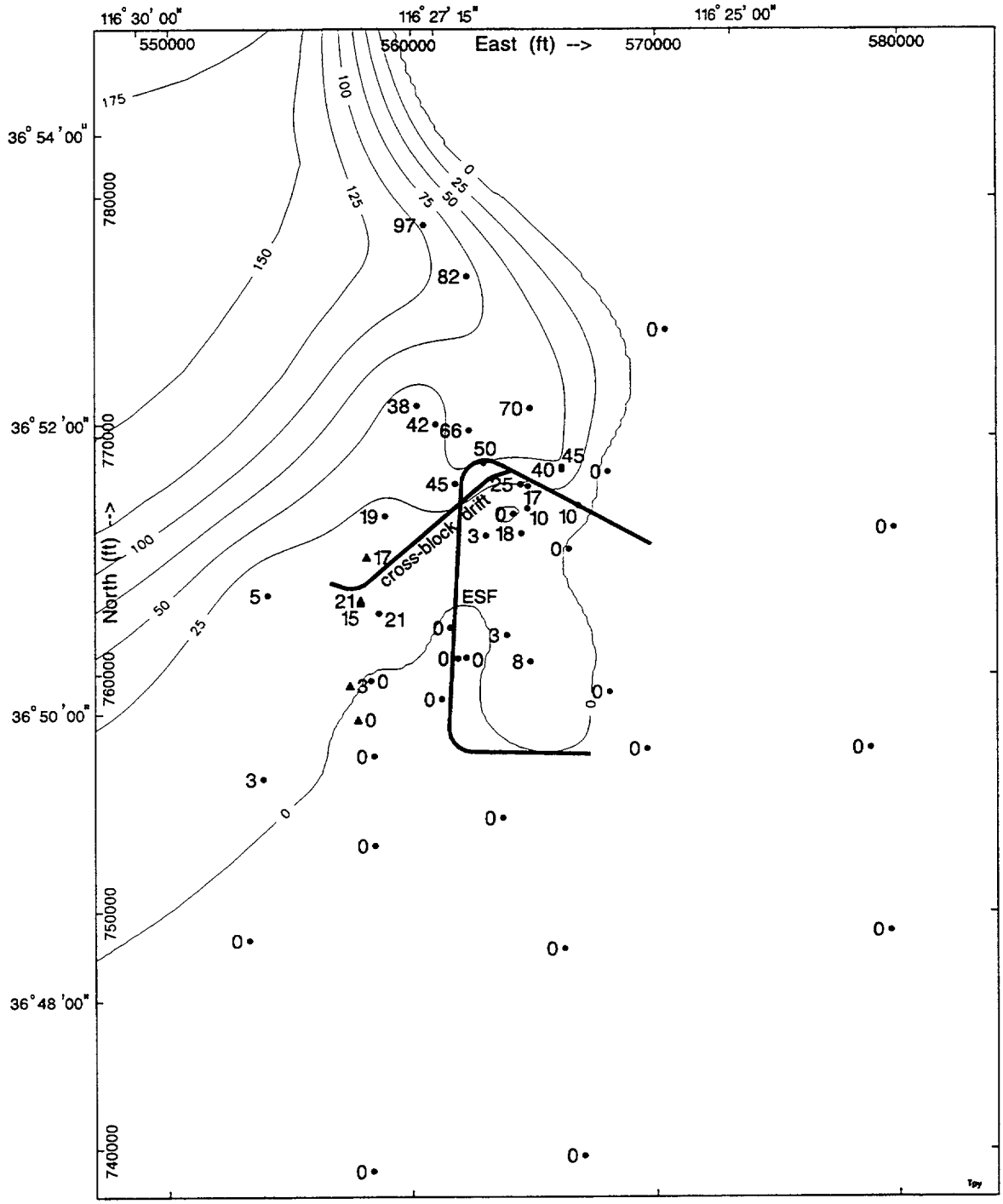

ESF - Exploratory Studies Facility

Contour Interval 25 Feet

- Borehole

▲ Measured Section

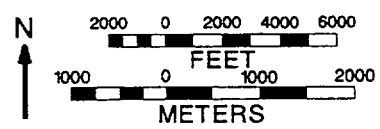

Figure 17. Model-Isochore Map of Yucca Mountain Tuff (Tpy)

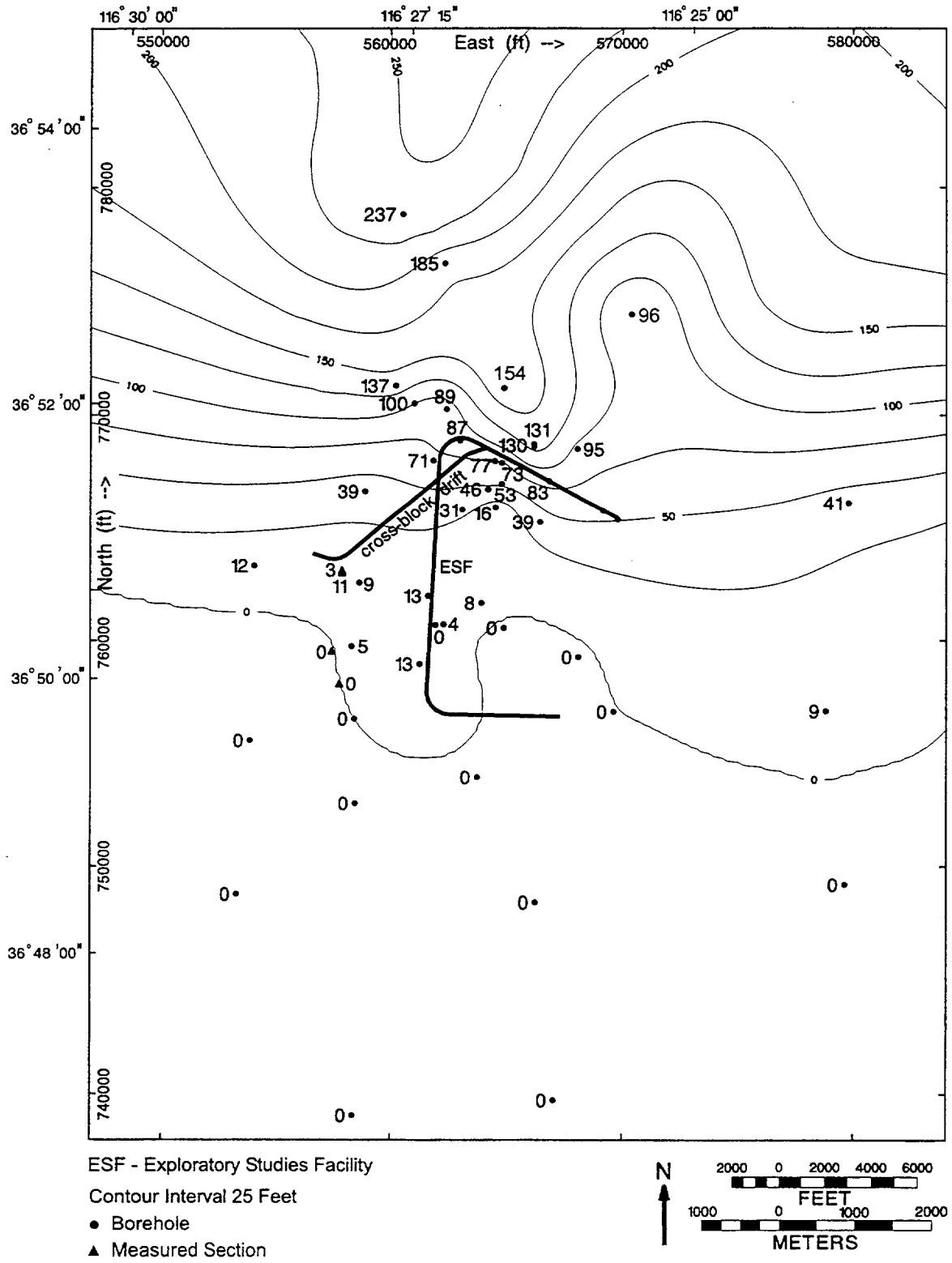

Figure 18. Model-Isochore Map of Pah Canyon Tuff (Tpp)

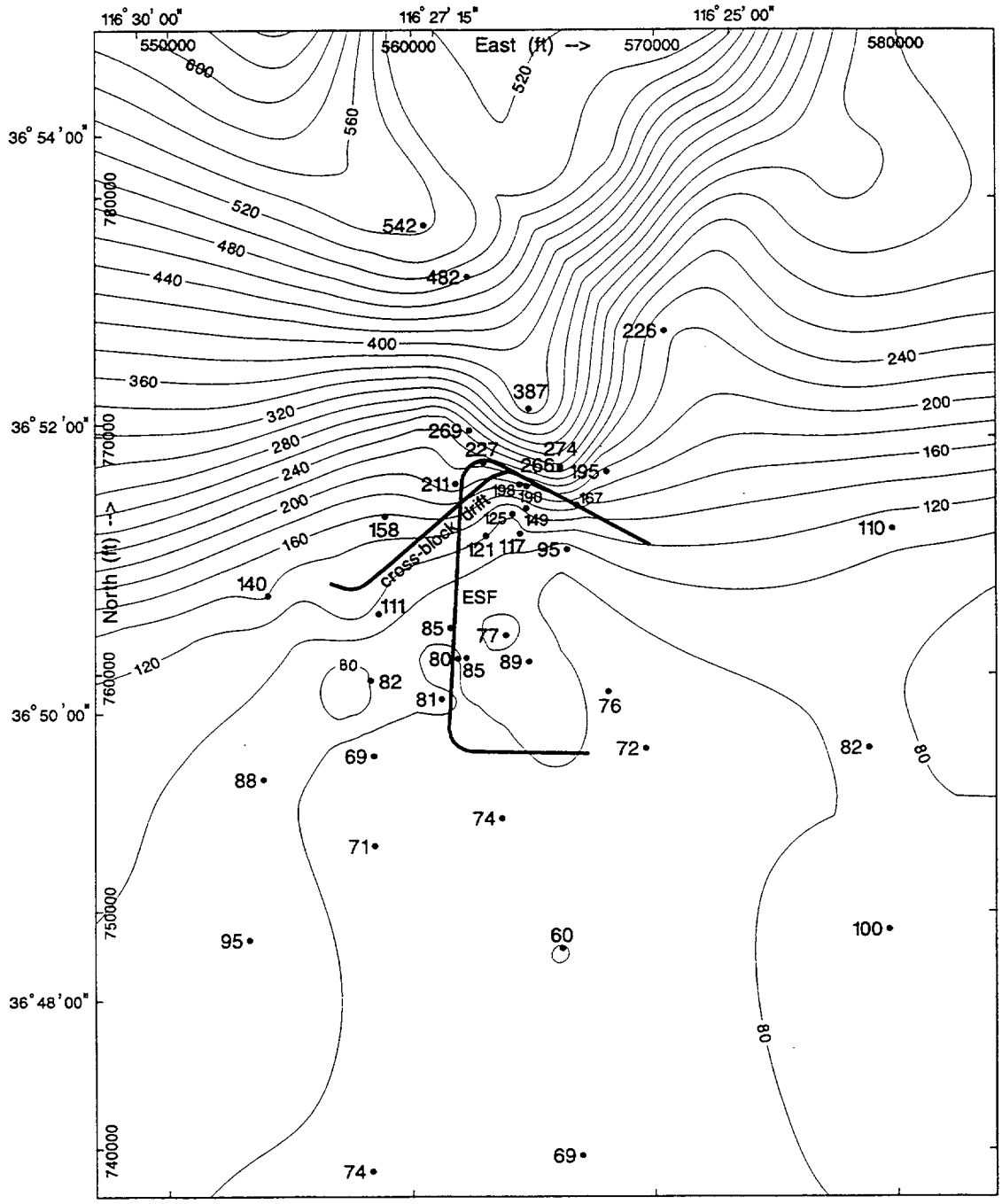

ESF - Exploratory Studies Facility

Contour Interval 20 Feet

• Borehole

N

2000 0 2000 4000 6000
FEET

1000 0 1000 2000
METERS

Figure 19. Model-Isochore Map of Paintbrush Tuff Nonwelded Unit (Ptn)

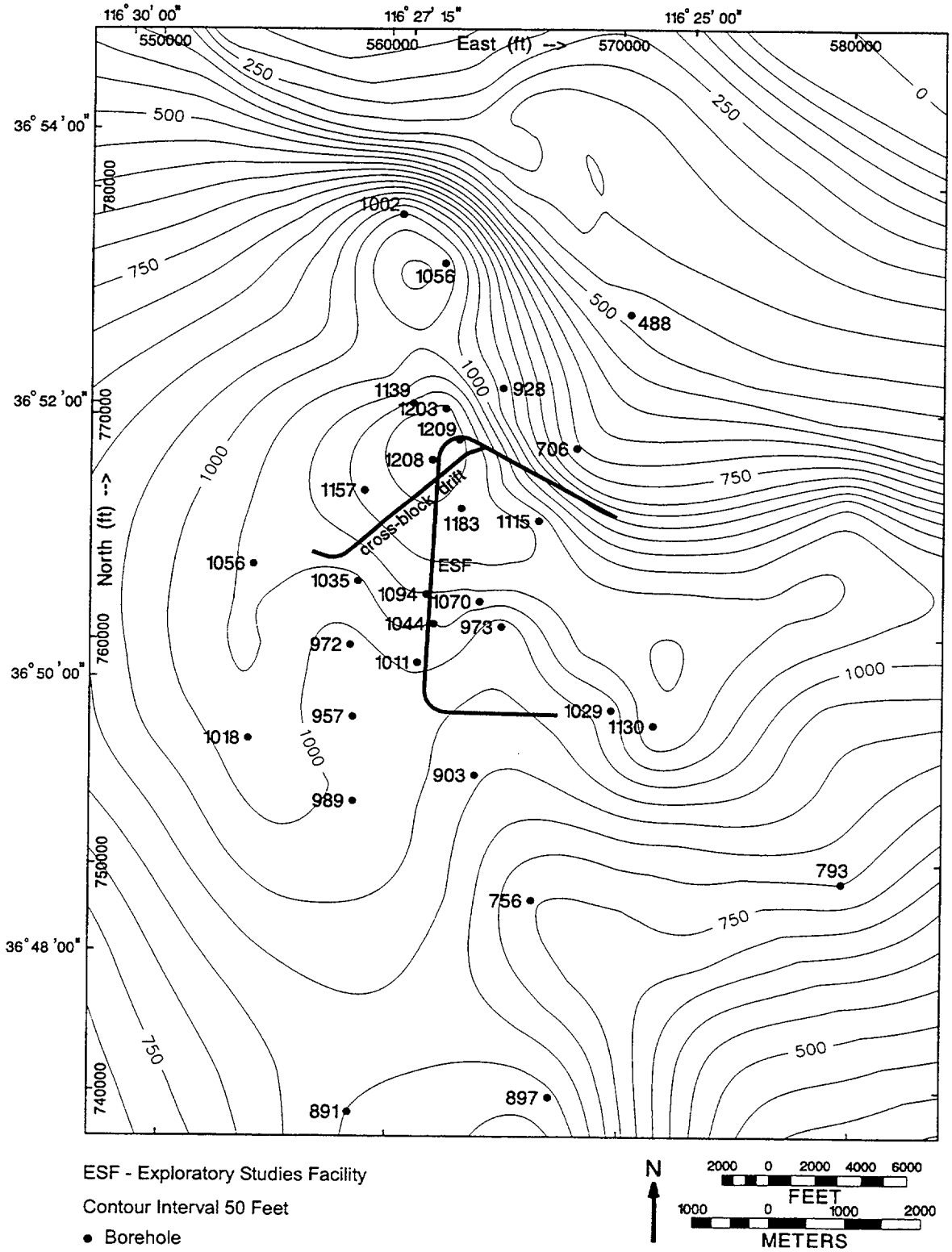

ESF - Exploratory Studies Facility

Contour Interval 50 Feet

• Borehole

N

2000 0 2000 4000 6000
FEET

1000 0 1000 2000
METERS

Figure 20. Model-Isochore Map of Topopah Spring Tuff (Tpt)

The anomalously thin Tptpv3 in borehole WT-1 is due to faulting of the unit. The faulted thickness was used in the model so that all stratigraphic contacts could be honored; if a projected true thickness were used and no fault explicitly modeled at this rock layer, the model could not honor the rest of the stratigraphic contacts in the borehole. No fault was included at this rock layer because no other information about the fault is available.

A xenolithic unit (defined in the GFM as Tptf) (Figure 22) straddles the Topopah Spring Tuff Crystal-Rich/Crystal-Poor Member boundary (Buesch et al. 1996, Appendix 2, p. 41). This unit is present only in the vicinity of Yucca Wash and northward and has not been observed in the vicinity of the ESF. It reaches a maximum known thickness of 68 feet (21 meters) in borehole G-2.

The RHH (identified in Table 5) includes model units RHHtop (representing the lower part of Tptpul), Tptpmn, Tptpll, and Tptpln within the Topopah Spring Tuff. The thickness of this unit mimics that of the total Topopah Spring Tuff—it reaches a maximum thickness of more than 750 feet (230 meters) along the same northwest-southeast axis (Figure 23). The thickness of the unit ranges from about 550 to 760 feet (170 to 230 meters) in the vicinity of the ESF and decreases to less than 400 feet (122 meters) to the south. Model unit RHHtop was incorrectly constructed locally at the Prow (Figure 1) in the far northwestern corner of the modeled area. As a result, the RHH in Figure 23 is approximately 40 feet (12 meters) too thick in this small area, and appears thicker than the Topopah Spring Tuff (Tpt) in Figure 20. No impact is anticipated on users of the GFM because model unit RHHtop and remaining model units comprising the complete RHH are used for subsurface repository design in the vicinity of the ESF.

6.4.1.5 Calico Hills Formation (Ta)

Overview–The Calico Hills Formation crops out in the northern part of the modeled area, as well as one isolated exposure at Busted Butte near the southern boundary of the modeled area. The Calico Hills Formation is lithologically distinct from the overlying Topopah Spring Tuff.

The Calico Hills Formation is important for hydrologic and radionuclide transport modeling because it lies in the flow path between the potential repository and the water table, as defined in the Reference Information Base (RIB) (DTN: MO9609RIB00038.000). Over much of the modeled area the formation has been altered to zeolites and clay minerals, which may retard certain radionuclides (DOE 1998b, p. 2-19).

Data Distribution and Unit Geometry–The model interpretation for this formation is based on input data from 25 boreholes that fully penetrated the formation (DTN: MO9811MWDGFM03.000) and geologic map data (DTN: GS970808314221.002).

Eleven additional input boreholes partially penetrated the formation but did not provide information on total thickness. The Calico Hills Formation ranges in thickness from less than 100 feet (30 meters) in the south to more than 1,500 feet (450 meters) in the northeast (Figure 24). In the northeast, geologic map data provide only a minimum thickness because the base of the formation is not exposed. In the vicinity of the ESF, the formation thickness ranges from less than 40 feet (12 meters) to greater than 300 feet (91 meters).

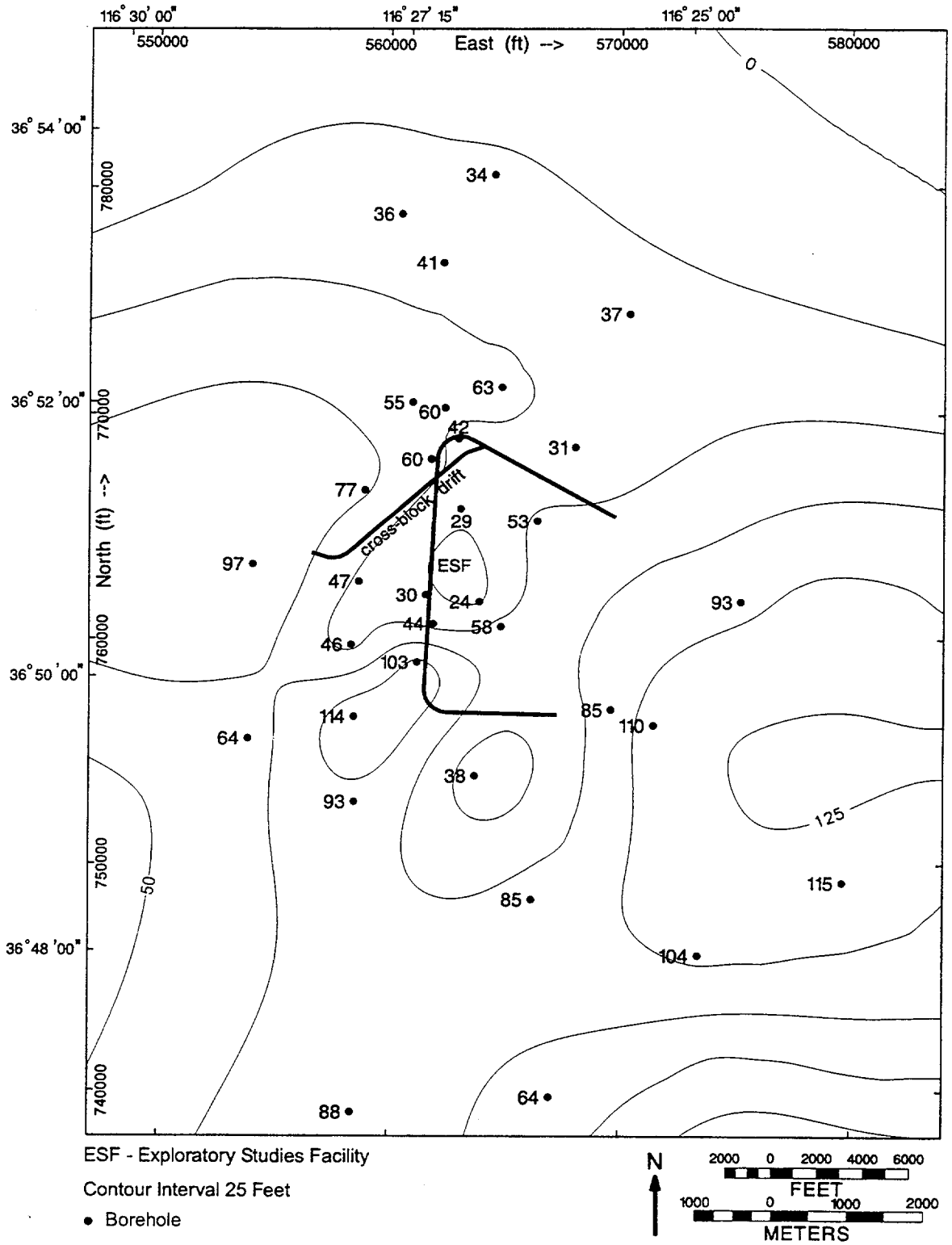

Figure 21. Model-Isochore Map of Topopah Spring Tuff Crystal-Poor Member Vitric Zone Densely Welded Subzone (Tptpv3)

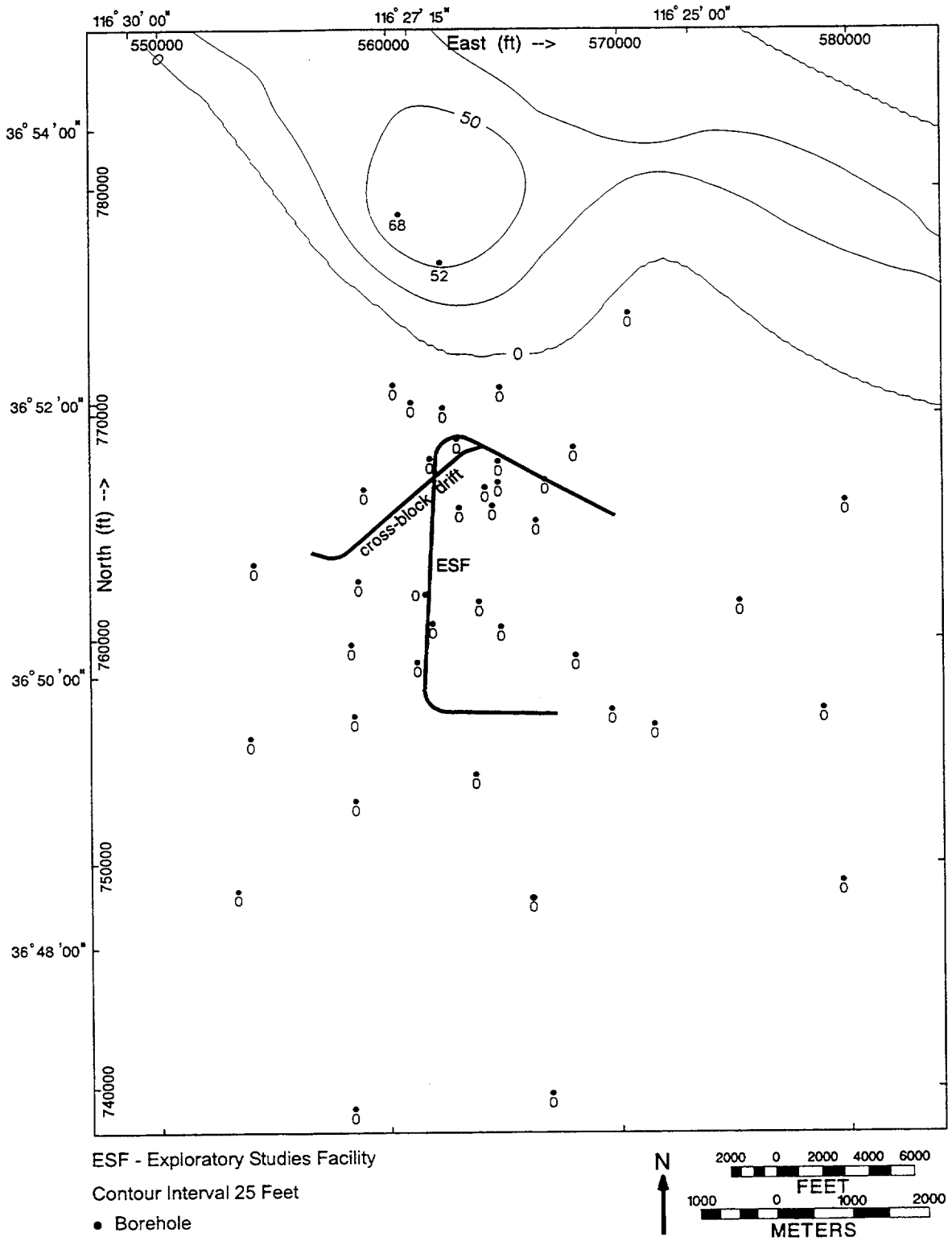

Figure 22. Model-Isochore Map of Topopah Spring Crystal-Poor Member Lithic-Rich Zone (Tptf)

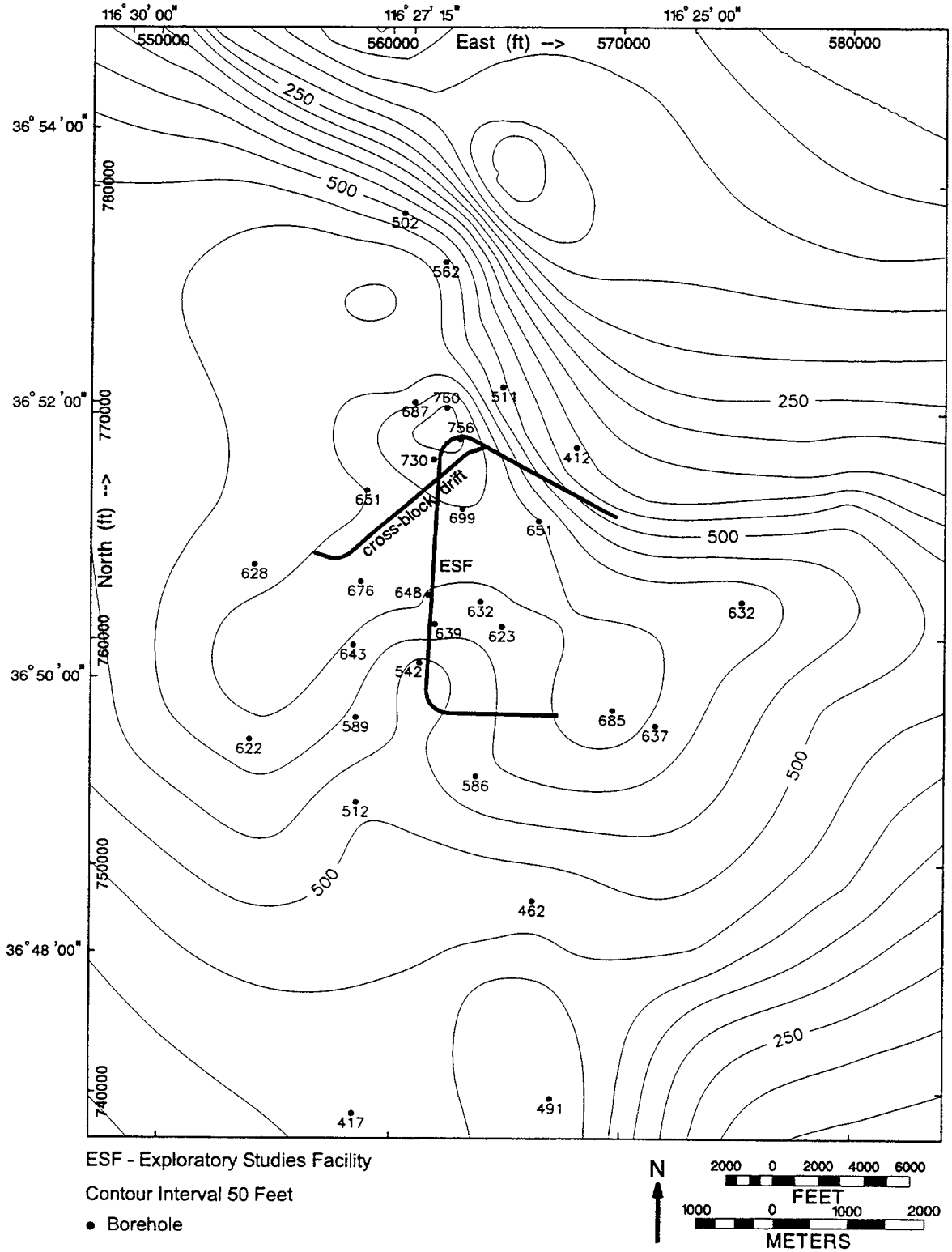

Figure 23. Model-Isochore Map of Repository Host Horizon (RHH)

6.4.1.6 Prow Pass Tuff (Tcp)

Overview–The Prow Pass Tuff is present beneath the entire modeled area but is exposed at the surface in only one small outcrop in the northwestern corner of the modeled area.

The Prow Pass Tuff is important for hydrologic and radionuclide transport modeling because, like the Calico Hills Formation, it lies in the flow path between the potential repository and the water table, as defined in the RIB (DTN: MO9609RIB00038.000), and has in part been altered to zeolites and clay minerals, which may retard certain radionuclides (DOE 1998b, p. 2-20).

Data Distribution and Unit Geometry–The model interpretation for this formation is based on input data from 18 boreholes that fully penetrated the formation (DTN: MO9811MWDGFM03.000) and geologic map data for the lone outcrop in the modeled area (DTN: GS970808314221.002). Five additional input boreholes partially penetrated the formation but did not provide information on total thickness. The formation is thickest along a north-south axis through the center of the modeled area, reaching a maximum observed thickness of 636 feet (194 meters) in borehole H-4 (Figure 25). In the vicinity of the ESF, the formation ranges in thickness from less than 300 feet (91 meters) to more than 550 feet (168 meters). The formation pinches out several miles northeast of the modeled area, according to geologic map data (Byers et al. 1976), which show the Calico Hills Formation depositionally overlying rocks of Devonian age. However, the exact location at which the Prow Pass Tuff pinches out is unknown. Although not used as direct input, a regional interpretation (Carr, et al. 1986a, Fig. 15) shows the pinchout in a similar area.

6.4.1.7 Bullfrog Tuff (Tcb)

Overview–The Bullfrog Tuff is present beneath the entire modeled area and is the deepest stratigraphic unit exposed at the surface in the modeled area. It is exposed in only one small outcrop in the far northwestern corner of the modeled area.

The Bullfrog Tuff is important for hydrologic and radionuclide transport modeling because, like the Calico Hills Formation and the Prow Pass Tuff, it lies in the flow path between the potential repository and the water table, as defined in the RIB (DTN: MO9609RIB00038.000). In addition, the Bullfrog Tuff has, in part, been altered to zeolites and clay minerals, which may retard certain radionuclides (DOE 1998b, p. 2-20).

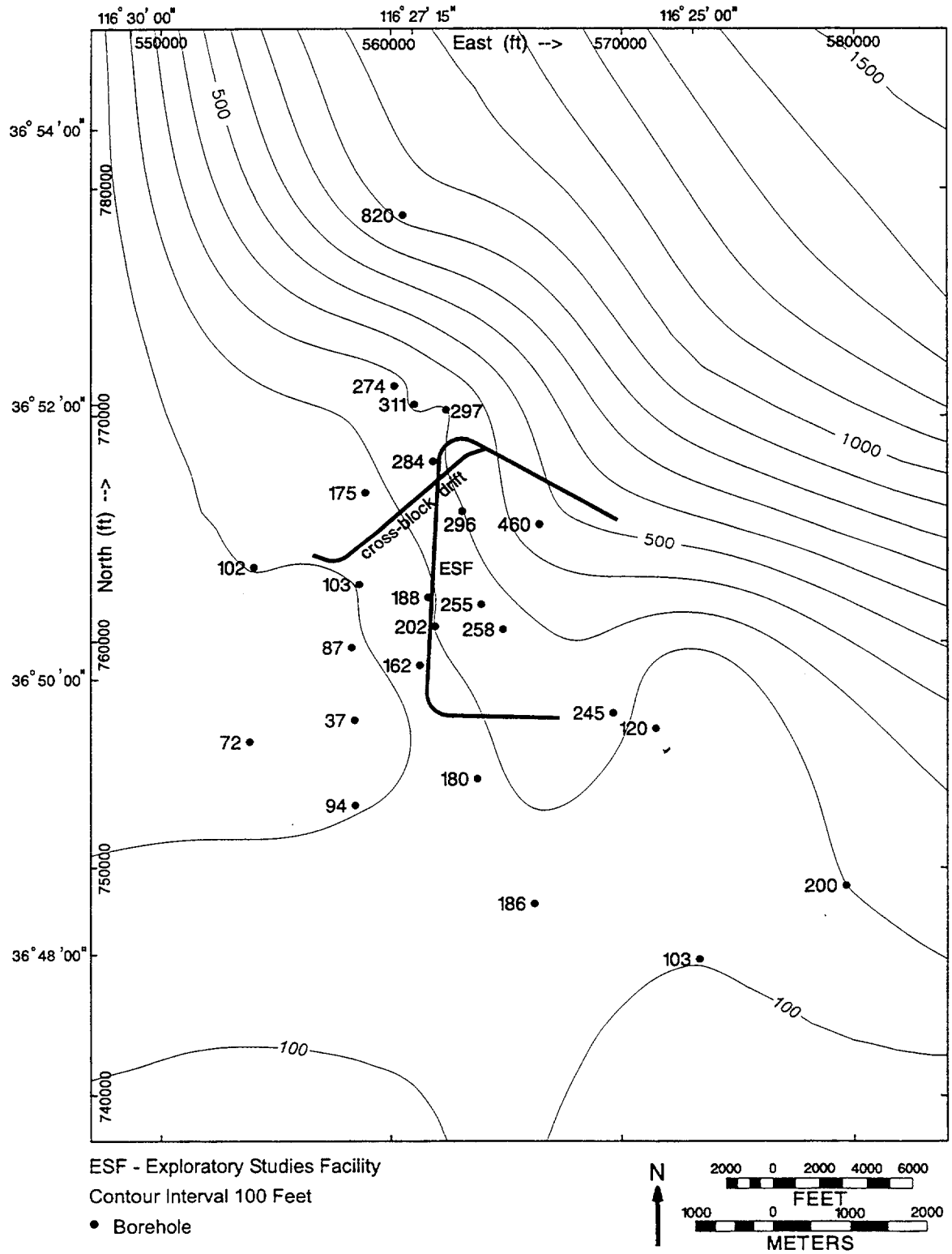

Figure 24. Model-Isochore Map of Calico Hills Formation (Ta)

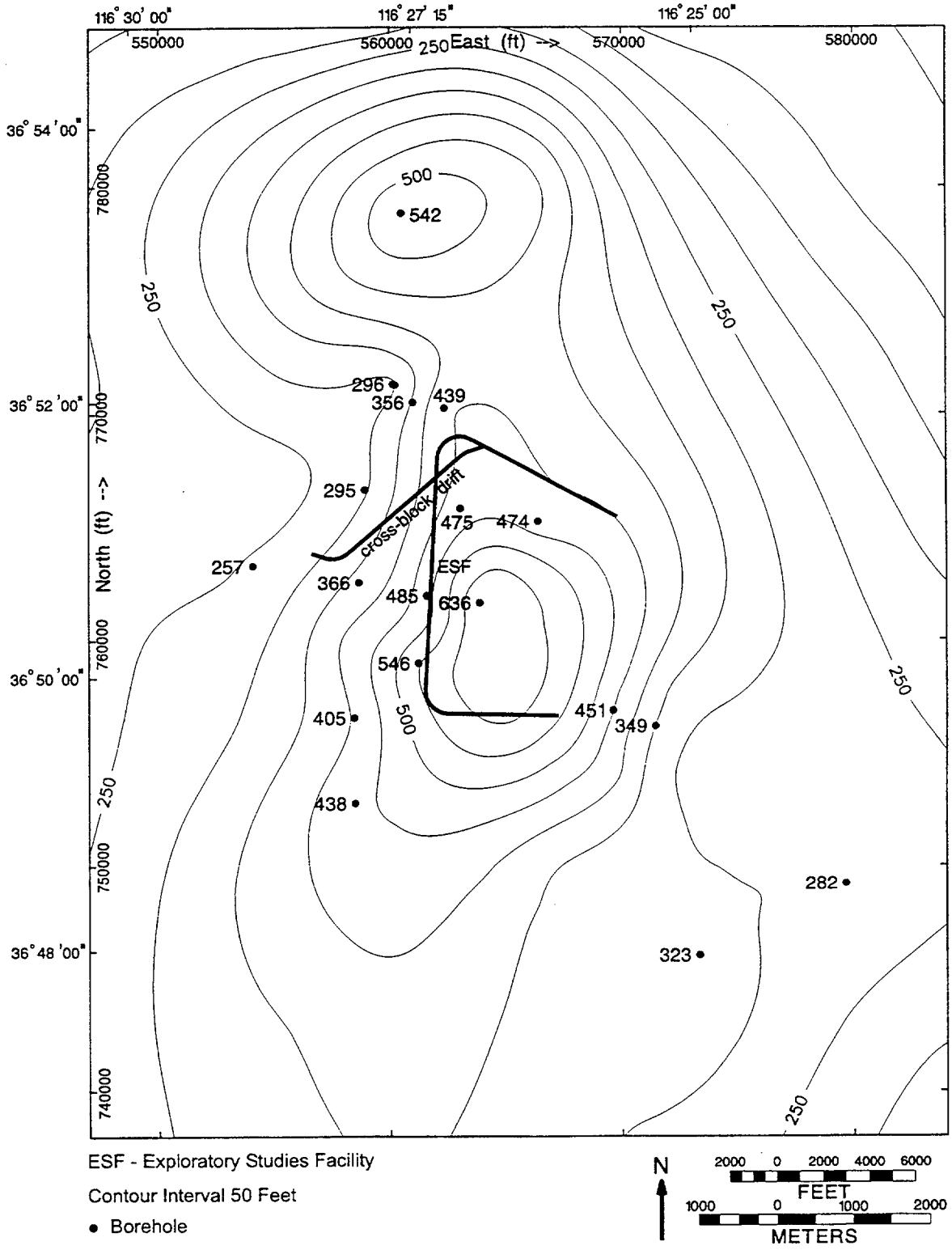

Figure 25. Model-Isochore Map of Prow Pass Tuff (Tcp)

Data Distribution and Unit Geometry–The model interpretation for this unit is based on input data from 14 boreholes that fully penetrated the formation (DTN: MO9811MWDGFM03.000) and the lone outcrop data from the geologic map (DTN: GS970808314221.002). Three additional input boreholes partially penetrated the formation but did not provide information on total thickness. The Bullfrog Tuff model-isochore is shown in Figure 26. The Bullfrog Tuff is thickest in the southwestern part of the central modeled area, reaching a maximum thickness of 618 feet (188 meters) in borehole G-3 (Figure 26). In the vicinity of the ESF, the formation ranges in thickness from 370 feet (113 meters) to 540 feet (165 meters). The formation pinches out several miles northeast of the modeled area, according to geologic map data (Byers et al. 1976. The exact location at which the Bullfrog Tuff pinches out is unknown. Units Tcblc and Tcblv in borehole J-13 are not present due to faulting; therefore, the thickness of the Bullfrog Tuff shown in Figure 26 is not a true thickness at borehole J-13. Although not used as direct input, a regional interpretation (Carr, et al. 1986a, Fig. 14) shows the pinchout in a similar area.

6.4.1.8 Tram Tuff (Tct)

Overview–The Tram Tuff is present beneath the entire modeled area but is not exposed in outcrop. The Tram Tuff is important for hydrologic and radionuclide transport modeling because, like the Calico Hills Formation, Prow Pass Tuff, and Bullfrog Tuff, it lies in the flow path between the potential repository and the water table, as defined in the RIB (DTN: MO9609RIB00038.000). In addition, the Tram Tuff is, in part, altered to zeolitic clays, which trap certain radionuclides (DOE 1998b, p. 2-20).

Data Distribution and Unit Geometry–The model interpretation for this unit is based on input data from 11 boreholes that fully penetrated the formation (DTN: MO9811MWDGFM03.000). Two additional input boreholes partially penetrated the formation but did not provide information on total thickness. In the GFM, the Tram Tuff is the thickest of the formations in the Crater Flat Group. It is thickest in a north-northeasterly trending axis over the central part of the modeled area (Figure 27) with a maximum thickness greater than 1,200 feet (365 meters) at borehole G-3. In the vicinity of the ESF, it ranges in thickness from about 650 feet (198 meters) to about 1,120 feet (340 meters). The formation pinches out several miles northeast of the modeled area, according to geologic map data (Byers et al. 1976). Although not used as direct input, a regional interpretation (Carr, et al. 1986a, Fig. 11) differs from the model and shows a thickness of more than 820 feet (250 meters) in northern Crater Flat northwest of the modeled area. In the northwestern part of the modeled area, thickness is constrained only by borehole G-2; however, this borehole may be located on a buried structural high and may not be representative of the regional trend.

In Figure 27, the anomalously thin Tram Tuff at borehole p#1 (601 feet (183 meters)) is interpreted in the model to be due to faulting. The faulted thickness had to be used in the model so that all stratigraphic contacts would be honored. This is true for any faulted contact, not just for p#1. If a hypothetical true thickness were used for the Tram Tuff in borehole p#1 and no fault explicitly modeled there, the model would not match the rest of the stratigraphic contacts in the borehole. The thickened Tram Tuff would have forced the other contacts to be out of place. (As described in Section 6.3, the model is built by thicknesses, not elevations.) No fault was included at this rock layer because no other information about the fault is available. An

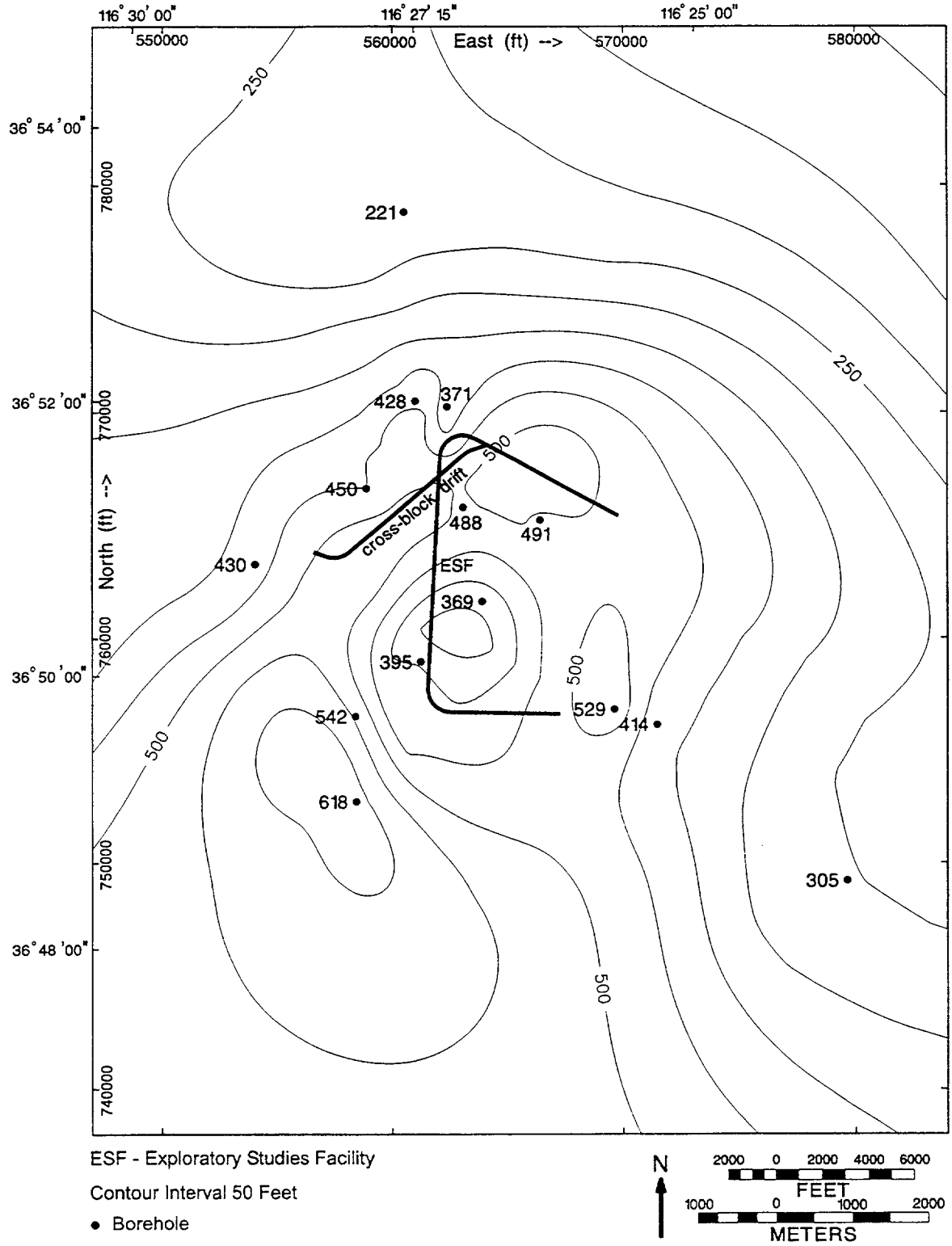

ESF - Exploratory Studies Facility

Contour Interval 50 Feet

• Borehole

N

2000 0 2000 4000 6000
FEET

1000 0 1000 2000
METERS

Figure 26. Model-Isochore Map of Bullfrog Tuff (Tcb)

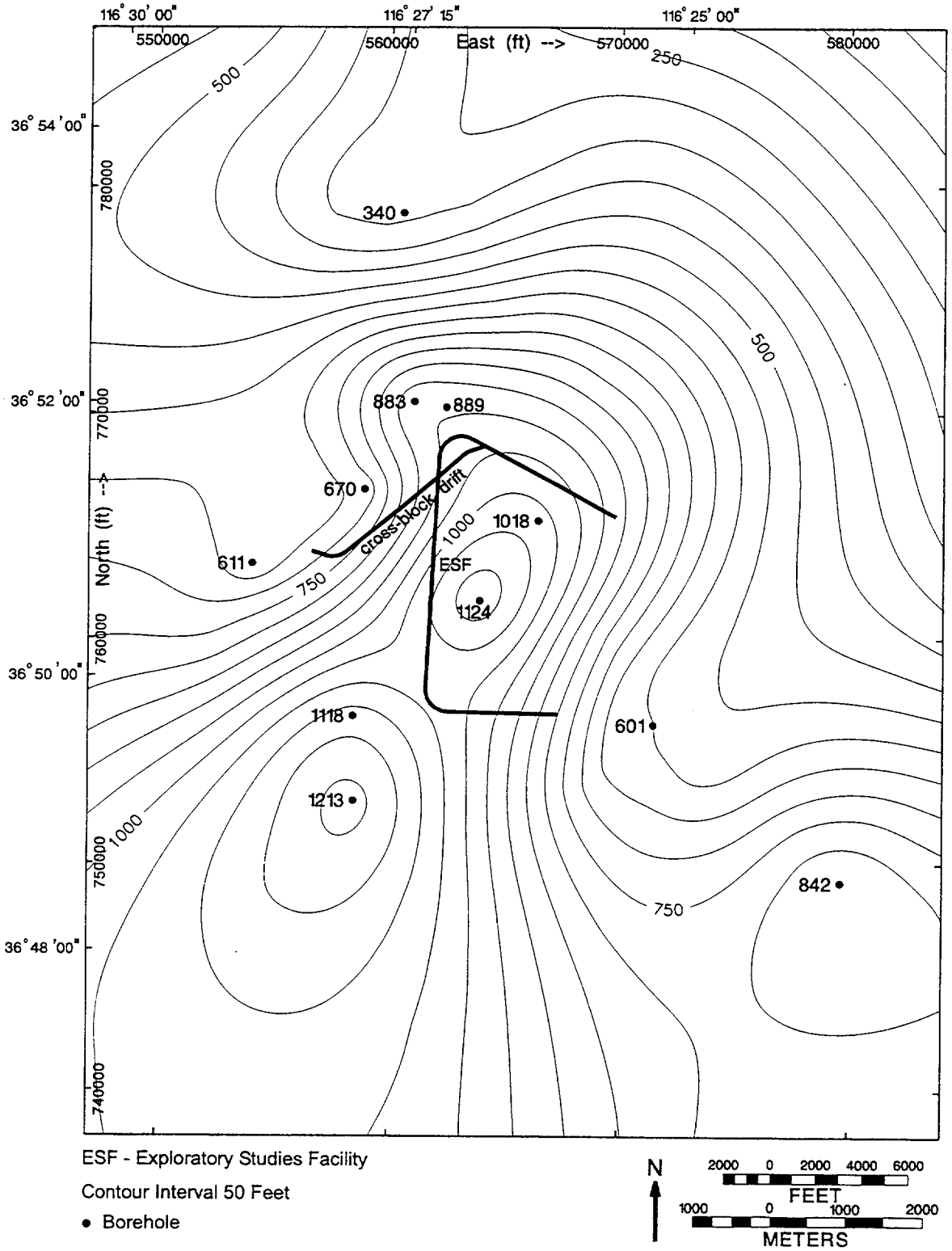

Figure 27. Model-Isochore Map of Tram Tuff (Tct)

alternative interpretation is that this fault is the Paintbrush Canyon fault and the Tertiary-Paleozoic contact in borehole p#1 is not the Paintbrush Canyon fault.

6.4.1.9 Older Tertiary Unit (Tund)

Overview–The Tertiary rocks older than the pre-Tram Tuff bedded tuff (Tctbt) are labeled as Tertiary undifferentiated (Tund) in the GFM. Although this unit represents the greatest share of the modeled volume, it is the least known of all the Tertiary units because few boreholes penetrate it.

The older Tertiary unit is important for hydrologic and radionuclide transport modeling because it lies in the flow path between the potential repository and the regional carbonate aquifer in the Paleozoic rocks below. It also makes up a large percentage of the saturated zone volume.

Data Distribution and Unit Geometry–The model interpretation for this unit is based on input data from 10 boreholes, only one of which fully penetrates the older Tertiary section (borehole p#1, DTN: MO9811MWDGFM03.000). The elevation of the top of this unit is shown in Figure 28. The unit thickness was not mapped because it is entirely dependent on the configuration of the Tertiary-Paleozoic unconformity derived from gravity data (DTN: LB980130123112.003). Because the Paleozoic surface was provided as an elevation grid, and the top of Tund was a reference horizon, no model-isochore map (grid) was generated for Tund during the model construction.

6.4.1.10 Tertiary-Paleozoic Unconformity

Overview–The configuration of the unconformity between Tertiary and Paleozoic rocks is subject to several interpretations, as described in the following paragraphs. The nature of the GFM is such that only one interpretation could be used, and the interpretation needed to cover the entire modeled area. These requirements limited the available sources to one, an interpretation of gravity data (DTN: LB980130123112.003), which is a recalculation of the Tertiary-Paleozoic unconformity that was initially used in GFM2.0. The interpretation incorporated in the GFM also had to be consistent with the other data from boreholes and the geologic map, which further narrowed the options.

The elevation of the Tertiary-Paleozoic unconformity is important for hydrologic modeling because it forms the top of the regional carbonate aquifer (Carr et al. 1986b, p. 6). Alternative interpretations are also potentially important because of the range of vertical differences between the interpreted surfaces, and consequent potential impacts on hydrologic and radionuclide transport modeling. According to the GFM interpretation, the unconformity occurs 8,000 to 11,000 feet (2,400 to 3,500 meters) below the ESF.

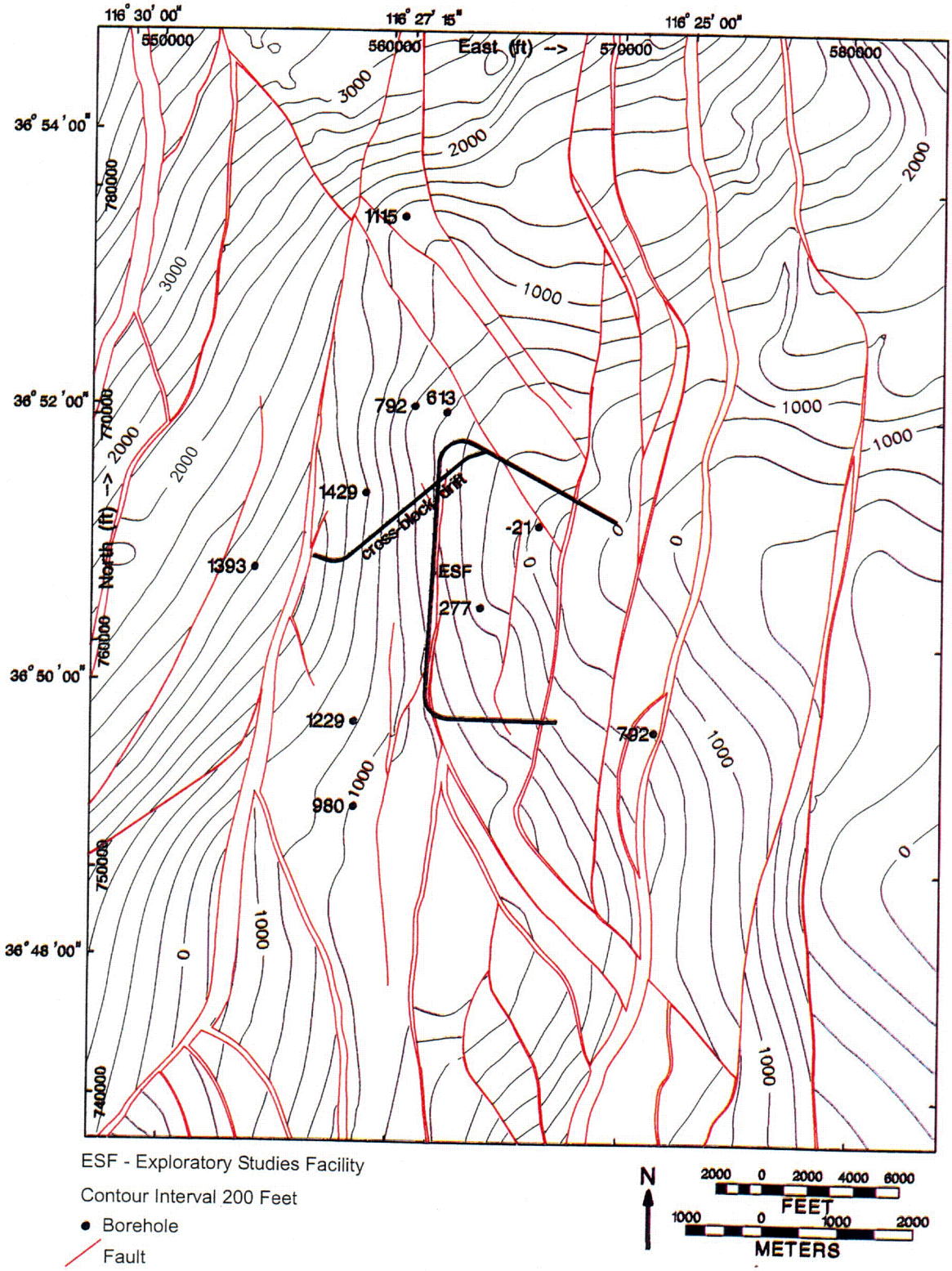

Figure 28. Elevation Map of Top of Older Tertiary Units (Tund)

C006

Data Distribution and Unit Geometry–The Tertiary-Paleozoic unconformity used in GFM3.1, shown in Figure 29, is modified from an interpretation of gravity data (DTN: LB980130123112.003). The surface in the GFM includes vertical displacements along the modeled faults, which were not included in the gravity interpretation. Fault displacements on the Tertiary-Paleozoic unconformity were constructed by matching the vertical displacements of the shallower modeled units and displacing the gravity interpretation. In the model area, only one borehole—p#1—penetrates the Paleozoic rocks which are encountered at an elevation of -400 feet (-122 meters) (DTN: MO9811MWDGFM03.000); therefore, the model relies primarily on the gravity interpretation.

The unconformity forms a high ridge beneath Busted Butte and Fran Ridge in the southeastern model area, falling away to deeper levels to the north and west. At its deepest point in the northwest, the unconformity is 13,000 feet (3,960 meters) below ground surface. At its shallowest point beneath Fran Ridge, it is 3,500 feet (1,060 meters) below ground surface. The deepening to the west can be explained by the combined down-to-the-west vertical displacement of several known north-trending Tertiary normal faults, but may also be enhanced by erosion and displacement on older, unknown faults. The deepening to the north may be a result of caldera subsidence and deposition of the thick Tertiary volcanic pile, or older deformation.

Discussion of Alternative Interpretations–There are several interpretations of the Tertiary-Paleozoic unconformity in the vicinity of borehole p#1 (DTN: LB980130123112.003; Brocher et al. 1998, Figures 7, 8, and 14; Feigner et al. 1998, Figure 7b). Although they are local interpretations, they coincide with part of the GFM interpretation (Figure 30; adapted from DTN: LB980130123112.003). No definitive data (such as another borehole or conclusive geophysical data) are available to distinguish between the alternatives; available data permit a variety of interpretations. This section discusses the reason for choosing the interpretation in the GFM over the others.

The GFM was constructed with the interpretation that the Tertiary-Paleozoic contact in borehole p#1 is the Paintbrush Canyon fault, as first interpreted in a USGS open file report in which the fault was called the Fran Ridge fault (Carr et al. 1986b, pp. 16 and 41, Figure 12). However, because the borehole data are inconclusive, other interpretations are possible, including an unfaulted unconformity at the Tertiary-Paleozoic contact, correlation of the fault at the unconformity to a fault other than the Paintbrush Canyon fault, or placement of the Paintbrush Canyon fault higher in the borehole.

On the other hand, an important observation is that the geologic map relations across the borehole p#1 vicinity (DTN: GS970808314221.002) show approximately 700 feet (210 meters) of vertical displacement along the Paintbrush Canyon fault and 400 feet (120 meters) of vertical displacement on the splay (labeled "PJ" in Figure 4) that arcs around the hill south of borehole p#1. These relations require at least a 1,100-foot (330-meter) down-to-the-west vertical displacement in the immediate vicinity of borehole p#1. The interpretation from the borehole report was accepted for the GFM because it is consistent with the geologic map data and formed a reasonable interpretation in three dimensions.

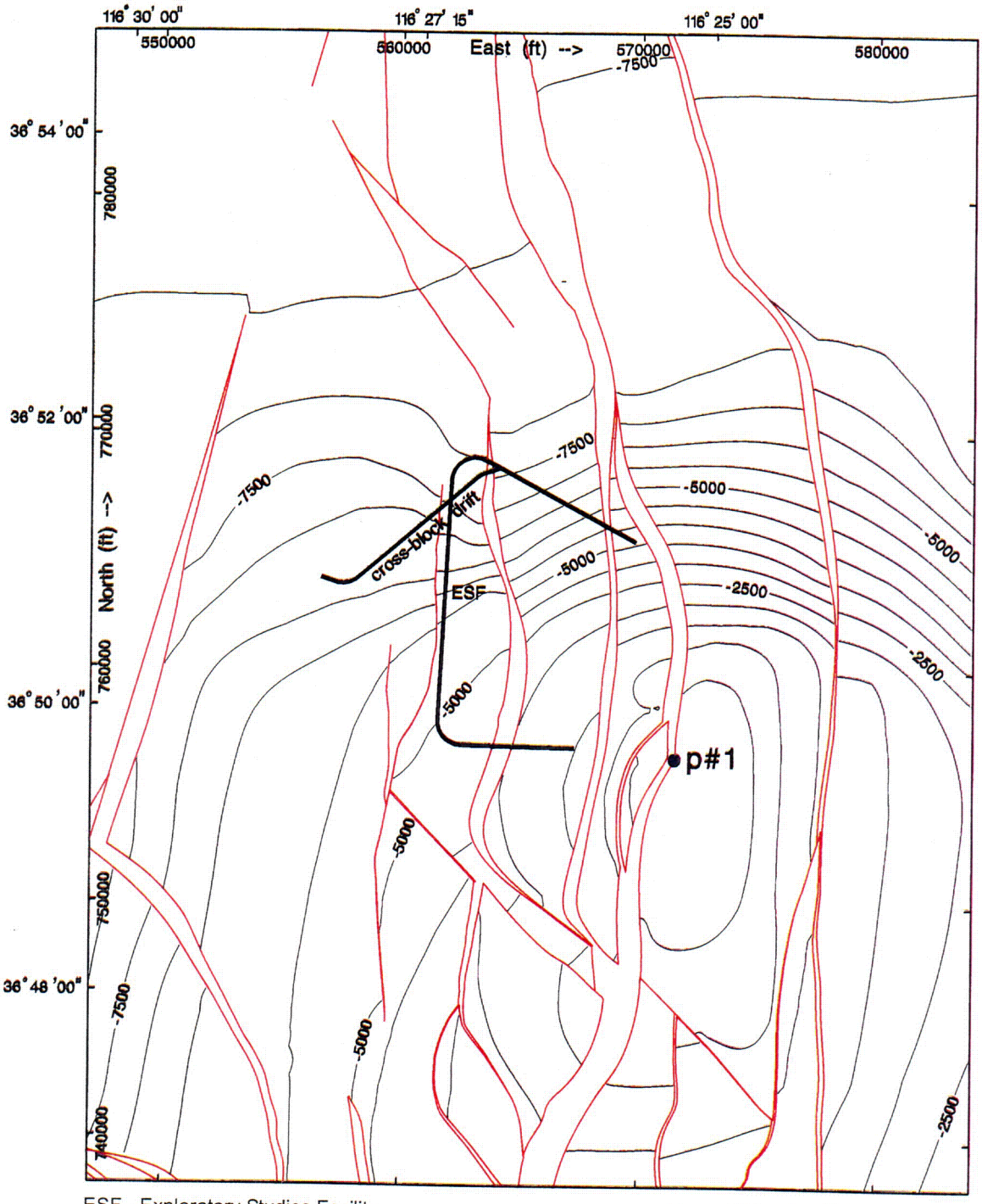

Figure 29. Elevation Map of Tertiary-Paleozoic Unconformity

C007

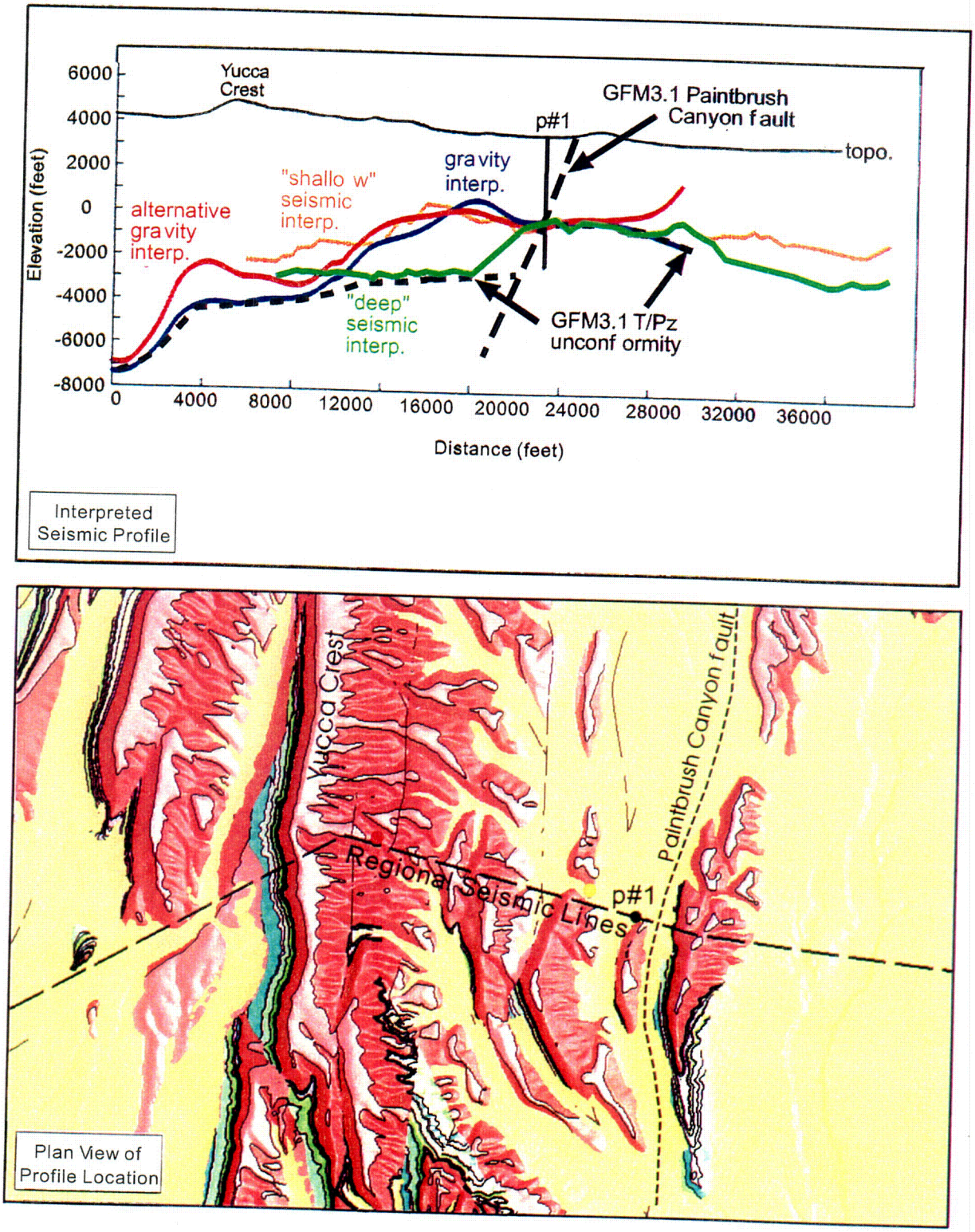

Figure 30. Comparison of Geophysical and GFM Interpretations of Tertiary-Paleozoic Unconformity

C008

An alternative interpretation would be that the Paintbrush Canyon fault is intersected at the base of the Tram Tuff and there is no fault at the Tertiary-Paleozoic contact. This configuration is plausible if the Tertiary-Paleozoic contact in borehole p#1 is interpreted as an erosional surface and not as a fault. To be consistent with published interpretations, however, the GFM represents the contact as a fault (Carr et al 1986b pp 16 and 41, Figure 12).

The gravity and seismic interpretations summarized by Majer et al. (1998) show the Tertiary-Paleozoic unconformity at shallow levels west of borehole p#1 (shown in Figure 30 as the red, orange, and blue lines), conflict with the geologic map relations discussed previously. The interpretations do not allow for 1,100-foot (330-meter) vertical displacement on normal faults in the vicinity of borehole p#1. Because the GFM could not be constructed with the use of the shallower interpretations and still be consistent with the data from the borehole and geologic map, the shallower interpretations were not used. To construct the Tertiary-Paleozoic unconformity in the GFM, it was necessary to modify the gravity interpretation (DTN: LB980130123112.003) to be consistent with the data from the borehole and geologic map. The gravity interpretation is shown in Figure 30 as the blue line.

As shown in Figure 30, the GFM interpretation is also consistent with the regional seismic profile (Brocher et al. 1998, Figure 14) and closely resembles the deep seismic interpretation (DTN: LB980130123112.003) by extending the high-amplitude, subparallel reflections (interpreted here to represent lower Tertiary rocks) 2,000 feet (610 meters) farther east. Although available data do not provide a unique solution, the consistency of the GFM interpretation with data from the borehole, geologic map, and seismic profile supports the interpretation.

Impacts of Alternative Interpretations–The alternative interpretations of the elevation of the Tertiary-Paleozoic unconformity show marked vertical differences 2 to 4 kilometers east of the ESF. The vertical differences between deep and shallow interpretations are on the order of 3,000 feet (1,000 meters) for a distance of 7,000 feet (2,100 meters) along the regional seismic profile west of borehole p#1. This produces a cross-sectional area of approximately 21,000 square feet (1,950 square meters) and a corresponding volume of disputed pre-Cenozoic rock between the potential repository horizon and the regional carbonate aquifer. The impacts of this difference on downstream models would need to be assessed in those modeling activities.

6.4.2 Interpretation of Faults

This section discusses the construction of faults for the GFM. Faults depicted in the GFM were constructed with the use of the methodology described in Section 6.3.3, and were intended to be consistent with current YMP structural and tectonic models (CRWMS M&O 1998b, Sections 3.3 and 3.6). The patterns of faulting, structural domains, and relative ages of the faults are discussed in previous work (CRWMS M&O 1998b, Section 3.6). The following sections discuss the particular features of the faults modeled in the GFM.

6.4.2.1 Fault Curvature

In the GFM interpretation, the dominant faults were constructed as slightly curved (i.e., a slight decrease in dip with depth) in cross section. The faults could also have been depicted with

greater curvature; however, in practical terms the uncertainty of fault geometries at depth outweighs any fine details that could be applied to the modeled faults.

6.4.2.2 Fault Patterns

The north-trending fault system (Figure 4) dominates the model. The largest of these faults are the Solitario Canyon and Paintbrush Canyon faults, both of which displace strata down to the west by more than 1,400 feet (425 meters) (DTN: GS970808314221.002). The Windy Wash fault is as large but is present only in the far northwestern edge of the model (DTN: GS970808314221.002). Other north-trending faults of note include the Fatigue Wash, Iron Ridge, and Bow Ridge faults, which form major topographic features of the site area. A system of faults beneath Midway Valley produces a series of small horst-graben bedrock structures now buried by alluvium.

Prominent topographic features have also formed along northwest-trending faults in the site area. A series of northwest-trending faults is present in the prominent drainages (Drillhole, Pagany, and Sever Washes) in the north-central part of the area. The vertical displacements on these faults are small and, therefore, are not significant in the model. In the southern part of the area, Dune Wash contains a complex pattern of intersecting north- and northwest-trending faults including the Dune Wash fault, which has a maximum vertical displacement of more than 200 feet (61 meters). The mapped pattern of faults in Dune Wash is complex (DTN: GS970808314221.002), so much so that only a few of these faults could be included in the GFM. The actual structure in Dune Wash is, therefore, more complex than represented in the GFM.

6.4.2.3 Features of Individual Faults

The Paintbrush Canyon fault (Figure 4) is the longest of the faults in the GFM and has the greatest Tertiary vertical displacement. The main strand of the fault passes along the west side of Fran Ridge. The report for borehole p#1 called this the Fran Ridge fault (Carr et al. 1986b, Figure 12) and indicated that it intersects borehole p#1 at the Tertiary-Paleozoic unconformity. This is the interpretation used to construct the Paintbrush Canyon fault in the GFM. The Paintbrush Canyon fault reaches its maximum vertical displacement of approximately 1,400 feet (425 meters) in the model area at the mouth of Dune Wash, where several faults intersect the Paintbrush Canyon fault and increase the total vertical displacement.

The Solitario Canyon fault is a scissor fault that changes dip direction at Tonsil Ridge from west-dipping in the south to east-dipping in the north (DTN: GS970808314221.002). The location of Tonsil Ridge is indicated in Figure 2. As described in Section 6.2.2.6, this dip change was generalized in the GFM as a single surface. Interpretations from the model from Tonsil Ridge northward should take this generalization into account. The uncertainties regarding fault dips and locations at great depth are expected to outweigh the potential impacts of the generalization.

The Bow Ridge fault (Figure 4) is also a scissor fault, with its hinge point covered by alluvium approximately at the mouth of Sever Wash (DTN: GS970808314221.002). Outcrop and borehole data indicate that the fault passes between borehole WT#16 and the outcrop to the west,

and that the apparent displacement is down-to-the-east (DTN: GS970808314221.002). North of the hinge point, the Bow Ridge fault is called the "Mid-E" fault in the GFM (Figure 4).

Minor faults, such as the Ghost Dance, Abandoned Wash, and numerous faults around Dune Wash, appear to be secondary features that accommodated strain between the dominant faults (DTN: GS970808314221.002). Their intersections with more dominant faults at depth are uncertain; however, the interpretation shown in the GFM is that the Dune Wash, Bow Ridge, and Midway Valley faults intersect the Paintbrush Canyon fault at depth. The Ghost Dance and Abandoned Wash faults do not intersect any major faults in the GFM, but could at deeper crustal levels.

6.4.2.4 Faulting and Deposition

In the GFM, model-isochore maps of the Paintbrush Group and older units do not show changes in thickness across faults, although some minor changes could be interpreted from the available data. Data distribution for this kind of detailed analysis is limited. Geologic map relations (DTN: GS970808314221.002) show that isolated thickness changes across faults in Solitario Canyon and Fatigue Wash are associated with pre-Tiva Canyon Tuff faulting. However, the greatest fault displacement and tilting of the stratigraphic section appear to have occurred after the deposition of the Tiva Canyon Tuff (CRWMS M&O 1998b, p. 3.3-3). Thickness changes across faults are, therefore, likely to be relatively small in the Paintbrush Group but are probably more common than that indicated by currently available data.

The YMP boreholes are too sparse to define pre-Topopah Spring Tuff structural relief in the modeled area. Some pre-Calico Hills Formation faulting may be implied by available borehole and geophysical data; however, details such as fault locations, strikes, dips, or vertical displacements are insufficiently well determined to be modeled.

6.5 UNCERTAINTIES AND LIMITATIONS

For the GFM, uncertainty is an estimation of how closely the model matches the real world. The primary factor affecting uncertainty in the GFM is distance from the data. Because borehole data are restricted in depth, uncertainty increases with vertical distance below the boreholes, as well as with horizontal distance away from them. Likewise, interpretations regarding deeper rock units, which have fewer borehole penetrations, have more uncertainty associated with them than do interpretations associated with shallower rock units. Rock layers near the surface are constrained by the geologic map (DTN: GS970808314221.002).

Because of the faulting and tilting of the rock layers in much of the modeled area and the sparseness of data, geostatistical techniques were not used to estimate uncertainty. Instead, methods that examine the modeling process were used to determine the amount of uncertainty associated with gridding, contouring, interpreting, and interpolating. The details of these methods are provided in Attachment V.

The modeled area is divided into *constrained* and *less constrained* areas for the purposes of estimating subsurface uncertainty (Figure 31). Constrained areas are those between at least two boreholes, whereas less constrained areas are those outside borehole control or are influenced by geologic complexity. Described in other terms, the constrained areas are those for which subsurface interpretations are *interpolated* between borehole data, and the less constrained areas are those for which subsurface interpretations are *extrapolated* from data. Because an interpolation is constrained on at least two sides, its uncertainty is generally less than that of an extrapolation. Note that in the vertical dimension, the boundaries of the constrained and less constrained areas vary because boreholes were drilled to various depths. Also, the uncertainty of interpolations increases with distance from the boreholes.

An inherent feature of all three-dimensional geologic models is that the subsurface is only partially known. Knowledge of the subsurface is defined by the number and distribution of boreholes and tunnels. For the modeled area at Yucca Mountain, approximately 1 percent of the subsurface volume (measured to the depth of the deepest borehole, 6,000 feet (1,830 meters) below ground surface) is within 500 feet (150 meters) of a borehole or tunnel. This means that uncertainty is unavoidable. Uncertainty is mitigated by the application of sound geologic principles to interpolate between the data and extrapolate into unknown areas.

Uncertainty regarding constrained areas and less constrained areas is discussed separately in the following subsections.

6.5.1 Uncertainty Estimates for Constrained Areas

6.5.1.1 Elevation Uncertainty

The results of elevation uncertainty estimation are discussed in this section. The details of the estimation process are presented in Attachment V. The uncertainty is greater for deeper units, for which there are fewer borehole data, and is less for shallower units, for which there are more data. As discussed in Attachment V, elevation uncertainty is summarized with the following expected windows:

- Surface to Tptrv1: ±30 feet (9 meters)
- Tptrv1 to Tac (includes the RHH): ±40 feet (12 meters)
- Base of Tac to Tctbt: ±50 feet (15 meters).

The term *expected window* means that the model is expected to predict the elevation of a horizon within that window. For the RHH, as an example, the maximum uncertainty of ±40 feet (12 meters) at a distance of about 3,280 feet (1,000 meters) from the borehole is the expected window. A prediction that is confirmed within the expected window is considered acceptable.

Beyond 3,280 feet (1,000 meters) from a data point, uncertainty is bounded only by what is known about the structure and/or stratigraphy of the area. Uncertainty estimates for the GFM are made with the knowledge that unknown geologic features in the subsurface may add an unquantifiable uncertainty. Therefore, the estimates described in this selection apply to relatively simple situations.

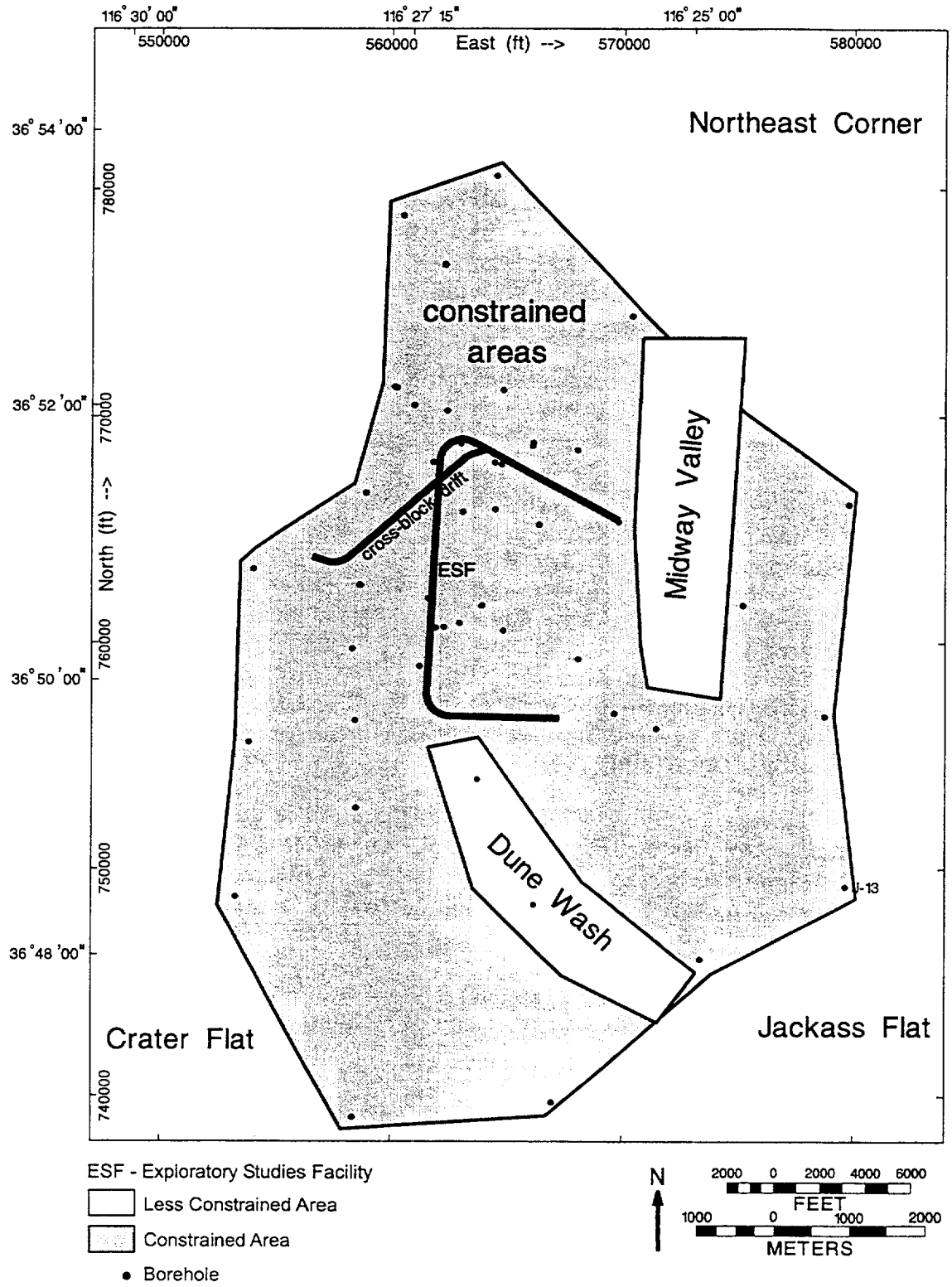

Figure 31. Map of Constrained and Less Constrained Areas

The uncertainty window was estimated by two empirical methods—an analysis of contouring and a piecewise reconstruction of the model. Both methods are discussed in more detail in Attachment V.

6.5.1.2 Thickness Uncertainty

Thickness uncertainty is used to evaluate the distributions of individual rock layers. It is a contributing factor to elevation uncertainty. Because the rock layers in the GFM were built with the use of the thicknesses of rock layers, thickness uncertainty is an important contributor to uncertainty in the model. As discussed in Section 6.3, the elevations of the rock layers in the GFM were calculated by the addition or subtraction of model-isochores from three reference horizons (elevation control surfaces), which are located near the top, middle, and bottom of the model. Therefore, the effects of thickness uncertainty are cumulative, such that each model-isochore added to (or subtracted from) the previous layer contributes its own uncertainty to the resulting elevation of the rock layer. Cumulative thickness uncertainty is controlled in the model, however, by the three reference horizons and adherence of the model to the input borehole data, which are fixed in space. Because of these controls, cumulative thickness uncertainty is not expected to exceed the elevation uncertainty discussed in the previous section.

In addition to distance from data, thickness uncertainty depends on the range of thickness of a unit. Because of the nature of the volcanic rocks that comprise Yucca Mountain, thickness uncertainty is also a function of the depositional and postdepositional processes that affected a particular unit. As a rough estimate of thickness uncertainty in practical terms, thickness uncertainty for a given unit is approximately equal to the contour interval shown in the figures of this report and discussed in Attachment V, Section V.2. Because there is no exact formula for calculating thickness uncertainty as a function of these factors and because an model-isochore is dependent on the interpretation of geologic processes, the estimates given below are approximate and semiquantitative.

To illustrate the dependence of uncertainty on thickness range and geologic processes, Figure 32 shows the thickness of the Topopah Spring Tuff crystal-rich vitrophyre (Tptrv1), which formed in response to specific thermal and chemical processes. The nature of those processes was such that the unit thicknesses indicated by the data range from 0 to 10 feet (0 to 3 meters) but ranged from 2 to 5 feet (1 to 2 meters) over most of the modeled area. The conceptual model (Section 6.3.1) and corroborating data (DTN: GS950608314211.025) suggest a thicker lobe at the northwestern edge of the modeled area. Because of the relative thinness of the unit, the uncertainty is limited to a very small numerical value (approximately 5 feet (2 meters)) but a high percentage of the unit's total thickness range.

In contrast, Figure 33 shows the model-isochore map for the RHH, which is a group of layers that formed in response to broader geologic processes. The RHH has a much greater thickness range than the crystal-rich vitrophyre Tptrv1—from about 200 to 760 feet (about 61 to 230 meters); however, uncertainty within the constrained area is a much smaller percentage of the thickness range—on the order of 50 feet (15 meters).

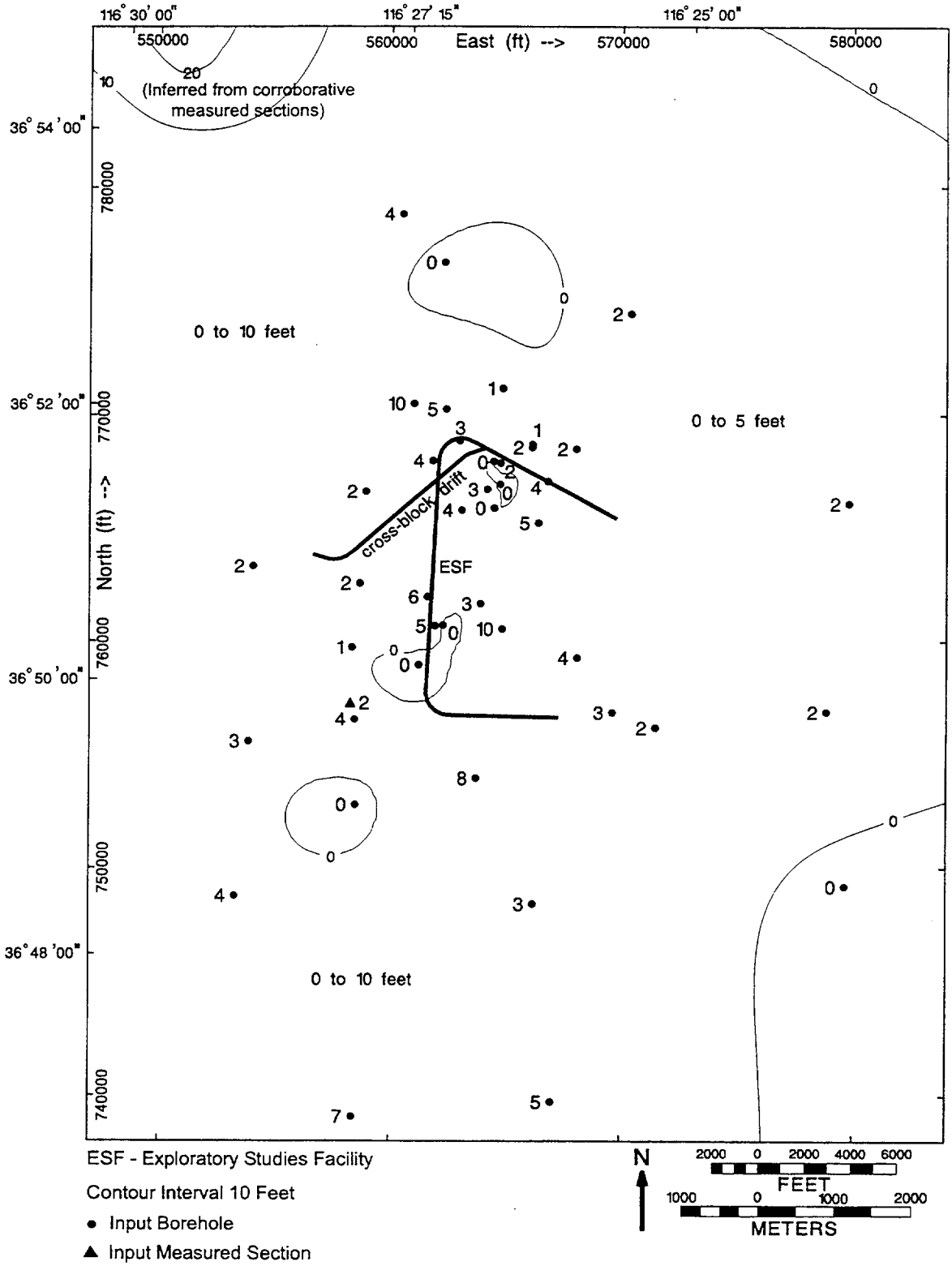

Figure 32. Model-Isochore Map of Topopah Spring Tuff Crystal-Rich Member Vitric Zone Densely Welded Subzone (Tptrv1)

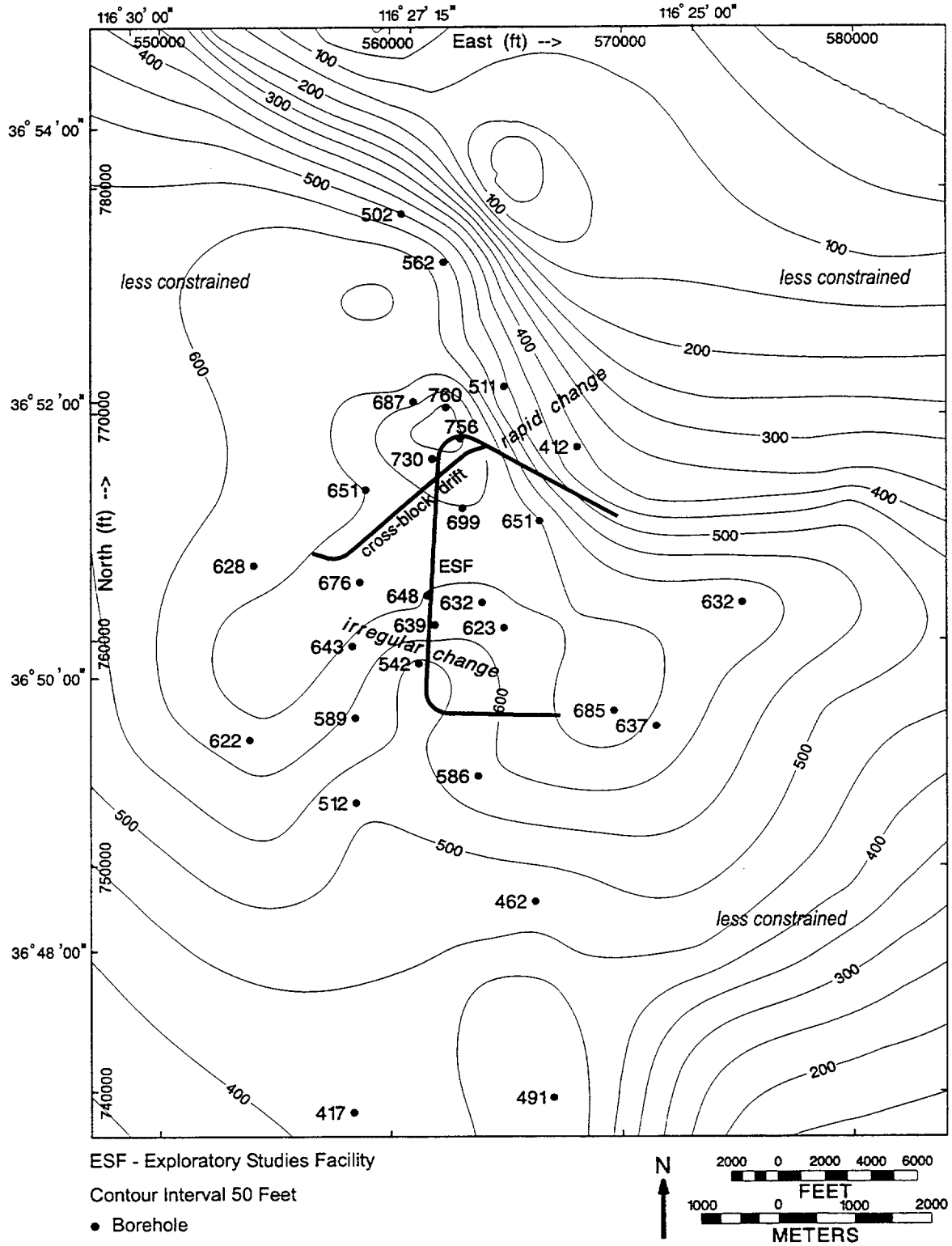

ESF - Exploratory Studies Facility

Contour Interval 50 Feet

• Borehole

N

2000 0 2000 4000 6000
FEET

1000 0 1000 2000
METERS

Figure 33. Model-Isochore Map of Repository Host Horizon Showing Less Constrained Areas

6.5.2 Uncertainty Estimates for Less Constrained Areas

In addition to distance from data, other factors contribute to uncertainty in some areas of the modeled block. These factors include uncertain amounts of fault displacements, unsampled fault blocks, and structural complexity buried by alluvium. The affected areas are the northeastern corner of the modeled area, Midway Valley, Crater Flat, Jackass Flat, and the Dune Wash area (Figure 31). In addition, much of the subsurface in the corners of the model area is unconstrained by data. Collectively, these areas are called the *less constrained areas* because they are physically outside borehole control or because of geologic complexity. Finally, the deeper geologic units (older Tertiary and pre-Tertiary units) are sufficiently deeper than most data so they are also considered to be less constrained. Uncertainty in these areas can be estimated only qualitatively because the only available constraints are distant data or conceptual models.

Northeastern Corner–The greatest uncertainty in the model is associated with the northeastern corner of the modeled area. It is unquantifiable from the lower Calico Hills Formation and below because the base of the Calico Hills Formation is not exposed in the area and no subsurface data are available.

Midway Valley, Crater Flat, and Jackass Flat–Structure beneath Midway Valley is qualitatively constrained only by geophysical profiles, which do not provide stratigraphic details. Crater Flat and Jackass Flat are large areas covered by alluvium and are constrained only by widely scattered boreholes, so structural details are not known with any degree of confidence.

Dune Wash–The uncertainty associated with the Dune Wash area is largely due to localized structural complexity, the details of which are largely buried by alluvium. Based on geologic mapping (DTN: GS970808314221.002), faults are likely to be present between boreholes WT-1 and WT#17 (shown on Figure 3), between the boreholes and outcrop so that little detail can be projected from one location to another.

Older Tertiary and pre-Tertiary Units–Because of their depth below ground surface and the minimal measured data available, the older Tertiary (Tund) and pre-Tertiary units have more uncertainty associated with them than the more recent Tertiary units. The depth of the Tertiary-Paleozoic unconformity is constrained at only one point (borehole p#1) and is extrapolated across the modeled area by means of a gravity model (DTN: LB980130123112.003). Because only the p#1 borehole provides data on the physical properties of the older Tertiary (Tund) and pre-Tertiary units for gravity calculations, vertical uncertainty for the depth of the unconformity is more than 3,280 feet (1,000 meters), except in the vicinity of borehole p#1.

6.5.3 Limitations and Alternative Interpretations

Because each reference horizon and model-isochore in the GFM is an interpretation, each is non-unique, and other viable interpretations are possible. All interpretations and predictions made by the GFM are bounded by an expected window of uncertainty, and it is implicitly recognized that alternative interpretations that fall within this window would also be considered valid. Changes to the GFM within the expected window of uncertainty would not, therefore, be considered significant. A significant change to the GFM (or a significant alternative interpretation) would be one that exceeds the expected window of uncertainty.

It is recognized that by inclusion of offsite boreholes (VH-1, VH-2, J#12, and JF#3) and regional data, the methodology applied in this AMR can generate viable alternative interpretations that differ from the interpretations presented by GFM3.1. This is especially true in the less constrained areas of the model (the model boundaries, corners, and deeper stratigraphic units). Additionally, selection of different modeling techniques (i.e. computer triangulation, hand contouring, or geostatistical methods) could also result in viable alternative interpretations.

As stated above, alternative interpretations can result from application of different conceptual models, gridding algorithms, modeling methods, or consideration of different data sets. Examples of alternative interpretations are discussed below.

The thickness of the Topopah Spring Tuff (Tpt) shown in Figure 20 could be alternatively interpreted using a conceptual model that it thickens into the structural low in Crater Flat. Using this conceptual model, the formation thickness could be shown to increase toward the southwest instead of decreasing as shown in the figure. The thickness of the Topopah Spring Tuff lower vitrophyre (Tptpv3) shown in Figure 18 could also be shown to thicken toward the southwest using the same conceptual model, or by using a different interpolation scheme to offsite borehole VH-2, which is 3.9 miles (6.4 kilometers) from the edge of the model and indicates a thick vitrophyre as discussed in Section 6.4.1.4.

The thickness of the Tram Tuff (Tct) shown in Figure 27 could be interpreted differently in the vicinity of borehole G-2. This borehole appears to be located on a buried structural high, so that the Tram Tuff is unusually thin in the borehole. Using a different conceptual model for this structural high, the thickness in G-2 could be illustrated with closed contours instead of the axis of thinning shown. The orientation of the structural high could also be illustrated on this map by imparting a trend to the contours based on a structural conceptual model.

In addition, the thickness of both the Tram Tuff (Tct) and the Prow Pass Tuff (Tcp) could be interpreted differently, particularly in the northeast corner of the model. Regional trends could be interpreted to suggest that these tuffs have a more pronounced and abrupt thinning to the northeast beneath the overlying Calico Hills Formation (Ta).

Alluvial thickness is of importance to the processes that control the rate and spatial distribution of net infiltration at land surface over the site area. Estimates of alluvial thickness for these purposes are discussed in an AMR that is being prepared in support of the UZ Flow and Transport PMR. These estimates, however, are concerned with establishing only minimum and bounding depths of alluvium and as such do not provide an alternative interpretation of alluvial thicknesses as embodied in the GFM and thus the ISM.

Finally, it should be noted that appropriate use of the GFM is inherently limited by scale and content. The grid spacing used in the GFM (200 feet, 61 meters), discussed in Section 6.3.2.1, limits the size of features that can be resolved by the model. Users of the GFM must also consider the data reduction discussed in Section 6.1.1 and the selection of faults discussed in Section 6.1.2 to determine whether the GFM is appropriate for specific applications.

6.5.4 Effect of To Be Verified (TBV) Input on the GFM

The data inputs having TBV status are indicated in the DIRS data base. Because the key inputs to the model are currently TBV, excluding them would prohibit construction of the model. Accordingly, the GFM itself (DTN: MO9901MWDGFM31.000) has been assigned a TBV number. Those TBV data on which the GFM is based currently are being evaluated to verify their quality-assurance status. Data identified to be unqualified through this verification activity will be subject to an independent qualification process, in accordance with AP-SIII.2Q, to ensure that those data on which the GFM is based are fully qualified. Because it is anticipated that all data on which the GFM is based ultimately will be qualified, there is no need at this time to develop criteria, pursuant to AP-3.10Q, by which to assess the impact and appropriateness of the use of unqualified data on the applicability or validity of the GFM.

6.6 GFM VALIDATION

The GFM was validated by predicting the subsurface geology for two boreholes and one tunnel, and comparing the predictions to the actual results. The purpose of the validation was to assess whether the GFM provides an adequate representation of the Yucca Mountain site geology.

6.6.1 Validation Criteria

To assess whether the GFM provides an adequate representation of the geology of the site, the validation criteria were formulated as follows:

- The model was considered valid if the majority of actual results were within the expected window of uncertainty (as described in Section 6.5).
- For results not within the expected window of uncertainty, the results were analyzed for a cause. Where the cause was determined to be a geologic feature that is unpredictable (i.e., not predictable to a high degree of accuracy) given the available data, the results did not affect the model validation.
- The model would be considered invalid if a majority of the predictions were not within the expected window of uncertainty and a reasonable geologic cause (i.e., an unpredictable geologic feature) could not be determined.
- Because the GFM was constructed by mapping (predicting) rock layer thicknesses, thickness predictions were given the greatest weight in the validation.

Some anomalous rock layer contacts or structures were expected given the geologically complex setting of Yucca Mountain on the flank of a major caldera complex, but the model was expected to provide an adequate representation of the total stratigraphic package.

Uncertainty is discussed in Section 6.5. Details of the uncertainty estimation methods are provided in Attachment V.

6.6.2 Predictions for Boreholes SD-6 and WT-24 and the ECRB Cross-Block Drift

Predictions were made from Version GFM3.0, which was completed before boreholes SD-6 and WT-24 and the ECRB cross-block drift were constructed. The model was then updated to incorporate the new data in Version GFM3.1 (the current version). The predictions for SD-6 and the ECRB cross-block drift illustrate the model's predictive capability and uncertainty in an area constrained by borehole data, whereas the predictions for WT-24 do so for a less constrained area.

6.6.2.1 Predictions for Borehole SD-6

Table 6 and Figure 34 show the predicted stratigraphy for borehole SD-6 and the actual results. Of 26 predicted contact elevations, 22 (85 percent) were within the expected window of uncertainty. In borehole SD-6, the contact elevations not predicted within the expected window of uncertainty were Tpbt1, Ta, Tcp, and Tcb. The source of the elevation mismatches was thickness mismatches in two units. As listed on Table 6, model unit Tptpv1 was 22 feet (7 meters) thinner than predicted and unit Ta was 24 feet (8 meters) thinner than predicted. These two thickness errors caused the subsequent elevation prediction errors. In terms of the model validation criteria, the source of the thickness prediction errors for Tptpv1 and Ta must be examined.

Like all of the subunits within the Topopah Spring Tuff, unit Tptpv1 formed in response to multiple depositional processes and was subjected to postdepositional processes (Buesch et al. 1996, pp. 9–12), which resulted in variable thicknesses. The thickness of Tptpv1 is highly variable in the area of SD-6, ranging from 71 feet (22 meters) at SD-12, which is 3,000 feet (914 meters) east of SD-6, to 28 feet (9 meters) at UZ-6, which is 2,800 feet (853 meters) to the south (data from DTN: MO9811MWDGFM03.000). In view of the steep thickness gradient in this area, the prediction error for Tptpv1 in SD-6 is considered to be reasonable.

The Calico Hills Formation was 24 feet (7.3 meters) thinner than expected, which, in view of the model-isochore map (Figure 24), is within an acceptable uncertainty range as defined in Attachment V because of the thickness gradient that passes through the area surrounding SD-6.

The cumulative elevation error caused by the thickness differences of Tptpv1 and Ta also affected the elevation prediction at the top of the Prow Pass Tuff, which was 80 feet (24.4 meters) higher than predicted. The Prow Pass Tuff was only 9 feet (2.7 meters) thicker than expected, suggesting that the tuff may be on a structural high that formed after deposition of the Prow Pass Tuff but before deposition of the Calico Hills Formation. The Prow Pass Tuff thickness map is illustrated in Figure 25. The model shows no effect of possible pre-Calico structure on the RHH (Figure 20).

It is significant to note that the total Topopah Spring Tuff thickness prediction was within 4 percent of actual, suggesting that the observed thickness variations of the subunits are largely a function of depositional and postdepositional processes operating within the formation. The actual thickness was 1,035 feet (315 meters), and the predicted thickness was 1,083 feet (330 meters).

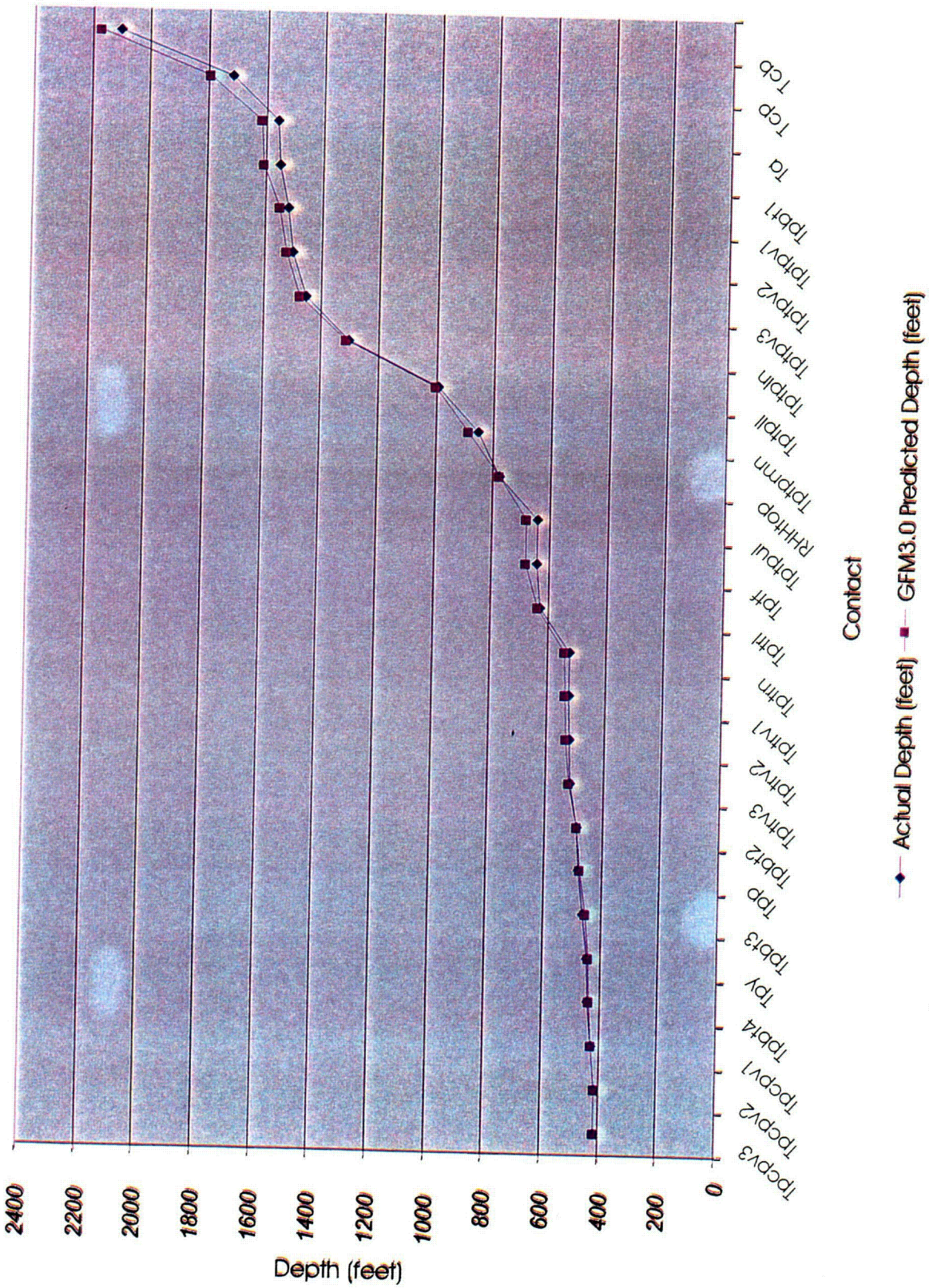

Figure 34. SD-6 Comparison of Predicted Versus Actual Contact Depths

C009

In summary, the model meets each validation criterion for the SD-6 predictions. Where contact elevations and thicknesses were not predicted within the expected window of uncertainty, the causes can be ascribed to unpredictable geologic features. Because it is relatively well constrained by surrounding boreholes, borehole SD-6 illustrates the model's predictive capabilities and the effects of geologic variability on model predictions in a constrained area.

6.6.2.2 Predictions for Borehole WT-24

Because borehole WT-24 was located outside the area constrained by boreholes when it was drilled, it provides an assessment of uncertainty for the GFM in a less constrained area. In addition, WT-24 is located in an area that is more stratigraphically and structurally complex than borehole SD-6, so the predictions at WT-24 are expected to be less accurate (that is, the window of uncertainty is greater due to geologic complexity and lack of subsurface data). The nearest borehole to WT-24 is approximately 3,200 feet (975 meters) away (borehole G-2; Figure 3) and no others are within 5,000 feet (1,500 meters). For evaluation purposes, however, the predictions will be compared to the maximum uncertainty windows for constrained areas discussed in Section 6.5.

Table 7 and Figure 35 show the predicted stratigraphy for borehole WT-24 and the actual results. Only 12 of 24 elevation predictions (50 percent) were within the expected window of uncertainty; however, it is readily apparent from Table 7 that the mismatch for the other 12 units is the result of cumulative errors. The thicknesses of 5 model units (Tpp, Tptpul, RHHtop, Tptpmn, and Tptpln) caused elevation errors in all 12 units. The causes of error in the 5 unit thickness predictions are discussed below.

As illustrated in Figure 18, the Pah Canyon Tuff (model unit Tpp) thickens toward the north in the area of WT-24. Without the constraint of WT-24, little data are available to constrain the thickness of Tpp in this area, and the thickness is not predictable with a high degree of precision. In this context, the thickness prediction error is reasonable.

The Topopah Spring Tuff units Tptpul, RHHtop, Tptpmn, and Tptpln, which were the source of additional cumulative elevation errors, were formed by multiple depositional and postdepositional processes (Buesch et al. 1996, pp. 9–12), which resulted in variable thicknesses that are not predictable to a high degree of accuracy. The model-isochore map for the RHH (Figure 23), which includes units RHHtop, Tptpmn, and Tptpln (and also Tptpll), shows that this interval is changing thickness rapidly through the area of WT-24. In view of the steep thickness gradient and the variable nature of the units, the thickness prediction errors for these units are reasonable.

It is important to note that the Topopah Spring Tuff was 93 feet (28 meters) thicker than expected, 55 feet (17 meters) of which was contributed by the anomalous Tptpln, which was predicted to be absent in the borehole. Without this anomalous unit, the predicted thickness of the formation was close to actual (1,057 - 55 = 1,002 feet (305 meters)) versus 964 feet (294 meters) predicted—a difference of 37 feet (11 meters), or within about 3.7 percent—suggesting that the overall modeling approach is appropriate for the geology of the modeled area. Observed differences are most likely caused by singular geologic variability related to the depositional and postdepositional processes that affected individual rock layers.

Table 6. Predicted Versus Actual Contacts in Borehole SD-6

Unit	Actual Depth (feet)[a]	GFM3.0 Predicted Depth (feet)	Difference in Depth (Predicted Minus Actual) (feet)	Actual Unit Thickness (feet)	GFM3.0 Predicted Thickness (feet)	Difference in Thickness (Predicted Minus Actual) (feet)
Tpcpv3	415	414	-1	0	0	0
Tpcpv2	415	414	-1	14	15	1
Tpcpv1	429	429	0	13	8	-5
Tpbt4	442	437	-5	3	7	4
Tpy	445	444	-1	21	13	-8
Tpbt3	466	457	-9	14	22	8
Tpp	480	479	-1	9	11	2
Tpbt2	489	490	1	29	33	4
Tptrv3	517	523	6	3	13	10
Tptrv2	521	536	15	5	4	-1
Tptrv1	526	540	14	2	3	1
Tptrn	527	543	16	105	98	-7
Tptrl	632	641	9	14	44	30
Tptf	646	685	39	0	0	0
Tptpul	646	685	39	134	96	-38
RHHtop	780	781	1	73	106	33
Tptpmn	853	887	34	142	118	-24
Tptpll	995	1,005	10	310	308	-2
Tptpln	1,305	1,313	8	151	164	13
Tptpv3	1,456	1,477	21	47	49	2
Tptpv2	1,503	1,526	23	17	26	9
Tptpv1	1,520	1,552	32	32	54	22
Tpbt1	1,552	1,606	54	9	11	2
Ta+Tacbt	1,561	1,617	56	154	178	24
Tcp	1,715	1,795	80	388	379	-9
Tcb	2,103	2,174	71	Not fully penetrated		

[a]Source: DTN: SNF40060298001.001

The bottom of the Calico Hills Formation (Ta) was not penetrated in borehole WT-24, even though drilling progressed to more than 300 feet (91 meters) below the predicted depth. There is no subsurface control for Calico thickness east of borehole G-2, and the bottom of Calico is not exposed anywhere to the northeast, so its maximum thickness is unknown. The poor subsurface constraints in the northern part of the modeled area do not permit definition of the maximum expected uncertainty regarding the thickness of the Calico Hills Formation in this area.

In summary, the model meets each validation criterion for the WT-24 predictions. Where contact elevations and thicknesses were not predicted within the expected window of uncertainty, the causes can be ascribed to unpredictable geologic features. Because it is not well constrained by surrounding boreholes, borehole WT-24 illustrates the geologic variability expected to be found in less constrained areas.

6.6.2.3 Predictions for Enhanced Characterization of the Repository Block (ECRB) Cross-Block Drift

Table 8 shows predicted and actual locations of stratigraphy contacts for the ECRB cross-block drift. The vertical difference between predicted and actual stratigraphic contacts was calculated by the transformation of tunnel stations into elevations, correction for stratal tilt, and subtraction of one from the other. Two of the three contacts were encountered within the expected window of uncertainty for these horizons at this location (±40 feet (12 meters)). In the west end of the tunnel, where faults having vertical displacements of 10 feet to greater than 16 feet (3 meters to greater than 5 meters) appear to have caused most of the difference between predicted and actual elevations for the Tptpln contact. Although the faults in the west end of the tunnel were not mapped at the surface, they were not wholly unanticipated because it was known beforehand that structural deformation increases in proximity to the Solitario Canyon fault and that small faults are present in the mountain. In the ECRB cross-block drift, the Tptpln contact is within 650 feet (200 meters) horizontally of the Solitario Canyon fault. As a result, the prediction error for the Tptpln contact, while outside the expected window of uncertainty, can be explained in terms of geologic variability without affecting validation of the model (the faults are too small to have been included in the model). Had they been known beforehand, the small faults could have been accounted for by adjusting stratigraphic elevations without modeling the faults.

The predictions for the cross-block drift suggest that the GFM will provide predictions of subsurface stratigraphy for future repository tunneling within the expected window of uncertainty. Predictions may be affected on the far western edge near the Solitario Canyon fault and elsewhere if small, unmapped faults like those in the cross-block drift are encountered at other locations.

6.6.3 Validation Results

The predictions of subsurface geology made from the GFM for boreholes SD-6 and WT-24 and the ECRB cross-block drift were used to validate the GFM. The results show that the preponderance of subsurface stratigraphy was predicted within the expected window of uncertainty, and the model satisfied all validation criteria. Predictions that lay outside the window of uncertainty can be explained in terms of geologic variability and not as deficiencies in the model. Because a certain amount of geologic variability was known to be an inherent part of Yucca Mountain and some anomalies were anticipated, the results of the predictions are considered to demonstrate that the GFM provides an adequate representation of the geology of Yucca Mountain.

In addition to the stratigraphic predictions, a structural prediction was also made. Based on geologic map data, the west dipping Solitario Canyon fault was predicted to intersect the cross-block drift at station 25+55. The fault was encountered at station 25+83, indicating that the fault dips slightly more shallowly than predicted. Given that the Solitario Canyon fault has highly variable dip at the surface (DTN: GS970808314221.002), the prediction was determined to be adequate. Unlike the stratigraphic predictions, no window of uncertainty was estimated for the fault prediction because of the highly variable nature of fault geometries in the subsurface and the paucity of subsurface data defining them.

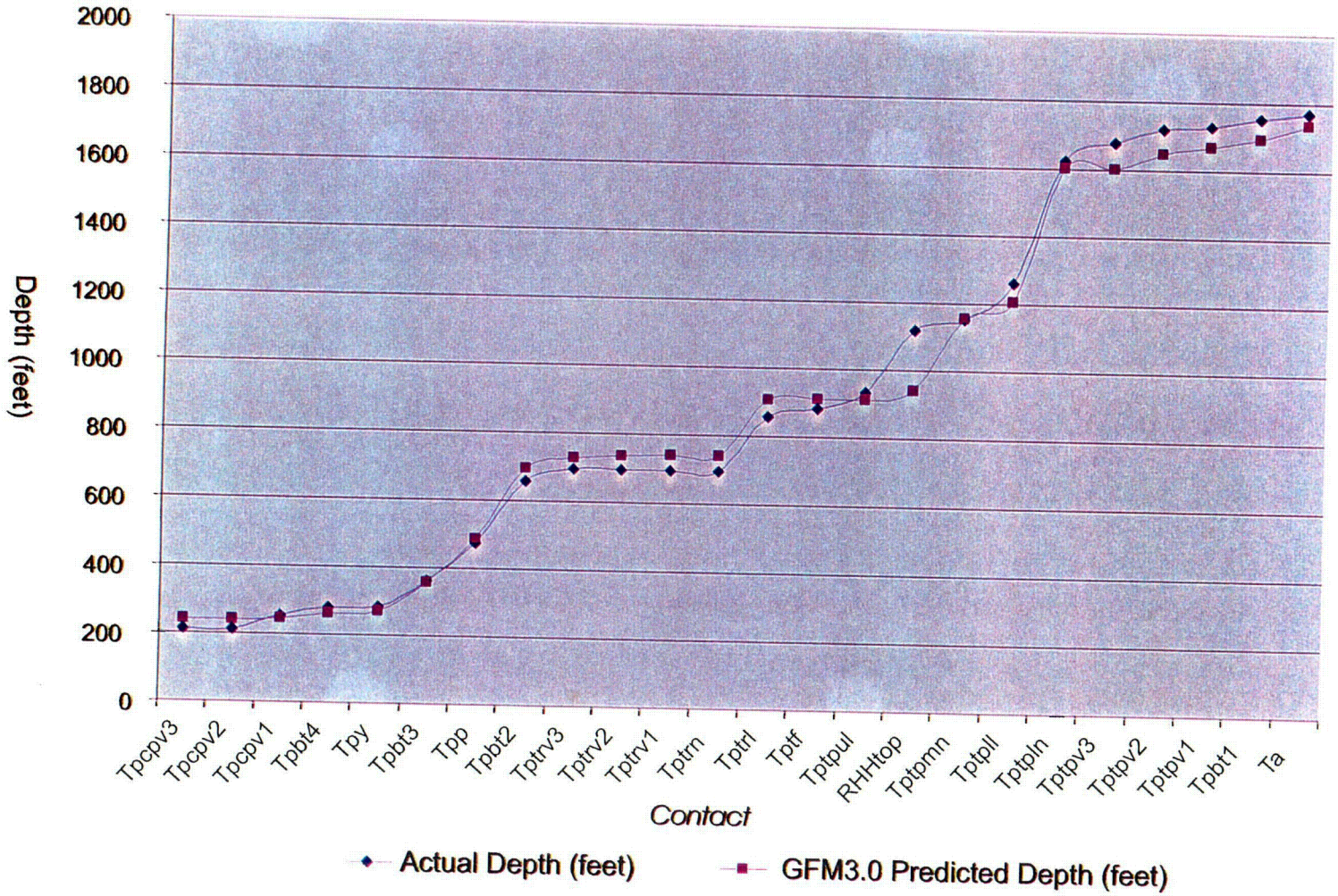

Figure 35. WT-24 Comparison of Predicted Versus Actual Contact Depths

C010

Table 7. Predicted Versus Actual Contacts in Borehole WT-24

Unit	Actual Depth (feet)[a]	GFM3.0 Predicted Depth (feet)	Difference in Depth (Predicted Minus Actual) (feet)	Actual Thickness (feet)	GFM3.0 Predicted Thickness (feet)	Difference in Thickness (feet)
Tpcpv3	215	241	26	0	0	0
Tpcpv2	215	241	26	40	5	-35
Tpcpv1	255	246	-9	24	17	-7
Tpbt4	279	263	-16	3	7	4
Tpy	282	270	-12	83	88	6
Tpbt3	365	358	-7	110	129	20
Tpp	474	487	13	185	212	27
Tpbt2	659	699	40	36	32	-4
Tptrv3	695	731	36	0	7	7
Tptrv2	695	738	43	2	4	2
Tptrv1	697	742	45	0	2	2
Tptrn	697	744	47	164	166	2
Tptrl	861	910	49	24	5	-19
Tptf	885	915	31	53	0	-53
Tptpul	937	915	-22	181	28	-153
RHHtop	1,118	943	-175	34	213	179
Tptpmn	1,152	1,156	4	110	51	-59
Tptpll	1,262	1,207	-55	363	398	35
Tptpln	1,625	1,605	-20	55	0	-55
Tptpv3	1,680	1,605	-75	41	44	3
Tptpv2	1,721	1,649	-72	9	20	11
Tptpv1	1,730	1,669	-61	22	26	4
Tptbt1	1,752	1,695	-57	17	40	23
Tac	1,769	1,735	-34	Not fully penetrated		

[a]Source: DTN: SNF40060198001.001

Table 8. Locations of Predicted and Actual Stratigraphic Contacts for the ECRB Cross-Block Drift

Contact	Predicted Station	Actual Station[a]	Vertical Difference
Tptpmn (top)	10+78	10+15	23 feet (7 meters)
Tptpll (top)	15+21	14+44	26 feet (8 meters)
Tptpln (top)	24+10	23+26	75.5 feet (23 meters)

[a]Source: DTN: GS981108314224.005

7. CONCLUSIONS

The GFM is one component of the ISM, which also includes the RPM and the MM. The GFM provides a baseline representation of the locations and distributions of 50 rock layers and 43 faults in the subsurface of the Yucca Mountain area for use in geoscientific modeling and repository design. The input data from the geologic map and boreholes provide controls at the ground surface and to the total depths of the boreholes; however, most of the modeled volume is unsampled. The GFM is an interpretative and predictive tool that provides an approximate representation of reality.

Elevation uncertainty in the geologic model increases with distance from the data and is also a function of geologic processes like deposition, faulting, and erosion. Thickness uncertainty of individual units is a contributing factor to elevation uncertainty and is strongly influenced by the thickness range of a unit and the geologic processes that formed it. Uncertainty in the model is mitigated by the application of established geologic principles.

The most uncertain areas in the model are the four corners, the less constrained areas, and the volume deeper than the borehole penetrations. For locations between boreholes in the central part of the model (the constrained areas), model predictions and acceptable alternative interpretations would be expected to fall within the following maximum vertical (elevation) ranges:

- Surface to Tptrv1: ±30 feet (9 meters)
- Tptrv1 to Tac (includes the RHH): ±40 feet (12 meters)
- Base of Tac to Tctbt: ±50 feet (15 meters).

The GFM shows the distribution of rock layers that are of greatest interest to TSPA-related models and analyses, some of which are summarized here. The Paintbrush Tuff nonwelded (PTn) unit thickens dramatically to the northwest and thins southward throughout the vicinity of the ESF. The RHH is several hundred feet thick in the vicinity of the ESF. The Calico Hills Formation (Ta) thickens to an unknown maximum thickness toward the northeast. The Tertiary-Paleozoic unconformity, which is the top of the regional Paleozoic carbonate aquifer, is poorly constrained by data but appears to deepen dramatically from east to west in the vicinity of the ESF. The vertical uncertainty for the depth of the Paleozoic unconformity is more than 3280 feet (1,000 meters), except in the vicinity of borehole p#1. This surface is between 8,000 and 11,000 feet (2,400 to 3,500 meters) below the ESF.

Analysis of model predictions for boreholes SD-6 and WT-24 and the ECRB cross-block drift indicates that the GFM will provide predictions of subsurface stratigraphy within the expected window of uncertainty.

The GFM is intended to be used in a variety of YMP studies and activities. Because the GFM is an interactive three-dimensional database and volumetric representation of Yucca Mountain, it is a useful tool for geoscientific analyses of all types, including hydrologic modeling, juxtaposition of permeable units across faults for flow analysis, confirmation test planning, site geotechnical analysis, uncertainty analysis, model integration, data analysis, and repository facilities design. However, users of the GFM should consider the limitations of scale and content to determine whether the GFM is appropriate to specific applications.

The key inputs to the model are currently TBV; excluding them would prohibit construction of the model. Accordingly, the GFM also has a TBV qualification status.

This document and its conclusions may be affected by technical product input information that requires confirmation. Any changes to the document or its conclusions that may occur as a result of completing the confirmation activities will be reflected in subsequent revisions. The status of the input information quality may be confirmed by review of the Document Input Reference System database.

8. INPUTS AND REFERENCES

8.1 DOCUMENTS CITED

Brocher, T.M.; Hunter, W.C.; and Langenheim, V.E. 1998. "Implications of Seismic Reflection and Potential Field Geophysical Data on the Structural Framework of the Yucca Mountain-Crater Flat Region, Nevada." *Geological Society of America Bulletin, 110, (8)* 947–971. Boulder, Colorado: Geological Society of America. TIC: 238643.

Buesch, D.C. and Spengler, R.W. 1999. "Correlations of Lithostratigraphic Features With Hydrogeologic Properties, a Facies-Based Approach to Model Development in Volcanic Rocks at Yucca Mountain, Nevada." *Proceedings of Conference on Status of Geologic Research and Mapping in Death Valley National Park, Las Vegas, Nevada, April 9-11, 1999,* Open File Report 99-153, 62-64. Denver, Colorado: U.S. Geologic Survey. TIC: 245245.

Buesch, D.C.; Spengler, R.W.; Moyer, T.C.; and Geslin, J.K. 1996. *Proposed Stratigraphic Nomenclature and Macroscopic Identification of Lithostratigraphic Units of the Paintbrush Group Exposed at Yucca Mountain, Nevada.* Open File Report 94-469. Denver, Colorado: U.S. Geological Survey. ACC: MOL.19970205.0061.

Byers, F.M., Jr.; Carr, W.J.; Christiansen, R.L.; Lipman, P.W.; Orkild, P.P.; and Quinlivan, W.D. 1976. *Geologic Map of the Timber Mountain Caldera Area, Nye County, Nevada.* Miscellaneous Investigations Series Map I-891. Denver, Colorado: U.S. Geological Survey. TIC: 204573.

Carr, W.J.; Byers, Jr., F.M.; and Orkild, P.P. 1986a. *Stratigraphic and Volcano-Tectonic Relations of Crater Flat Tuff and Some Older Volcanic Units, Nye County, Nevada.* USGS Professional Paper 1323. Denver, Colorado: U.S. Geological Survey. TIC: 216598.

Carr, M.D.; Waddell, S.J.; Vick, G.S.; Stock, J.M.; Monsen, S.A.; Harris, A.G.; Cork, B.W.; and Byers, F.M., Jr. 1986b. *Geology of Drill Hole UE25p#1: A Test Hole Into Pre-Tertiary Rocks Near Yucca Mountain, Southern Nevada.* Open File Report 86-175. Menlo Park, California: U.S. Geological Survey. ACC: HQS.19880517.2633.

Clayton, R.W. 1998a. *ISM2.1 Scientific Notebook.* SN-M&O-SCI-001-V1. ACC: MOL.19981021.0286.

Clayton, R.W. 1998b. *Scientific Notebook: Integrated Site Model (ISM) Version 3.0.* SN-M&O-SCI-003-V1. ACC: MOL.19990521.0202.

Clayton, R.W. 1999. *Scientific Notebook: GFM/ISM 3.1.* SN-M&O-SCI-008-V1. ACC: MOL.19991019.0478.

CRWMS M&O (Civilian Radioactive Waste Management System Management and Operating Contractor). 1999a. *M&O Site Investigations.* Activity Evaluation, January 23, 1999. Las Vegas, Nevada: CRWMS M&O. ACC: MOL.19990317.0330.

CRWMS M&O. 1999b. *M&O Site Investigations.* Activity Evaluation, September 28, 1999. Las Vegas, Nevada: CRWMS M&O. ACC: MOL.19990928.0224.

CRWMS M&O. 1999c. Analysis and Modeling Report (AMR), Work Direction and Planning Document for Geologic Framework Model (GFM) Version 3.1, Integrated Site Model (ISM). 14012210M5 ISM PMR. Las Vegas, Nevada: CRWMS M&O. ACC: MOL.19990707.0294.

CRWMS M&O. 1998a. *Work Plan for Integrated Site Model.* Rev 0. Las Vegas, Nevada: CRWMS M&O. ACC: MOL.19990819.0022.

CRWMS M&O. 1998b. *Yucca Mountain Site Description.* B00000000-01717-5700-00019 REV 00. Las Vegas, Nevada: CRWMS M&O. ACC: MOL.19981202.0492.

CRWMS M&O. 1998c. Not used.

CRWMS M&O. 1998d. Not used.

CRWMS M&O. 1998e. Not used.

CRWMS M&O 1998f. *Software Qualification Report, Rev. 0, EARTHVISION Version 4.0(c).* Las Vegas, Nevada: CRWMS M&O. ACC: MOL.19980507.004.

CRWMS M&O. 1997. *Determination of Available Volume for Repository Siting: YMP.M03.* BCA000000-01717-0200-00007 REV 00. Las Vegas, Nevada: CRWMS M&O. ACC: MOL.19971009.0699.

DOE (U.S. Department of Energy). 1998a. *Quality Assurance Requirements and Description.* DOE/RW-0333P, Rev. 8. Washington, D.C.: U.S. Department of Energy, Office of Civilian Radioactive Waste Management. ACC: MOL.19980601.0022.

DOE. 1998b. *Introduction and Site Characteristics.* Volume I of *Viability Assessment of a Repository at Yucca Mountain.* DOE/RW-0508. Washington, D.C.: U.S. Department of Energy, Office of Civilian Radioactive Waste Management. ACC: MOL.19981007.0028.

Dyer, J.R. 1999. "Revised Interim Guidance Pending Issuance of New U.S. Nuclear Regulatory Commission (NRC) Regulations (Revision 01, July 22, 1999), for Yucca Mountain, Nevada." Letter from J. Russell Dyer (DOE) to Dr. D.R. Wilkins (CRWMS M&O), September 3, 1999, OL&RC: SB-1714, with enclosure, "Interim Guidance Pending Issuance of New NRC Regulations for Yucca Mountain (Revision 01)." ACC: MOL.19990910.0079.

Feighner, M.A.; Daley, T.M.; Gritto, R.; and Majer, E.L. 1998. *Report: Results of VSP Analysis in P #1.* Milestone SP3B6AM4. Berkeley, California: Lawrence Berkeley National Laboratory. ACC: MOL.19980507.0948.

Majer, E.L.; Feighner, M.; Johnson, L.; Daley, T.; Karageorgi, E.; Kaelin, B.; Lee, K.; Williams, K. and McEvilly, T. 1996. *Synthesis of Borehole and Surface Geophysical Studies at Yucca Mountain, Nevada and Vicinity, Volume I: Surface Geophysics.* LBL-39319. Berkeley, California: Lawrence Berkeley National Laboratory. ACC: MOL.19970610.0150.

Majer, E.L.; Johnson, L.R.; Vasco, D.W.; and Parker, P. 1998. *Results of Gravity Modeling of the Paleozoic Basement.* Milestone SP3B6DM4. Berkeley, California: Lawrence Berkeley National Laboratory. ACC: MOL.19980507.0940.

Oliver, H.W.; Ponce, D.A.; and Hunter, W.C., Eds. 1995. *Major Results of Geophysical Investigations at Yucca Mountain and Vicinity, Southern Nevada.* USCA-OFR-95-74. Denver, Colorado: U.S. Geological Survey. ACC: MOL.19980305.0122.

Ponce, D.A.; Kohrn, S.B.; and Waddell, S. 1992. *Gravity and Magnetic Data of Fortymile Wash, Nevada Test Site, Nevada.* USGS-OFR-92-343. Denver, Colorado: U.S. Geological Survey. TIC: 206271.

Ponce, D.A. and Langenheim, V.E. 1994. *Preliminary Gravity and Magnetic Models Across Midway Valley and Yucca Wash, Yucca Mountain, Nevada.* Open-File Report 94-572. Menlo Park, California: U.S. Geological Survey. ACC: MOL.19990406.0399.

Rautman, C.A. and McKenna, S.A. 1997. *Three-Dimensional Hydrological and Thermal Property Models of Yucca Mountain, Nevada.* SAND97-1730. Albuquerque, New Mexico: Sandia National Laboratories. ACC: MOL.19980311.0317.

Sawyer, D.A.; Fleck, R.J.; Lanphere, M.A.; Warren, R.G.; and Broxton, D.E. 1994, "Episodic Caldera Volcanism In The Miocene Southwestern Nevada Volcanic Field: Revised Stratigraphic Framework, $^{40}Ar/^{39}$ Ar Geochronology, And Implications for Magmatism and Extension." *Geological Society of American Bulletin*, 106, 1304-1318. Boulder, Colorado: Geological Society of America. TIC: 222523.

8.2 CODES, STANDARDS, REGULATIONS, AND PROCEDURES

AP-3.10Q, Rev. 1, ICN 0. *Analyses and Models.* Washington, D.C.: U.S. Department of Energy, Office of Civilian Radioactive Waste Management. ACC: MOL.19990702.0314.

AP-SI.1Q, Rev. 1, ICN 0. *Software Management.* Washington, D.C.: U.S. Department of Energy, Office of Civilian Radioactive Waste Management. ACC: MOL.19990630.0395.

AP-SIII.1Q, Rev. 0, ICN 0. *Scientific Notebooks.* Washington, D.C.: U.S. Department of Energy, Office of Civilian Radioactive Waste Management. ACC: MOL.19990702.0311.

QAP-2-0, Rev. 5. *Conduct of Activities.* Las Vegas, Nevada: CRWMS M&O. ACC: MOL.19980826.0209.

QAP-SI-0, Rev. 3. *Computer Software Qualification.* Las Vegas, Nevada: CRWMS M&O. ACC: MOL.19980205.0304.

QAP-SI-3Q, Rev. 3. *Software Configuration Management.* CRWMS M&O. ACC: MOL.19980923.0125.

QAP-SIII-1, Rev. 3. *Scientific Investigation Control.* Las Vegas, Nevada: CRWMS M&O. ACC: MOL.19980929.0029.

QAP-SIII-2, Rev. 1. *Review of Scientific Documents and Data.* Las Vegas, Nevada: CRWMS M&O. ACC: MOL.19980219.0733.

QAP-SIII-3, Rev 2. *Scientific Notebooks.* Las Vegas, Nevada: CRWMS M&O. ACC: MOL.19971105.0040.

8.3 SOURCE DATA, LISTED BY DATA TRACKING NUMBER

GS940708314211.035. Measured Stratigraphic Section on the Eastern Side of Solitario Canyon (Section SC#1). Submittal date: 07/19/1994.

GS950108314211.001. Measured Stratigraphic Section on Isolation Ridge (Section PTn#1). Submittal date: 01/20/1995.

GS950108314211.002. Measured Stratigraphic Section on the Eastern Side of Solitario Canyon (Section PTn#2). Submittal date: 01/20/1995.

GS950108314211.003. Measured Stratigraphic Section on the Eastern Side of Solitario Canyon (Section PTn#3). Submittal date: 01/20/1995.

GS950108314211.004. Measured Stratigraphic Section on the Eastern Side of Solitario Canyon (Section PTn#4). Submittal date: 01/27/1995.

GS950108314211.005. Measured Stratigraphic Section on the Eastern Side of Solitario Canyon (Section PTn#5). Submittal date: 01/27/1995.

GS950608314211.025. 44 Measured Sections Measured in 1985 and 1986 in the Vicinity of Yucca Mountain. Submittal date: 06/28/1995.

GS960908314224.020. Analysis Report: Geology of the North Ramp - Stations 4+00 to 28+00 and Data: Detailed Line Survey and Full-Periphery Geotechnical Map - Alcoves 3 (UPCA) and 4 (LPCA), and Comparative Geologic Cross Section - Stations 0+60 to 28+00. Submittal date: 09/09/1996.

GS970808314221.002. Bedrock Geologic Map of the Yucca Mountain Area, Nye County, Nevada. Submittal date: 08/07/1997. (Note: These data superseded by DTN: GS980608314221.002.)

GS970808314224.016. Geology of the South Ramp – Station 55+00 to 78+77, Exploratory Studies Facility, Yucca Mountain Project, Yucca Mountain, Nevada. Submittal date: 08/27/1997.

GS980608314221.002. Revised Bedrock Geologic Map of the Yucca Mountain Area, Nye County, Nevada. Submittal date: 06/09/1998.

GS981108314224.005. Locations of Lithostratigraphic Contacts in the ECRB Cross Drift. Submittal date: 11/30/1998.

LB980130123112.003. Figure 3B of Report "Results of Gravity Modeling of the Paleozoic Basement". Submittal date: Submitted 10/20/1999.

MO9510RIB00002.004. RIB Item #2/Rev. 4: Stratigraphic Characteristics: Geologic/Lithologic Stratigraphy. Submittal date: 06/26/1996.

MO9607ISM10MOD.001. A 3-D Geologic Framework and Integrated Site Model of Yucca Mountain: ISM1.0. Submittal date: 07/25/1996.

MO9609RIB00038.000. RIB Item: 38/Rev. 0: Hydrologic Characteristics: Potentiometric Surface. Submittal date: 05/07/1997.

MO9804MWDGFM03.001. An Update to GFM3.0; Corrected Horizon Grids for Four Fault Blocks. Submittal date: 04/14/1998.

MO9807COV98003.000. Coverage: Global Positioning System (GPS) Field Survey of Final Data Borehole Locations. Submittal date: 03/26/1998.

MO9807MWDGFM02.000. ISM2.0: A 3-D Geologic Framework and Integrated Site Model of Yucca Mountain. Submittal date: 04/03/1998.

MO9811COV98591.000. Coverage: TOPO20S. Submittal date: 11/09/1998.

MO9811MWDGFM03.000. Input Data to the Geologic Framework Model GFM3.0. Submittal date: 11/30/98.

MO9901MWDGFM31.000. Geologic Framework Model Version GFM3.1. Submittal date: 01/06/1999.

MO9906GPS98410.000. Yucca Mountain Project (YMP) Borehole Locations. Submittal date: 06/23/1999.

SNF40060198001.001. Unsaturated Zone Lithostratigraphic Contacts in Borehole USW WT-24. Submittal date: 10/15/1998.

SNF40060298001.001. Unsaturated Zone Lithostratigraphic Contacts in Borehole USW SD-6. Submittal date: 10/15/1998.

8.4 SOFTWARE

EARTHVISION Version 4.0. STN: 30035 V4.0.

ATTACHMENT II

EXCLUDED BOREHOLE DATA

Borehole data not used in the GFM are shown in the following table. In the table, letters A through D indicate the reasons for data omission, which are summarized here.

A: Closely spaced clusters of boreholes can not be adequately modeled, as discussed in Section 6.1.1. One borehole was selected to represent each group. The omitted boreholes are a#1, c#1, and c#3.

B: With a few exceptions which are discussed in Section 6.1.1, data were not used if geophysical logs of acceptable quality were not available. This includes the UZN boreholes, the upper part of UZ-14, the lower part of UZ-1, and shorter intervals in other boreholes as indicated below.

C: Several values were omitted to provide correct input to the model. In these cases, rock units were thinned or omitted by faulting. To prevent incorrect calculation of the thicknesses of these units, the data were removed from the input spreadsheet.

D: The data entry errors resulted from inadvertent insertion of a pound sign (#) at the beginning of a row of data, which by convention in the UNIX operating system causes the line to not be read. Borehole a#7 was at one time omitted by using the initial pound sign because it is an angled hole, and its data must be corrected for the inclination of the borehole. Even after correcting the data, the pound sign was never deleted. Borehole NRG#2b was inadvertently omitted the same way.

Bold Cell Border: During model construction, questions frequently arose concerning specific data values. These data were analyzed, and the issues resolved with the principal investigators responsible for the input data. Data values (in DTN: MO9811MWDGFM03.000) that were changed are marked with a bold cell border in the table below.

Data excluded from the GFM are further discussed in Section 6.1.1.

	A	B	C	D	E	F	G	H	I	J	K	L	M	N	O	P	Q	R	S	T	U
1	Criteria for exclusion from GFM3.1 Input																				
2	A -- Used other nearby borehole instead																				
3	B -- No geophysical logs for correlation to other borehole data																				
4	C -- Value omitted from model input to avoid incorrect thickness calculation; due to faulting																				
5	D -- Omitted because of data entry error																				
6	Bold cell border -- Value corrected during modeling																				
7		source DTN: MO9811MWDGFM03.000 (D.C. Buesch)																			
8		DTN for GFM3.1 model input data: MO9901MWDGFM31.000, filename "pix99md.dat"; elevations are "pix99el.dat"																			
9	well id	easting	northing	grelev	TD	NC	Qa	Tmr	Tpk	Tpc_un	Tpcpv3	Tpcpv2	Tpcpv1	Tpbt4	Tpy	Tpbt3	Tpp	Tpbt2	Tptrv3	Tptrv2	Tptrv1
10	a#1	566350	764901	3935	2501	A	A	A	A	A	A	A	A	A	A	A	A	A	A	A	A
11	a#4	564472	767972	4102	500	0	0	""	""	30	119	119	135	150.7	154.3	179.2	197	273.6	301.9	309	316.8
12	a#5	564755	766956	4061	487	0	0	""	""	90	128	128	136	149	155	164.5	180	233	262	269	277
13	a#6	564501	765900	4053	500	0	0	""	""	20	124.5	124.5	135	144.2	149.3	167	186	201.5	229.8	236	241.7
14	a#7	565468	766250	4006	1002	D	D	D	D	D	D	D	D	D	D	D	D	D	D	D	D
15	b#1	566416	765244	3939	4003	0	0	""	""	156	180	180	182	189	192	192	204	243	259	267	275
16	c#1	569681	757097	3708	3000	A	A	A	A	A	A	A	A	A	A	A	A	A	A	A	A
17	c#2	569634	756850	3714	3000	0	0	""	""	70	243	243	257	264	267	267	286	286	306	313	315
18	c#3	569555	756911	3714	3000	A	A	A	A	A	A	A	A	A	A	A	A	A	A	A	A
19	G-1	561001	770502	4350	6000	0	0	""	""	""	""	""	""	""	60	102	135	235	265	265	270
20	G-2	560504	778826	5097	6006	0	0	""	""	""	225	225	228	235	245	341.5	494.2	730.8	755.2	761.7	766.8
21	G-3	558483	752780	4856	2644	0	0	""	""	""	348.1	357	368.4	372.5	375.5	375.5	391.7	391.7	417.7	424.9	427.8
22	G-4	563082	765808	4166	3001	0	0	""	""	30	118	118	130	141	146	148.8	168.2	198.9	224	236.5	239
23	H-1	562388	770255	4274	6000	0	0	""	""	""	61	61	70	90	95	161	190	279	295	320	330
24	H-3	558452	756542	4866	4000	0	0	""	""	""	369.8	376	388	400	403.9	403.9	417	417	435	441.9	445
25	H-4	563911	761644	4096	4004	0	0	""	""	""	173.9	173.9	185	193	195	198	216	224	242	248.5	251
26	H-5	558908	766634	4851	4000	0	0	""	""	""	404	404	420	437.5	438	457	471	510	542	560	562
27	H-6	554075	763299	4271	4002	0	0	""	""	30	190	190	200	260	270	275	278	290	300	330	330
28	J-13	579648	749202	3317	3498	0	0	""	""	435	587	591	610	629	632	632	650	650	682	686	691
29	NRG#1	569803	765359	3753	150	0	0	""	""	9.5	""	""	""	""	""	""	""	""	""	""	""
30	NRG#2	569162	765764	3800	294	0	0	""	164.6	164.6	276.3	276.3	282.8	""	""	""	""	""	""	""	""
31	NRG#2a	569001	765700	3781	266	B	B	B	B	B	""	""	""	""	""	""	""	""	""	""	""
32	NRG#2b	569215	765765	3801	330	D	D	D	D	D	D	D	D	D	D	D	D	D	""	""	""
33	NRG#2c	569190	765772	3801	151	B	B	B	B	""	""	""	""	""	""	""	""	""	""	""	""
34	NRG#2d	569132	765825	3792	170	B	B	B	B	""	""	""	""	""	""	""	""	""	""	""	""
35	NRG#3	568316	766251	3823	330	B	B	""	""	""	""	""	""	""	""	""	""	""	""	""	""
36	NRG#4	566820	767080	4099	726	0	0	""	""	""	318	318	323	338	344	354	375	458	477	481.5	485
37	NRG#5	564770	767890	4107	1350	0	0	""	""	""	140	140	154	163	170	187	215	288	321	327	330
38	NRG-6	564187	766726	4092	1100	0	0	""	""	""	135.3	135.3	151.8	158.6	162.8	162.8	174.9	220.8	244.7	257.4	259.8
39	NRG-7A	562984	768880	4207	1513	0	0	""	""	17	69.7	69.7	79.2	102	106.4	156	172	258.8	284.3	292.7	296.2
40	ONC#1	568093	759257	3815	1478	0	0	98	193	206	578	578	589	597	600	600	621	621	643	653	654
41	p#1	571484	756173	3655	5923	0	0	""	""	""	""	""	""	""	""	""	""	""	140	145	148
42	SD-6	558650	762548	4909	2563	0	0	""	""	0	414.6	414.6	429	442.4	445	466.4	480	488.8	517.4	520.7	525.7
43	SD-7	561240	758950	4472	1632	0	0	""	""	50.1	305	305	316	325.8	330.6	330.6	343	356	384.3	384.3	386.3
44	SD-9	561818	767998	4273	2223	0	0	""	""	53.6	57.2	57.2	76.5	91.5	95.9	140.8	155.5	226.6	255.6	266.7	268.5
45	SD-12	561606	761957	4343	2000	0	0	""	""	5.3	239.5	239.5	256	263.7	266	266	278.3	291.2	314.1	320.8	324.5
46	UZ-1	560222	771277	4425	1260	0	0	""	""	""	""	""	""	""	40	78	105	242	272	282.5	284
47	UZ#4	566140	768716	3940	366	0	0	""	""	39	71.4	71.4	78	99	106	151.5	173.9	305	333	343	345
48	UZ#5	566136	768593	3953	363	0	0	""	""	3	89	89	100	118	122	162	186	316	345	352.5	354.5
49	UZ-6	558325	759730	4925	1887	0	0	""	""	""	383	407	422	432.5	437.2	437.2	450.1	455.5	478.2	483	489
50	UZ-7a	562270	760693	4228	770	0	0	""	""	38.5	163.9	163.9	184	197.7	203.6	203.6	214.9	218.6	243	247.3	248.6
51	UZ-14	560142	771310	4425	2207	B	B	B	B	B	B	B	B	B	B	B	B	B	B	B	B

	V	W	X	Y	Z	AA	AB	AC	AD	AE	AF	AG	AH	AI	AJ	AK	AL	AM	AN
1																			
2																			
3																			
4																			
5																			
6																			
7																			
8																			
9	well id	Tptrm	Tptrl	Tptf	Tptpul	RHH	Tptpmn	Tptpll	Tptpln	Tptpv3	Tptpv2	Tptpv1	Tpbt1	Tac	Tacbt	Tcpuv	Tcpuc	Tcpm	
10	a#1	A	A	A	A	A	A	A	A	A	A	A	A	A	A	A	A	A	
11	a#4	317	""	""	""	""	""	""	""	""	""	""	""	""	""	""	""	""	
12	a#5	277	442.4	475	475	""	""	""	""	""	""	""	""	""	""	""	""	""	
13	a#6	242	402	422	422	""	""	""	""	""	""	""	""	""	""	""	""	""	
14	a#7	D	D	D	D	D	D	D	""	""	""	""	""	""	""	""	""	""	
15	b#1	280	413	440	440	632	680.5	765	1130	1283	1336	1352	1374	1385	1845	1882	1896	1992	
16	c#1	A	A	A	A	A	A	A	A	A	A	A	A	A	A	A	A	A	
17	c#2	318	423	457	457	520	591	725	1038	1205	1290	1320	1335	1335	1580	1658	1658	1773	
18	c#3	A	A	A	A	A	A	A	A	A	A	A	A	A	A	A	A	A	
19	G-1	280	438	456.5	456.5	600	713.4	814.8	1199.2	1287	1342.4	1360.5	1403.9	1425.5	1736.4	1799	1862.5	1920	
20	G-2	771.2	909.1	909.1	977.2	1131.9	1246	1280	1604	1633.8	1670	1684.5	1702.1	1757	2576.7	2704.7	2704.7	2704.7	
21	G-3	427.8	542	548	548	675	688	830	1044	1186.7	1280	1317	1406.3	1412.5	1506.3	1553.9	1597	1663	
22	G-4	242.8	400.4	420	420	618	674	774	1127.9	1316.5	1345.4	1353.6	1406.8	1409.4	1705.4	1762.7	1793.6	1880	
23	H-1	335	505	538	538	650	788	897	1324	1410	1469.5	1486.2	1498	1505	1802	1861	1911	1969	
24	H-3	449	526.9	540	540	605	680.1	848.1	1049.9	1194	1308	1341	1392	1400	1437	1495	1518	1640	
25	H-4	254	376	376	376	553	576	703	987	1185	1209	1247	1312	1317	1572	1626.9	1662	1746	
26	H-5	564	700	741	741	931	988	1088	1450	1582	1659	1672	1699.1	1705	1879.9	1944.9	1967	2085	
27	H-6	332	409	435	435	585	653	795	1097	1213	1310	1322	1356	1356	1458	1508	1555	1602	
28	J-13	691	755	801	801	""	905	1003	1193	1300	1415	1450	1475	1482	1682	1711	1742	1848	
29	NRG#1	""	""	""	""	""	""	""	""	""	""	""	""	""	""	""	""	""	
30	NRG#2	""	""	""	""	""	""	""	""	""	""	""	""	""	""	""	""	""	
31	NRG#2a	""	""	""	""	""	""	""	""	""	""	""	""	""	""	""	""	""	
32	NRG#2b	""	""	""	""	""	""	""	""	""	""	""	""	""	""	""	""	""	
33	NRG#2c	""	""	""	""	""	""	""	""	""	""	""	""	""	""	""	""	""	
34	NRG#2d	""	""	""	""	""	""	""	""	""	""	""	""	""	""	""	""	""	
35	NRG#3	""	""	""	""	""	""	""	""	""	""	""	""	""	""	""	""	""	
36	NRG#4	488.9	660.5	700	700	""	""	""	""	""	""	""	""	""	""	""	""	""	
37	NRG#5	332	517	565	565	681	770	901.5	1230	""	""	""	""	""	""	""	""	""	
38	NRG-6	263.2	429	465.5	465.5	620	713	810	""	""	""	""	""	""	""	""	""	""	
39	NRG-7A	299	478.2	518.4	518.4	659	740	877.6	1243	1414.8	1457	1474.6	1493	1498	""	""	""	""	
40	ONC#1	658	774	810	810	927	977	C	C	C	C	1213	1253	1274	""	""	""	""	
41	p#1	150	228	248	248	453	493	640	958	1090	1200	1243	1270	1270	1390	1441	1468	1535	
42	SD-6	527.4	632	645.7	645.7	780	853	995	1305	1456	1503	1520	1552	1561	1664	1715	1739.9	1872	
43	SD-7	386.3	480	490	490	640	682.5	803.3	1020	1182	1285	1308	1395.4	1405.6	1567.2	1621.5	1646.5	1765	
44	SD-9	272.2	450	473	473	628	730	845.8	1182	1358	1418.4	1425.7	1464.1	1479.9	1764.4	1820.7	1868.7	1938.5	
45	SD-12	330.7	436.4	470.2	470.2	630	663.7	786.9	1065.5	1278.1	1308	1337.5	1408.1	1411.5	1599.5	1648.4	1677	1787	
46	UZ-1	288	436	470	470	585	717	830	1145	B	B	B	B	B	B	B	B	B	
47	UZ#4	346	""	""	""	""	""	""	""	""	""	""	""	""	""	""	""	""	
48	UZ#5	356.1	""	""	""	""	""	""	""	""	""	""	""	""	""	""	""	""	
49	UZ-6	490	575	610	610	690	778	917	1190	1333	1379	1422	1450	1460	1547.2	1592	1614	1750	
50	UZ-7a	248.6	377.8	C	C	C	480	607	""	""	""	""	""	""	""	""	""	""	
51	UZ-14	B	B	B	B	B	B	B	B	B	1358	1383	1404.2	1420.2	1694	1750.2	1815.1	1850	

	AO	AP	AQ	AR	AS	AT	AU	AV	AW	AX	AY	AZ	BA	BB	BC	BD	BE	BF	BG
1																			
2																			
3																			
4																			
5																			
6																			
7																			
8																			
9	well id	Tcplc	Tcplv	Tcpbt	Tcbuv	Tcbuc	Tcbm	Tcblc	Tcblv	Tcbbt	Tctuv	Tctuc	Tctm	Tctlc	Tctlv	Tctbt	Tund	Pz	V-Z
10	a#1	A	A	A	A	A	A	"	"	"	"	"	"	"	"	"	"	"	1360
11	a#4	"	"	"	"	"	"	"	"	"	"	"	"	"	"	"	"	"	"
12	a#5	"	"	"	"	"	"	"	"	"	"	"	"	"	"	"	"	"	"
13	a#6	"	"	"	"	"	"	"	"	"	"	"	"	"	"	"	"	"	"
14	a#7	"	"	"	"	"	"	"	"	"	"	"	"	"	"	"	"	"	"
15	b#1	2039	2071	2355.6	2361.3	2361.3	2468	2782.8	2799.5	2852.7	2882.5	2933	3158	3322	3360	3901	3960.3	"	1336
16	c#1	A	A	A	A	A	A	A	A	A	A	A	"	"	"	"	"	"	1293
17	c#2	1849	1872	2109.5	2138	2227	2262	2445	2550	2667	2725	2725	"	"	"	"	"	"	1290
18	c#3	A	A	A	A	A	A	A	A	A	A	A	"	"	"	"	"	"	1270
19	G-1	1960	1985.7	2154.9	2173.2	2337	2461	2547	2547	2601.6	2639.4	2800	2840	2956	3005	3522	3558.2	"	1394.3
20	G-2	2963.7	2980	3246.5	3281.9	3302.5	3320	3447	3485	3503.4	3574	3574	3574	3574	3574	3914	3982	"	1670
21	G-3	1744	1755	1992.3	1998.7	2021.3	2102	2549.5	2550.8	2617	2637	2719	2890	3265	3290	3850	3876.3	"	1816
22	G-4	1946	1954.6	2238	2245.7	2255	2560	2677	2677	2733.3	2755.6	2839	2950	"	"	"	"	"	1376
23	H-1	2021	2053	2300	2319.5	2337	2533	2629	2676	2690.3	2729.6	2823	2862	3073	3111	3619	3661.4	"	1490
24	H-3	1690	1702	1899.9	1907.1	1922	2092	2350	2397	2449.1	2477	2567	2692	3086	3120	3595	3637.1	"	1762
25	H-4	1820	1840	2263.1	2274.9	2369	2494	2559	2635	2644	2664	2745	2835	3200	3228	3788	3818.9	"	1330
26	H-5	2113	2130	2240.1	2263.1	2310	2388	2468	2510	2712.9	2742.1	2845	2897	3130	3150	3412	3421.9	"	1888
27	H-6	1670	1685	1765.1	1794.9	1881	1894	1990	2138.1	2225	2258	2348	2439	2655	2667	2869	2877.9	"	1429
28	J-13	1942	1961	1993	2017	2017	2082	2322	2322	2322	2358	2465	2658	2862	2991	3200	3220	"	1415
29	NRG#1	"	"	"	"	"	"	"	"	"	"	"	"	"	"	"	"	"	"
30	NRG#2	"	"	"	"	"	"	"	"	"	"	"	"	"	"	"	"	"	"
31	NRG#2a	"	"	"	"	"	"	"	"	"	"	"	"	"	"	"	"	"	"
32	NRG#2b	"	"	"	"	"	"	"	"	"	"	"	"	"	"	"	"	"	"
33	NRG#2c	"	"	"	"	"	"	"	"	"	"	"	"	"	"	"	"	"	"
34	NRG#2d	"	"	"	"	"	"	"	"	"	"	"	"	"	"	"	"	"	"
35	NRG#3	"	"	"	"	"	"	"	"	"	"	"	"	"	"	"	"	"	"
36	NRG#4	"	"	"	"	"	"	"	"	"	"	"	"	"	"	"	"	"	"
37	NRG#5	"	"	"	"	"	"	"	"	"	"	"	"	"	"	"	"	"	"
38	NRG-6	"	"	"	"	"	"	"	"	"	"	"	"	"	"	"	"	"	"
39	NRG-7A	"	"	"	"	"	"	"	"	"	"	"	"	"	"	"	"	"	1466
40	ONC#1	"	"	"	"	"	"	"	"	"	"	"	"	"	"	"	"	"	1153
41	p#1	1630	1680	1790	1826	1826	1953	2130	2162	2240	2262	2340	2395	2595	2616	2863	2863	4080	1200
42	SD-6	1885	1908	2081	2103	2122.4	2217	2477	2506	"	"	"	"	"	"	"	"	"	"
43	SD-7	1832	1872	2167.8	2183.9	2183.9	2183.9	2450	2478	2579.4	2598	2611.8	"	"	"	"	"	"	1562
44	SD-9	1991.4	2015.8	"	"	"	"	"	"	"	"	"	"	"	"	"	"	"	1457
45	SD-12	1842	1865	2133	2137.8	"	"	"	"	"	"	"	"	"	"	"	"	"	1600
46	UZ-1	B	B	B	B	"	"	"	"	"	"	"	"	"	"	"	"	"	"
47	UZ#4	"	"	"	"	"	"	"	"	"	"	"	"	"	"	"	"	"	"
48	UZ#5	"	"	"	"	"	"	"	"	"	"	"	"	"	"	"	"	"	"
49	UZ-6	1802	1829	"	"	"	"	"	"	"	"	"	"	"	"	"	"	"	"
50	UZ-7a	"	"	"	"	"	"	"	"	"	"	"	"	"	"	"	"	"	"
51	UZ-14	1893	1899	2046.6	2072.1	"	"	"	"	"	"	"	"	"	"	"	"	"	1392.5

	A	B	C	D	E	F	G	H	I	J	K	L	M	N	O	P	Q	R	S	T	U
52	UZ#16	564857	760535	4000	1686	0	0	""	""	39.7	140.8	140.8	153	160.7	165.9	173.4	188.8	188.8	217	228.1	229.4
53	WT-1	563739	753942	3940	1689	0	0	""	""	30	395	410	417	431	435	435	446	446	477	481	484
54	WT-2	561924	760662	4268	2060	0	0	""	""	60	193	200	215	227	230	230	247	247	271	275	280
55	WT#3	573385	745996	3379	1142	0	0	""	""	""	""	""	""	""	""	""	""	""	""	""	""
56	WT#4	568038	768512	3836	1580	0	0	""	""	51	261	261	270	281	293	293	324	419	444	448	456
57	WT#6	564524	780576	4313	1258	0	0	""	""	""	""	""	""	""	""	""	""	""	""	""	""
58	WT-7	553892	755571	3926	1610	0	0	""	""	40	344	344	355	369.5	372	374.5	391	391	415	426	432
59	WT-10	553302	748772	3686	1412	0	0	60	627	627	863	872	880	887	894	894	924	924	954	960.5	967
60	WT-11	558377	739071	3589	1446	0	0	""	""	40	239	243.5	263	271	272	272	287	287	307	313	317
61	WT#12	567012	739727	3526	1308	0	0	""	""	60	297	300	306	319	323	323	339	339	362	365	369
62	WT#13	578842	756885	3386	1154	0	0	""	""	220	416	416	427	440	450	450	460	469	490	497	498
63	WT#14	575210	761651	3530	1310	0	0	""	""	""	""	""	""	""	""	""	""	""	B	B	B
64	WT#15	579806	766117	3553	1360	0	0	""	""	210	332	332	334	349	356	356	372	413	436	440	442
65	WT#16	570395	774420	3971	1709	0	0	""	""	137	368	368	375	386	395	395	462	558	580	588	594
66	WT#17	566212	748422	3687	1450	0	0	""	""	B	188	188	194	197	203	203	217	217	242	245	248
67	WT#18	564855	771167	4384	2043	0	0	""	""	""	314	314	332	340	353	423	497	651	692	698	701
68	WT#24	562306	776673	4902	2834	0	0	""	""	0	215	215	255	278.6	282	364.5	474	659.3	695.4	695.4	697
69	wellid	easting	northi	ground	TD	NC	Qa	Tmr	Tpk	Tpc_un	Tpcpv3	Tpcpv2	Tpcpv1	Tpbt4	Tpy	Tpbt3	Tpp	Tpbt2	Tptrv3	Tptrv2	Tptrv1
70	UZ-N11	559021	780574	5224	84	B	B	B	B	B	B	B	B	B	B	""	""	""	""	""	""
71	UZ-N15	559552	778091	5109	60	B	B	B	B	B	""	""	""	""	""	""	""	""	""	""	""
72	UZ-N16	559626	778151	5117	60	B	B	B	B	B	""	""	""	""	""	""	""	""	""	""	""
73	UZ-N17	559995	778224	5128	60	B	B	B	B	B	""	""	""	""	""	""	""	""	""	""	""
74	UZ-N27	558872	771570	4860	202	B	""	""	""	""	""	""	""	""	""	""	""	""	""	""	""
75	UZ-N31	562752	764246	4152	193	B	B	B	B	B	B	B	B	B	B	B	B	B	B	B	B
76	UZ-N32	562800	764303	4156	207	B	B	B	B	B	B	B	B	B	B	B	B	B	B	B	B
77	UZ-N33	561239	769760	4331	75	B	B	B	B	B	B	B	B	B	B	""	""	""	""	""	""
78	UZ-N34	561252	770159	4324	84	B	B	B	B	B	B	B	B	B	B	""	""	""	""	""	""
79	UZ-N35	562310	762264	4247	176	B	B	B	B	B	""	""	""	""	""	""	""	""	""	""	""
80	UZ-N36	563583	773900	4642	60	B	B	B	B	B	""	""	""	""	""	""	""	""	""	""	""
81	UZ-N37	563714	767499	4124	271	B	B	B	B	B	B	B	B	B	B	B	B	B	B	B	B
82	UZ-N38	563343	767466	4149	89	B	B	B	B	B	B	B	""	""	""	""	""	""	""	""	""
83	UZ-N53	564237	760096	4056	234	B	B	B	B	B	B	B	B	B	B	B	B	B	B	B	B
84	UZ-N54	564262	760272	4046	245	B	B	B	B	B	B	B	B	B	B	B	B	B	B	B	B
85	UZ-N55	564248	760503	4073	255	B	B	B	B	B	B	B	B	B	B	B	B	B	B	B	B
86	UZ-N57	560830	755165	4184	119	B	B	B	B	B	""	""	""	""	""	""	""	""	""	""	""
87	UZ-N58	560862	755240	4179	119	B	B	B	B	B	""	""	""	""	""	""	""	""	""	""	""
88	UZ-N59	560888	755321	4178	119	B	B	B	B	B	""	""	""	""	""	""	""	""	""	""	""
89	UZ-N61	560894	755376	4182	119	B	B	B	B	B	""	""	""	""	""	""	""	""	""	""	""
90	UZ-N62	558303	757125	4882	60	B	B	B	B	B	""	""	""	""	""	""	""	""	""	""	""
91	UZ-N63	566169	768837	3944	60	B	B	B	B	B	""	""	""	""	""	""	""	""	""	""	""
92	UZ-N64	559436	765729	4791	60	B	B	B	B	B	""	""	""	""	""	""	""	""	""	""	""

	V	W	X	Y	Z	AA	AB	AC	AD	AE	AF	AG	AH	AI	AJ	AK	AL	AM	AN
52	UZ#16	238.9	357.8	371	371	485	545	669	935	1107.5	1165.2	1178	1190	1197	1455.4	1485	1497.7	1571	
53	WT-1	492	575	593	593	713	733	888	1187	1299	1337	1368	1380	1384	1564	C	C	C	
54	WT-2	285	380	421	421	540	590	727	1014	1179	1223	1264	1315	1319	1521	1594	1594	1706	
55	WT#3	**	**	**	**	**	**	**	35	189	293	327	351	358	461	512	554	660	
56	WT#4	458	630	660	660	679	727	785	1091	1091	1122	1141	1150	1156	**	**	**	**	
57	WT#6	**	**	**	**	**	250	250	303	303	337	352	369	383	**	**	**	**	
58	WT-7	435	515	546	546	665	706	959	1091	1287	1351	1360	1433	1438	1510	1571	1598	**	
59	WT-10	971	1035	1049	1049	1233	1250	**	**	**	**	**	**	**	**	**	**	**	
60	WT-11	324	430	430	430	641	661	782	875	1058	1146	1186	1198	1208	**	**	**	**	
61	WT#12	374	478	478	478	660	680	760	890	1151	1215	1250	1259	1276	**	**	**	**	
62	WT#13	500	612	630	630	740	755	868	1103	**	**	**	**	**	**	**	**	**	
63	WT#14	B	247	275	275	392	446	534	830	1024	1117	1137	1157	1210	**	**	**	**	
64	WT#15	444	608	641	641	840	852	919	1260	**	**	**	**	**	**	**	**	**	
65	WT#16	596	818	830	830	**	830	830	1013	1013	1050	1057	1068	1068	**	**	**	**	
66	WT#17	251	312	336	336	412	472	535	668	874	959	989	998	998	1184	1271	1313	1318	
67	WT#18	702	879	900	900	990	1078	1170	1501	1501	1564	1592	1620	1620	**	**	**	**	
68	WT#24	697	861	884.5	937.4	1118	1151.7	1261.7	1625	1680	1720.8	1730.2	1751.8	1768.8	**	**	**	**	
69	wellid	Tptrm	Tptrl	Tptf	Tptpul	RHH	Tptpmn	Tptpll	Tptpln	Tptpv3	Tptpv2	Tptpv1	Tpbt1	Tac	Tacbt	Tcpuv	Tcpuc	Tcpm	
70	UZ-N11	**	**	**	**	**	**	**	**	**	**	**	**	**	**	**	**	**	
71	UZ-N15	**	**	**	**	**	**	**	**	**	**	**	**	**	**	**	**	**	
72	UZ-N16	**	**	**	**	**	**	**	**	**	**	**	**	**	**	**	**	**	
73	UZ-N17	**	**	**	**	**	**	**	**	**	**	**	**	**	**	**	**	**	
74	UZ-N27	**	**	**	**	**	**	**	**	**	**	**	**	**	**	**	**	**	
75	UZ-N31	B	**	**	**	**	**	**	**	**	**	**	**	**	**	**	**	**	
76	UZ-N32	B	**	**	**	**	**	**	**	**	**	**	**	**	**	**	**	**	
77	UZ-N33	**	**	**	**	**	**	**	**	**	**	**	**	**	**	**	**	**	
78	UZ-N34	**	**	**	**	**	**	**	**	**	**	**	**	**	**	**	**	**	
79	UZ-N35	**	**	**	**	**	**	**	**	**	**	**	**	**	**	**	**	**	
80	UZ-N36	**	**	**	**	**	**	**	**	**	**	**	**	**	**	**	**	**	
81	UZ-N37	B	**	**	**	**	**	**	**	**	**	**	**	**	**	**	**	**	
82	UZ-N38	**	**	**	**	**	**	**	**	**	**	**	**	**	**	**	**	**	
83	UZ-N53	B	**	**	**	**	**	**	**	**	**	**	**	**	**	**	**	**	
84	UZ-N54	B	**	**	**	**	**	**	**	**	**	**	**	**	**	**	**	**	
85	UZ-N55	B	**	**	**	**	**	**	**	**	**	**	**	**	**	**	**	**	
86	UZ-N57	**	**	**	**	**	**	**	**	**	**	**	**	**	**	**	**	**	
87	UZ-N58	**	**	**	**	**	**	**	**	**	**	**	**	**	**	**	**	**	
88	UZ-N59	**	**	**	**	**	**	**	**	**	**	**	**	**	**	**	**	**	
89	UZ-N61	**	**	**	**	**	**	**	**	**	**	**	**	**	**	**	**	**	
90	UZ-N62	**	**	**	**	**	**	**	**	**	**	**	**	**	**	**	**	**	
91	UZ-N63	**	**	**	**	**	**	**	**	**	**	**	**	**	**	**	**	**	
92	UZ-N64	**	**	**	**	**	**	**	**	**	**	**	**	**	**	**	**	**	

	AO	AP	AQ	AR	AS	AT	AU	AV	AW	AX	AY	AZ	BA	BB	BC	BD	BE	BF	BG
52	UZ#16	1638	1669.2																1165.2
53	WT-1	C	C	C	C	C	1564												1337
54	WT-2	1776	1794																1452
55	WT#3	704	710	835	846	850	909												293
56	WT#4																		1122
57	WT#6																		305
58	WT-7																		1351
59	WT-10																		
60	WT-11																		1271
61	WT#12																		1180
62	WT#13																		
63	WT#14																		1117
64	WT#15																		
65	WT#16																		1050
66	WT#17																		961
67	WT#18																		1564
68	WT#24																		1723.5
69	wellid	Tcplc	Tcplv	Tcpbt	Tcbuv	Tcbuc	Tcbm	Tcblc	Tcblv	Tcbbt	Tctuv	Tctuc	Tctm	Tctlc	Tctlv	Tctbt	Tund	Pz	V-Z
70	UZ-N11																		
71	UZ-N15																		
72	UZ-N16																		
73	UZ-N17																		
74	UZ-N27																		
75	UZ-N31																		
76	UZ-N32																		
77	UZ-N33																		
78	UZ-N34																		
79	UZ-N35																		
80	UZ-N36																		
81	UZ-N37																		
82	UZ-N38																		
83	UZ-N53																		
84	UZ-N54																		
85	UZ-N55																		
86	UZ-N57																		
87	UZ-N58																		
88	UZ-N59																		
89	UZ-N61																		
90	UZ-N62																		
91	UZ-N63																		
92	UZ-N64																		

INTENTIONALLY LEFT BLANK

ATTACHMENT III

PREDICTED AND ACTUAL UNIT THICKNESSES FOR THE UZN BOREHOLES

ATTACHMENT III

PREDICTED AND ACTUAL UNIT THICKNESSES

FOR THE UZN BOREHOLES

borehole	Tpcpv3	Tpcpv2	Tpcpv1	Tpbt4	Tpy	Tpbt3	Tpp	Tpbt2	Tptrv3	Tptrv2	Tptrv1
UZ-N11	0	5	17	14	N/A	N/A	N/A	N/A	N/A	N/A	N/A
GFM	0	0	6	10	N/A	N/A	N/A	N/A	N/A	N/A	N/A
difference	*0*	*-5*	*-11*	*-4*							
UZ-N15	N/A	N/A	N/A	N/A	N/A	N/A	N/A	N/A	N/A	N/A	N/A
GFM	N/A	N/A	N/A	N/A	N/A	N/A	N/A	N/A	N/A	N/A	N/A
UZ-N16	N/A	N/A	N/A	N/A	N/A	N/A	N/A	N/A	N/A	N/A	N/A
GFM	N/A	N/A	N/A	N/A	N/A	N/A	N/A	N/A	N/A	N/A	N/A
UZ-N17	N/A	N/A	N/A	N/A	N/A	N/A	N/A	N/A	N/A	N/A	N/A
GFM	N/A	N/A	N/A	N/A	N/A	N/A	N/A	N/A	N/A	N/A	N/A
UZ-N27	N/A	N/A	N/A	N/A	N/A	N/A	N/A	N/A	N/A	N/A	N/A
GFM	N/A	N/A	N/A	N/A	N/A	N/A	N/A	N/A	N/A	N/A	N/A
UZ-N31	0	15	4	5	0	8	25	24	12	1	4
GFM	0	13	8	3	4	18	16	23	9	3	4
difference	*0*	*-2*	*4*	*-2*	*4*	*10*	*-9*	*-1*	*-3*	*2*	*0*
UZ-N32	0	12	6	5	0	12	29	28	12	1	3
GFM	0	12	8	3	4	18	16	23	10	3	4
difference	*0*	*0*	*2*	*-2*	*4*	*6*	*-13*	*-5*	*-2*	*2*	*1*
UZ-N33	0	10	22	3	N/A	N/A	N/A	N/A	N/A	N/A	N/A
GFM	0	13	22	4	N/A	N/A	N/A	N/A	N/A	N/A	N/A
difference	*0*	*3*	*0*	*1*							
UZ-N34	0	0	0	0	N/A	N/A	N/A	N/A	N/A	N/A	N/A
GFM	0	12	22	4	N/A	N/A	N/A	N/A	N/A	N/A	N/A
difference	*0*	*12*	*22*	*4*							
UZ-N35	N/A	N/A	N/A	N/A	N/A	N/A	N/A	N/A	N/A	N/A	N/A
GFM	N/A	N/A	N/A	N/A	N/A	N/A	N/A	N/A	N/A	N/A	N/A
UZ-N36	N/A	N/A	N/A	N/A	N/A	N/A	N/A	N/A	N/A	N/A	N/A
GFM	N/A	N/A	N/A	N/A	N/A	N/A	N/A	N/A	N/A	N/A	N/A
UZ-N37	0	12	7	6	0	15	71	25	6	6	1
GFM	0	17	12	4	11	13	63	26	11	4	2
difference	*0*	*5*	*5*	*-2*	*11*	*-2*	*-8*	*1*	*5*	*-2*	*1*
UZ-N38	0	N/A	N/A	N/A	N/A	N/A	N/A	N/A	N/A	N/A	N/A
GFM	0	N/A	N/A	N/A	N/A	N/A	N/A	N/A	N/A	N/A	N/A
difference	*0*										
UZ-N53	0	9	14	2	5	15	0	25	7	2	0
GFM	0	14	9	6	5	15	0	29	9	1	7
difference	*0*	*5*	*-5*	*4*	*0*	*0*	*0*	*4*	*2*	*-1*	*7*
UZ-N54	0	13	9	1	7	16	0	26	10	5	0
GFM	0	14	9	5	5	15	0	28	9	1	7
difference	*0*	*1*	*0*	*4*	*-2*	*-1*	*0*	*2*	*-1*	*-4*	*7*
UZ-N55	0	13	14	4	6	8	0	12	8	3	3
GFM	0	13	9	5	5	15	0	27	9	1	6
difference	*0*	*0*	*-5*	*1*	*-1*	*7*	*0*	*15*	*1*	*-2*	*3*

borehole	Tpcpv3	Tpcpv2	Tpcpv1	Tpbt4	Tpy	Tpbt3	Tpp	Tpbt2	Tptrv3	Tptrv2	Tptrv1
UZ-N57	N/A	N/A	N/A	N/A	N/A	N/A	N/A	N/A	N/A	N/A	N/A
GFM	N/A	N/A	N/A	N/A	N/A	N/A	N/A	N/A	N/A	N/A	N/A
UZ-N58	N/A	N/A	N/A	N/A	N/A	N/A	N/A	N/A	N/A	N/A	N/A
GFM	N/A	N/A	N/A	N/A	N/A	N/A	N/A	N/A	N/A	N/A	N/A
UZ-N59	N/A	N/A	N/A	N/A	N/A	N/A	N/A	N/A	N/A	N/A	N/A
GFM	N/A	N/A	N/A	N/A	N/A	N/A	N/A	N/A	N/A	N/A	N/A
UZ-N61	N/A	N/A	N/A	N/A	N/A	N/A	N/A	N/A	N/A	N/A	N/A
GFM	N/A	N/A	N/A	N/A	N/A	N/A	N/A	N/A	N/A	N/A	N/A
UZ-N62	N/A	N/A	N/A	N/A	N/A	N/A	N/A	N/A	N/A	N/A	N/A
GFM	N/A	N/A	N/A	N/A	N/A	N/A	N/A	N/A	N/A	N/A	N/A
UZ-N63	N/A	N/A	N/A	N/A	N/A	N/A	N/A	N/A	N/A	N/A	N/A
GFM	N/A	N/A	N/A	N/A	N/A	N/A	N/A	N/A	N/A	N/A	N/A
UZ-N64	N/A	N/A	N/A	N/A	N/A	N/A	N/A	N/A	N/A	N/A	N/A
GFM	N/A	N/A	N/A	N/A	N/A	N/A	N/A	N/A	N/A	N/A	N/A
N/A = not penetrated or partially penetrated											
Bars indicate closely spaced boreholes											
Values are thicknesses											

ATTACHMENT IV

PREDICTED AND ACTUAL UNIT THICKNESSES

FOR BOREHOLES a#1, a#7, c#1 AND c#3

ATTACHMENT IV

PREDICTED AND ACTUAL UNIT THICKNESSES

FOR BOREHOLES a#1, a#7, c#1 AND c#3

Borehole	Unit	Predicted Thickness	Actual Thickness	Difference (feet)
"a#1"	Tpcpv3	0	0	0
"a#1"	Tpcpv2	2	9	-7
"a#1"	Tpcpv1	6	5	1
"a#1"	Tpbt4	2	7	-5
"a#1"	Tpy	0	0	0
"a#1"	Tpbt3	12	1	11
"a#1"	Tpp	33	28	5
"a#1"	Tpbt2	16	21	-5
"a#1"	Tptrv3	8	6	2
"a#1"	Tptrv2	8	3	5
"a#1"	Tptrv1	5	4	1
"a#1"	Tptrn	130	130	0
"a#1"	Tptrl	23	28	-5
"a#1"	Tptpul	245	235	10
"a#1"	Tptpmn	86	72	14
"a#1"	Tptpll	363	339	24
"a#1"	Tptpln	164	188	-24
"a#1"	Tptpv3	54	39	16
"a#1"	Tptpv2	16	15	2
"a#1"	Tptpv1	28	35	-7
"a#1"	Tpbt1	11	9	2
"a#1"	Tac	446	421	25
"a#1"	Tacbt	36	43	-7
"a#1"	Tcpuv	15	13	2
"a#1"	Tcpuc	97	99	-2
"a#1"	Tcpmd	49	62	-13
"a#1"	Tcplc	31	24	7
"a#1"	Tcplv	296	301	-5
"a#1"	Tcpbt	6	2	4
"a#1"	Tcbuv	1	0	1
"a#1"	Tcbuc	107	82	25
"a#1"	Tcbmd	312	N/A	N/A
"a#7"	Tpcpv3	0	0	0
"a#7"	Tpcpv2	6	5	1
"a#7"	Tpcpv1	11	13	-2
"a#7"	Tpbt4	6	4	2
"a#7"	Tpy	14	16	-2
"a#7"	Tpbt3	17	13	4
"a#7"	Tpp	40	36	4
"a#7"	Tpbt2	26	23	3
"a#7"	Tptrv3	5	11	-6
"a#7"	Tptrv2	8	1	7
"a#7"	Tptrv1	0.4	6	-5.6
"a#7"	Tptrn	157	155	2
"a#7"	Tptrl	28	22	6
"a#7"	Tptpul	232	235	-3
"a#7"	Tptpmn	93	98	-5
"a#7"	Tptpll	351	N/A	N/A

Borehole	Unit	Predicted Thickness	Actual Thickness	Difference (feet)
"c#1"	Tptrv3	7	N/A	N/A
"c#1"	Tptrv2	2	2	0
"c#1"	Tptrv1	3	3	0
"c#1"	Tptrn	106	92	14
"c#1"	Tptrl	34	14	20
"c#1"	Tptpul	139	157	-18
"c#1"	Tptpmn	133	131	2
"c#1"	Tptpll	314	314	0
"c#1"	Tptpln	168	176	-8
"c#1"	Tptpv3	86	77	9
"c#1"	Tptpv2	29	27	2
"c#1"	Tptpv1	17	14	3
"c#1"	Tpbt1	0	0	0
"c#1"	Tac	245	247	-2
"c#1"	Tacbt	77	111	-34
"c#1"	Tcpuv	1	0	1
"c#1"	Tcpuc	114	95	19
"c#1"	Tcpmd	76	76	0
"c#1"	Tcplc	23	21	2
"c#1"	Tcplv	239	235	4
"c#1"	Tcpbt	29	34	-5
"c#1"	Tcbuv	86	87	-1
"c#1"	Tcbuc	38	35	3
"c#1"	Tcbmd	182	171	11
"c#1"	Tcblc	105	129	-24
"c#1"	Tcblv	115	117	-2
"c#1"	Tcbbt	57	62	-5
"c#1"	Tctuv	0	0	0
"c#1"	Tctuc	67	N/A	N/A
"c#3"	Tptrv3	7	N/A	N/A
"c#3"	Tptrv2	2	3	-1
"c#3"	Tptrv1	3	5	-2
"c#3"	Tptrn	106	97	9
"c#3"	Tptrl	34	38	-4
"c#3"	Tptpul	132	125	7
"c#3"	Tptpmn	134	140	-6
"c#3"	Tptpll	313	327	-14
"c#3"	Tptpln	168	153	15
"c#3"	Tptpv3	84	87	-3
"c#3"	Tptpv2	29	28	1
"c#3"	Tptpv1	15	22	-
"c#3"	Tpbt1	0	0	0
"c#3"	Tac	248	260	-12
"c#3"	Tacbt	78	55	23
"c#3"	Tcpuv	0	0	0
"c#3"	Tcpuc	116	127	-11
"c#3"	Tcpmd	75	76	-1
"c#3"	Tcplc	22	25	-3
"c#3"	Tcplv	243	247	-4

Borehole	Unit	Predicted Thickness	Actual Thickness	Difference (feet)
"c#3"	Tcpbt	28	20	8
"c#3"	Tcbuv	90	88	2
"c#3"	Tcbuc	33	49	-16
"c#3"	Tcbmd	183	161	22
"c#3"	Tcblc	107	119	-12
"c#3"	Tcblv	117	123	-6
"c#3"	Tcbbt	58	34	24
"c#3"	Tctuv	0	0	0
"c#3"	Tctuc	67	N/A	N/A
N/A = unit not penetrated or not fully penetrated				

All values are thicknesses in feet

INTENTIONALLY LEFT BLANK

ATTACHMENT V

METHODOLOGY FOR UNCERTAINTY ANALYSIS

ATTACHMENT II

EXCLUDED BOREHOLE DATA

ATTACHMENT I

DOCUMENT INPUT REFERENCE SYSTEM (DIRS)

REMOVED

See electronic DIRS database.

ATTACHMENT V

METHODOLOGY FOR UNCERTAINTY ANALYSES

Uncertainty was estimated by means of two methods—a piecewise reconstruction method and an estimation of contouring uncertainty. Thickness uncertainty was estimated by contour estimation only. The piecewise reconstruction method provides a robust, practical estimation of elevation uncertainty that is specific to the modeled area and data set. The contouring uncertainty analysis was performed to estimate the contribution of model construction methods to elevation and thickness uncertainty in the GFM. Used together, these two methods provide bounds to uncertainty and add confidence to the estimation.

Surface data were not used in this analysis because of the complexity of calculating a fully 3-dimensional uncertainty analysis. Outcrop data introduce problems of dip, depth, erosion, and faulting that can not be adequately accounted for in terms of uncertainty. The analysis was restricted to subsurface (borehole) data to reduce the problem to 2 dimensions, and was further simplified to remove the potential effects of faulting, which introduces discontinuities to the analysis. These simplifications are not anticipated to have any effect on uncertainty analysis in the potential repository area where the effects of faulting are minor and borehole data are relatively abundant.

II.1 PIECEWISE RECONSTRUCTION UNCERTAINTY ESTIMATION

The first uncertainty estimation method involves a piecewise reconstruction of the model and a comparison of each piece to the others. In this method, the input data are divided into a few groups and used to reconstruct the model with one group of data at a time. The first group of data is used to build an initial model. That model is then used to predict rock layer elevations at the locations of the next group of data. The model is then rebuilt with the first and second groups of data, and so on. As groups of data are added, the model should become increasingly accurate in its predictions. The rounds of prediction accuracy provide an estimation of the model's ability to predict rock layer elevations at the location of new data (such as a borehole or tunnel).

Uncertainty was estimated for the Topopah Spring Tuff lower vitrophyre (Tptpv3) by means of piecewise reconstruction. Tptpv3 was chosen because it is an important stratigraphic boundary, which defines the lower boundary of the RHH for the repository design (CRWMS M&O 1997, p. v), and assessment of its spatial uncertainty is important for tunnel placement. The uncertainties calculated for Tptpv3 can be applied to the RHH as maximum values, because there are more borehole data for shallower horizons than for Tptpv3. Lower horizons would have greater uncertainty because fewer borehole data are available.

The YMP boreholes were sorted roughly by drilling date and borehole type. Boreholes that did not penetrate to the Tptpv3 were excluded. Each sorted group was chosen to provide a nonclustered distribution. The origin group consisted of the pre-1991 "WT" series of boreholes

because they are the most widely distributed group across the model area and, therefore, provide a tenable starting point. The successive borehole sets consisted of the following groups:

- Set 1: The a, b, c, p, and G series
- Set 2: The "H" series and J-13
- Set 3: NRG-7a, UZ-6, and UZ#16
- Set 4: SD-6, 7, 9, and 12, and WT-24.

The WT-series boreholes were chosen to provide a viable starting point for the analysis because they provide widespread data distribution across the model area. A widespread starting distribution is necessary to prevent extreme extrapolations, which would result in unrealistic predictions for subsequent borehole data sets. The successive boreholes were chosen approximately by date of drilling to provide a realistic assessment of how uncertainty has been reduced by drilling at Yucca Mountain. Additionally, the drilling program generally filled in the areas between existing boreholes, so that this analysis measures uncertainty as a function of distance and is directly applicable to potential future drilling, which would likely be based on similar criteria.

During subsurface exploration and characterization, several boreholes within the central block were constructed to investigate features of interest and not necessarily to fill in data gaps between existing boreholes. Based on this acknowledgement, this analysis may be inherently biased in the vicinity of the ESF.

Two types of piecewise reconstruction assessments were performed—the first using only the *minimum tension* gridding algorithm and the second using *interpretive* input in addition to field data as input to minimum tension gridding in the same way the GFM was constructed. In the interpretive method, contours were added to the data at each step to provide guidance by geologic interpretation, in the same manner that GFM3.1 was constructed.

The expected result of the piecewise reconstruction exercise is that the average predictive error should asymptotically approach some value that represents the model's predictive limit, which is referred to as the window of expected uncertainty. The results of the piecewise reconstruction exercise are shown in Figure V-1. As expected, in both the minimum tension and interpretive cases, the average predictive error decreases as the number of boreholes increases. The minimum tension method, however, averaged an error of 79 feet (24 meters), whereas the interpretive method averaged an error of only 40 feet (12 meters). Notice, too, that the range of predictive errors for the minimum tension method did not decrease with the addition of borehole set 4, suggesting that this method's error may not systematically decrease with additional boreholes.

This exercise suggests that lower Topopah Spring Tuff contacts are expected to be predicted in the subsurface within an uncertainty window of about 40 feet (12 meters) at locations away from existing boreholes up to about 3,280 feet (1,000 meters) distance. This distance is the average halfway distance between boreholes in the best constrained area, and therefore represents the

Using minimum tension method only (feet)

	set01	set02	set03	set04	
average	499	333	82	79	
median	241	169	56	68	
stand. dev.	493	395	55	71	
max.	1207	1174	145	198	(abs. value)
min.	29	69	44	19	(abs. value)
range	1178	1105	101	179	(abs. value)

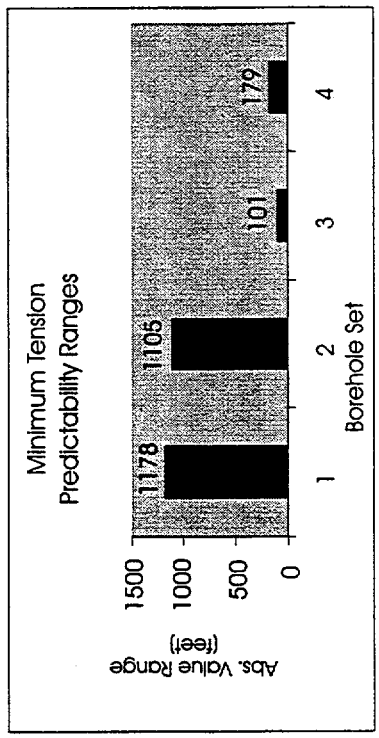

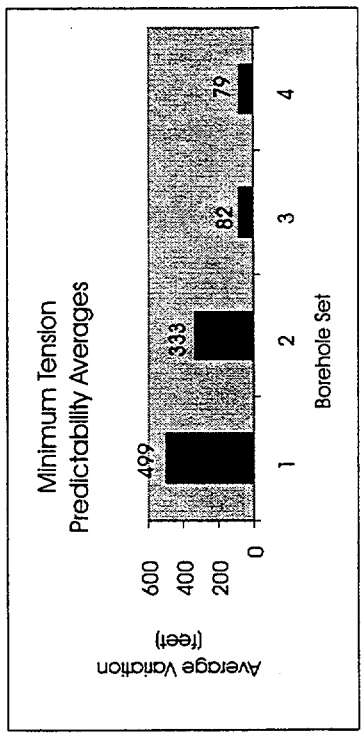

Using interpretive mapping in addition to minimum tension (feet)

	set01	set02	set03	set04	
average	282	133	57	39	
median	201	48	54	34	
stand. dev.	180	180	13	33	
max.	574	473	72	81	(abs. value)
min.	59	3	46	4	(abs. value)
range	633	476	118	85	(abs. value)

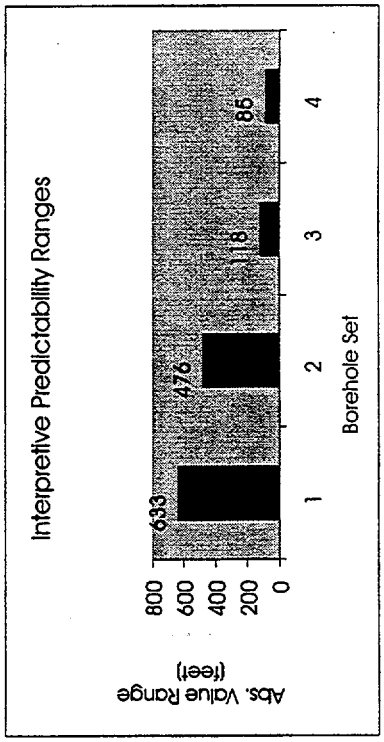

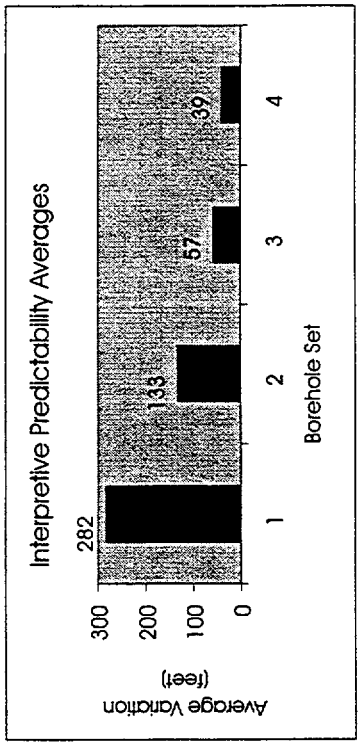

Figure V-1. Predictive Errors From the Piecewise Reconstruction Uncertainty Assessment for Tptpv3 (Lower Vitrophyre)

distance at which predictions begin to fall within the 40-foot (12-meter) average. Closer to existing boreholes, of course, uncertainty will be less, and it will be greater with distance from boreholes. This exercise was repeated for the pre- and post-Topopah contacts. Post-Topopah contact uncertainty window was about ±30 feet (9 meters), and pre-Topopah was about ±50 feet (15 meters).

II.2 CONTOURING UNCERTAINTY ESTIMATION

Figure V-2 illustrates the principles of estimating model-isochore contouring uncertainty for the GFM. This is a practical, empirical method that directly measures the uncertainty with which reference horizons in the GFM were constructed. The same principles could also be applied to model-isochore generation, but this discussion is focused on the reference horizons.

Interpretive constraints are used in addition to field data to create reference horizons (reference horizons are elevation control surfaces from which model-isochores are added or subtracted). The interpretive data consist of contours, which are hand-drawn by the modeler to constrain the shape of the reference horizon or model-isochore according to geologic principles and interpretation. The placement and shaping of these contours (in the context of the model interpretation) is, therefore, subjective—there is no "correct" answer. Measuring the range of acceptable or reasonable contour placements between data can make an estimate of contouring uncertainty. Because the data values are fixed, the range of reasonable contour placements between data behaves like a rubber band attached at the data, free to swing across the region in between. The dashed lines in Figure II-2 show the extreme contour placements in the analysis.

For the reference horizons in the GFM, this exercise yielded a contouring uncertainty increasing from 0 at data to ±50 feet (15 meters) at a distance of approximately 3,280 feet (1,000 meters) from data. Estimates for greater distances were not calculated because it was determined that beyond this distance, geologic factors like faulting, tilting, and erosion affect elevations to such a degree that the contouring uncertainty would be unidentified. In addition, 3,280 feet (1,000 meters) is the average halfway distance between boreholes in the most constrained area (the vicinity of the ESF). This value is reasonably consistent with the piecewise reconstruction uncertainty estimate of 40 feet (12 meters), although the piecewise reconstruction estimate was based on variable borehole spacing and is, therefore, not directly comparable.

II.3 SUMMARY

The more restrictive of the two uncertainty estimation methods discussed above (the piecewise reconstruction method) is used to summarize uncertainty in Section 6.5.1.

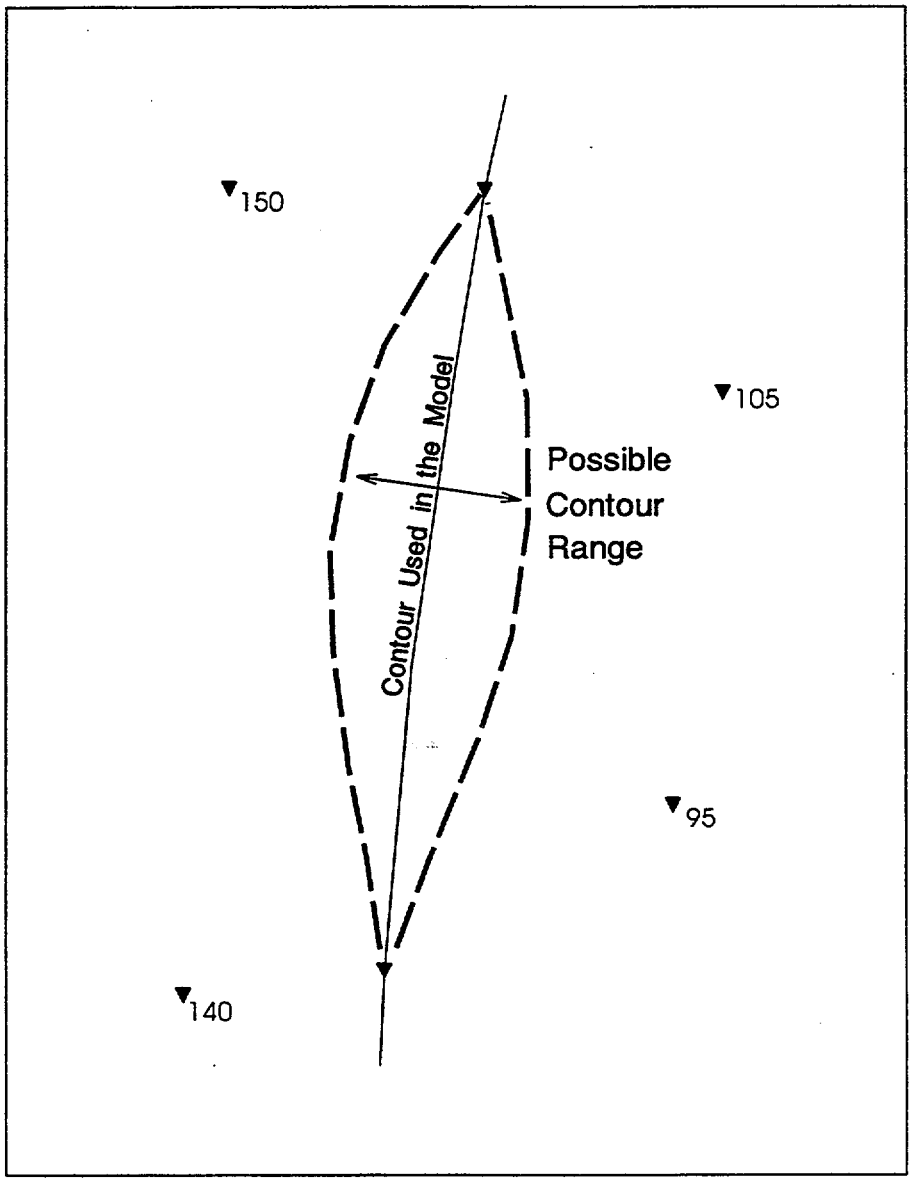

▼ Data

Figure V-2. Method for Evaluating Contouring Uncertainity

INTENTIONALLY LEFT BLANK